Convergent epigenetic consequences of mislocalization of ALS-linked RNA-binding proteins

by

Michael Tibshirani

Integrated Program in Neuroscience, McGill University, Montreal

December 2015

A thesis submitted to McGill University in partial fulfillment of the requirements of the degree of doctor of philosophy in science

Table of Contents

List of Figures:

Abstract

Amyotrophic Lateral Sclerosis (ALS) is a fatal neurodegenerative disease characterized by progressive paralysis resulting from dysfunction and loss of motor neurons. A common finding in ALS is retraction of motor neuron dendrites, expected to result in loss of vital central connections contributing to motor neuron dysfunction. Several genes have been linked to ALS, including the DNA/RNA-binding protein fused in sarcoma/translated in liposarcoma (FUS/TLS causing fALS6). Normally FUS is localized mainly in the nucleus and synaptic spines, but mutations lead to aberrant accumulation of the protein in cytoplasmic inclusions. This thesis investigates the hypothesis that cytoplasmic accumulation of FUS leads to loss of function of its interacting partners with consequences to transcriptional regulation underlying dendritic architecture. In a primary culture model of fALS6 established by expressing mutant FUS in motor neurons of dissociated murine spinal cord-dorsal root ganglion cultures, we measured attrition of terminal and intermediate dendritic branches in neurons expressing several FUS mutants, but not wild type human FUS, as well as nuclear depletion of two FUS-interacting proteins important for regulating gene expression. 1) Protein arginine methyltransferase 1 (PRMT1), which regulates nuclear-cytoplasmic shuttling of FUS. Nuclear depletion of PRMT1 (with FUS) was accompanied by decreased histone methylation (H4R3) and acetylation (H3K9/K14) and the rate of transcriptional activity. Treatment with the histone deacetylase inhibitor, SAHA, maintained histone acetylation and dendritic architecture. 2) The DNA-helicase Brahma-related gene 1 (Brg1), which in neurons, is associated with the neuronal Brg1-associated factor complex (nBAF). This chromatin remodeling complex is critical for neuronal differentiation, extension of dendrites and maintenance of synapse function, and is dependent on

critical nBAF subunits including Brg1, BAF53b and CREST. In cultured motor neurons expressing mutant FUS, Brg1, BAF53b and CREST were depleted from the nucleus. These mechanisms were not unique to fALS6; dendritic attrition, loss of nBAF subunits, decreased histone acetylation and rescue by SAHA occurred in motor neurons expressing mutant TDP43 (ALS10). nBAF subunits also were depleted from spinal motor neurons in cases of familial (SOD1A4V; C9ORF72 G_4C_2 expansion) and sporadic ALS. Disruption of nBAF function plays a critical role in dendritic attrition, since the effect of ALS-linked mutant proteins was reproduced by inhibiting Brg1 function and was delayed by ectopic expression of Brg1. Thus, this study supports the hypothesis that loss-of-function of FUS interacting partners does occur and identifies a new convergent mechanism in ALS pathogenesis and therapeutic target.

Résumé

La sclérose amyotrophique latérale (SLA) une maladie neurodégénérative caractérisée par une paralysie progressive causée par le dysfonctionnement et la perte des motoneurones dont l'origine est génétique ou sporadique. Une caractéristique commune aux différentes formes de la SLA est la rétraction des dendrites des motoneurones causant ainsi la déconnection des motoneurones spinaux d'avec leur connections centrales. Plusieurs gènes causant la maladie ont été identifiés, notamment le gène codant pour la DNA/RNA-binding protein fused in sarcoma/translated in liposarcoma (FUS/TLS) et responsable de SLA6. La localisation subcellulaire de FUS est principalement nucléaire et synaptique, cependant les mutants responsables de formes de SLA6 présentent une localisation cytoplasmique et forment des inclusions. Cette thèse se propose de vérifier l'hypothèse selon laquelle l'accumulation cytoplasmique de FUS abouti à une perte de fonction des partenaires de FUS et affecte la régulation de la transcription du programme génétique responsable de l'architecture dendritique. En utilisant un modèle *in vitro* reproduisant la SLA6 et consistant en l'expression de mutants FUS ou de la forme sauvage dans des motoneurones de souris en culture, nous avons mis en évidence l'attrition des branches terminales et intermédiaires des dendrites des motoneurones. De plus, la protéine arginine methyltransferase 1 (PRMT1) et la DNA-hélicase Brahma-related gene 1 (BRG1), deux partenaires de FUS impliqués dans la régulation de l'expression génique, présentent une déplétion nucléaire dans ce modèle *in vitro* suggérant ainsi une perte de fonction de ces deux protéines dans la SLA6. 1) PRMT1, est un partenaire important de FUS qui régule sa translocation nucléocytoplasmique. La déplétion nucléaire concomitante de PRMT1 et de FUS est accompagnée par un défaut de la méthylation (H3R3) et de l'acétylation des histones (H3K9/K14), et de la diminution de l'activité transcriptionelle. Le traitement avec l'inhibiteur d'histone deacétylase, SAHA, permet de maintenir l'acétylation des histones et de l'architecture

dendritique. 2) Brg1 est une protéine remodelant la chromatine et associée à un complexe de facteur de transcription dans les neurones (nBAF) crucial pour la différenciation neuronale, l'extension des dendrites et la maintenance des fonctions synaptiques. Il est composé de protéines clés comme Brg1, BAF53b et CREST dont la localisation nucléaire est affectée dans les neurones en culture exprimant les mutants de FUS responsables de la SLA6. L'attrition dendritique, la perte nucléaire des sous-unités composant le nBAF, la diminution de l'acétylation des histones sont aussi observés dans un modèle *in vitro* exprimant les mutants de TDP43, responsable de la SLA10. La perte nucléaire des sous-unités composant nBAF est aussi observée dans des cas de SLA familiales (SOD1A4V; C9ORF72 G_4C_2 expansion) ou sporadiques démontré par l'absence d'immunoreactivité dans les motoneurones d'échantillons anatomopathologiques. La perte des fonctions de nBAF, et plus particulièrement Brg1, joue un rôle important dans la rétraction dendritique car elle reproduit les effets de l'expression des mutants de FUS et peut être limitée par l'expression ectopique de Brg1. Ainsi notre étude confirme le rôle de FUS et des ses partenaires dans la SLA, et identifie de nouveaux mécanismes de la pathogenèse de la SLA et de nouvelles cibles thérapeutiques.

Acknowledgements

My accomplishments during graduate school are a culmination of the relationships I have forged throughout my time as a student in the Integrated Program for Neuroscience and these relationships must be acknowledged.

A student is only as good as his teacher; my supervisor Dr. Heather Durham is a testament to this fact. Her love of science and her professional and emotional support has kept me going strong during my graduate degree. Because of you, I have been able to explore with no limit, grow as a scientist and appreciate the patients we fight for in the lab. These are gifts I will cherish forever. Thank you, thank you, and thank you once more.

I would like to acknowledge the members of my thesis advisory committee Dr. Stéphane Richard, Dr. Ursula Stochaj and Dr. Kenneth Hastings for their time, effort and guidance in carefully carving a project of which I can be most proud.

I would also like to thank the members of the lab Dr. Miranda Tradewell, Dr. Benoit Gentil and Sandra Minotti for teaching me everything I know and for your never-ending guidance and patience.

To the wolf pack Luan Tran and Kyle St. Louis, your friendship and sense of humor in the lab made coming in to work an absolute joy. To Jessie Kulaga-Yoskovitz, you are a great confidant and friend. Having someone to listen to my seemingly never ending complaints about medical school applications had kept me sane.

To the breakfast club, Hana Antonicka, Karine Doiron, Liane Levasseur, and Joe Pogson, our morning coffee breaks and conversations are just what I needed to wake up and attack the day ahead of me with full force.

To my parents. You made me into the man I am today and my accomplishments are mirrored partly by my upbringing. Mom, thank you for your endearing support and making me feel like I couldn't fail no matter what I did in life. Dad, your ability to explain the science behind everything I saw in nature is what inspired my thirst for knowledge. Your hard-to-impress attitude and your no tolerance policy on being average kept me determined to accomplish anything I wanted in life and strive for perfection.

To my loving wife Lydia, this thesis was a team effort. You are a strong, loving wife and mother and your patience, encouragement, love and never-ending support for my pursuit of happiness has given me the ability to turn my life dreams into a reality.

Preface

In accordance with the guidelines for thesis preparation and under advisement of the thesis supervisor, the candidate has opted to present this thesis in standard format. A general introduction is presented in Chapter 1 followed by a hypothesis and rationale for the thesis project in Chapter 2. A detailed description of the experimental procedures used to address the specific aims of the thesis is presented in Chapter 3. Results are described in Chapter 4 and appear in the following articles:

Tibshirani M., Tradewell M.L., Mattina K.R., Minotti S., Yang W., Zhou H., Strong M.J., Hayward L.J., Durham H.D., Cytoplasmic sequestration of FUS/TLS associated with ALS alters histone marks through loss of nuclear protein arginine methyltransferase 1. Hum Mol Genet 24(3):773-86, 2014

Tibshirani M., Zhao B., Minotti S., Robertson J., Durham H.D., Depletion of nBAF chromatin remodeling complexes, a convergent mechanism of dendritic attrition in ALS. In Preparation.

Following the description of results, a general discussion of the thesis topic and results, as well as final conclusions and summary are presented followed by a bibliography. I planned and executed the experiments presented under the supervision of Dr. Durham and under advisement

of Dr. Stochaj, Dr. Richard and Dr. Hastings, members of my thesis advisory committee. I acknowledge the contributions of the following collaborators: Dr. Zhou and Dr. Hayward (University of Massachusetts Medical School, Worcester, MA) for immunohistochemical analysis of their mutant FUS transgenic mice; Drs. Wencheng Yang, Michael Strong (Robarts Research Institute, Western University, London, Ontario) and Beibei Zhao and Janice Robertson (Tanz Centre for Research in Neurodegenerative Diseases, Toronto, ON) for the immunohistochemistry experiments performed on human autopsy spinal cord; Katie Mattina for her assistance in the analysis of histone post-translational modifications, and Sandra Minotti for the generation of the spinal cord cultures as well as assistance with intranuclear injections.

I also contributed to the following published articles:

Tradewell M.L., Yu Z., **Tibshirani M**., Boulanger M.C., Durham H.D., Richard S., Arginine methylation by PRMT1 regulates nuclear-cytoplasmic localization and toxicity of FUS/TLS harbouring ALS-linked mutations. Hum Mol Genet 21(1):136-49, 2012

Cha J.R.C., St. Louis K.J.H., Gentil B.J., **Tibshirani M.**, Tradewell M.L., Minotti S., Jaffer Z.M., Chen R., Rubenstein A.E., Durham H.D. A novel small molecule HSP90 inhibitor, NXD30001, differentially induces heat shock proteins in nervous tissue in culture and in vivo. Cell Stress and Chaperones 19:421-435, 2014 (see erratum)

Gentil B.J-C., **Tibshirani M.,** Durham H.D. Neurofilament dynamics and disease mechanisms in neurofilament disorders. Cell Tissue Research 360(3):609-20, 2015 (Review)

My contribution to Tradewell *et al.* (2012) involved performing experiments, data collection and analysis and contributing to the writing of the manuscript as an undergraduate student. It was during this study when I observed the redistribution of PRMT1 in mutant FUS expressing neurons, which built the foundation for the hypothesis and rationale of my thesis.

Contribution to Original Knowledge

The growing list of ALS-linked genes encoding RNA binding proteins has revealed the importance of abnormal RNA metabolism in the pathogenesis of ALS. These normally nuclear proteins are implicated further in the pathology of ALS by their accumulation in the cytoplasm being a common neuropathological phenomenon, even in the absence of mutation. Furthermore, motor neurons are thought to become dysfunctional before cell death providing a window of opportunity for treatment. This thesis was driven by two main questions: How does cytoplasmic accumulation of RNA-binding proteins cause neuronal dysfunction? Are they involved in convergent pathological pathways that can be targeted for therapeutic interventions? To answer these questions, I employed a neuronal culture model in which the RNA-binding protein, FUS, with ALS-linked mutations was expressed in motor neurons of dissociated murine spinal cord cultures, as well as validating findings in ALS autopsy specimens. The original contributions of this work are: 1) The primary culture model of fALS6, which I assisted Dr. Tradewell in developing as an undergraduate student, was further characterized. By extending the timeline of FUS expression to six days post-injection, skein-like and linear mutant FUS inclusions formed in motor neurons. In addition dendritic retraction was identified as a main functional end-point of mutant FUS-related toxicity, reproducing a prominent phenotype of motor neurons in ALS (Nakano and Hirano, 1987, Karpati et al., 1988, Takeda et al., 2014). Quantifying dendritic retraction provided an endpoint in this culture model with which we could evaluate the efficacy of various interventions that would promote preservation of the connectivity of motor neurons. These results are described in Chapter 4.1.

2) The distribution of PRMT1, the enzyme responsible for asymmetric arginine methylation of FUS that regulates nuclear cytoplasmic trafficking, was disrupted concomitant with its binding

partner FUS. Nuclear depletion of PRMT1 compromised methylation of its nuclear substrates, specifically histone methylation, which had downstream effects on histone acetylation and transcriptional activity. Thus, in addition to the effect of the mutation directly on FUS localization and function, an important indirect mechanism of FUS-related toxicity was implicated; *i.e.*, loss of function of a FUS-interacting protein resulting in epigenetic modifications and consequences to gene expression. These results are described in Chapter 4.2.1 to Chapter 4.2.4.

3) The clinically approved histone deacetylase inhibitor, Vorinostat (SAHA), both maintained histone acetylation levels and prevented dendritic attrition in the fALS6 culture model, providing additional rationale for epigenetic drugs like HDAC inhibitors for treatment of ALS. If histone acetylation and gene expression profiles are altered in ALS, then HDAC inhibitors can be considered in combination with therapeutic candidates whose mechanism of action is to alter gene expression in motor neurons in an effort to upregulate the expression of prosurvival genes.

4) For our experiments to confirm these results in human archived tissue, we developed a protocol to evaluate the effect of post-mortem interval on antigen preservation and retrieval for immunohistochemistry. This variable must be considered when testing archived human autopsy tissue. These results are described in Chapter 4.2.6.

5) In keeping with the theme of changes in gene expression leading to dendritic attrition, I discovered depletion of the DNA helicase Brg1, and other critical subunits of the nBAF chromatin remodeling complex, important for neuronal differentiation and dendrite extension (Wu et al., 2007, Yoo et al., 2009, Chesi et al., 2013, Staahl et al., 2013, Vogel-Ciernia et al., 2013). The genetic heterogeneity of ALS and the number of sporadic cases with unidentified

mutations presents a challenge for ALS scientists to identify a common converging pathway that could be targeted for therapeutic intervention. We observed that, irrespective of the genetic background, depletion of critical nBAF subunits occurred in motor neurons of ALS patients indicating that dyregulation of the nBAF complex could be a converging pathway responsible for retraction of dendrites in ALS. The nBAF complex has mainly been implicated in neuronal development; others have demonstrated that it is important for extension of dendrites and mutations in nBAF subunits are linked to developmental disorders associated with mental retardation (Halgren et al., 2012, Neale et al., 2012, Tsurusaki et al., 2012). The results of the thesis project suggest that the nBAF complex must be maintained throughout adulthood and dysregulation can be associated with adult onset diseases as well. Re-introduction of Brg1 in cultured motor neurons was able to prevent dendritic retraction in the fALS6 culture model. These results are described in Chapter 4.3. Though gene replacement therapy is still far on the horizon, understanding the mechanisms of nBAF subunit depletion could reveal convergent pathways that could be targeted to maintain nBAF complex composition.

6) Using a primary culture model of fALS10 due to mutations in the RNA-binding protein, TDP43, I demonstrated that chromatin remodeling pathways are similarly affected in this form of ALS. These data are presented in Chapter 4.4.

Chapter 1: Introduction

1.1: What is ALS?

1.1.1 Demographics

Amyotrophic Lateral Sclerosis (ALS) is a neurodegenerative disease characterized by preferential loss of motor neurons leading to death typically 2-5 years after diagnosis due to respiratory insufficiency. The incidence of the disease is 2-3 people per 100,000 and the prevalence is 4-6 people per 100,000 (Kiernan et al., 2011). The average age of onset is 55-65 (Logroscino et al., 2010) and the lifetime risk of developing ALS is slightly higher in men than it is in women. There is no effective treatment for ALS, and the development of therapies is partly hindered due to the complexity of the disease, which involves multiple cell types and dysregulation of multiple cellular pathways.

1.1.2 Clinical Phenotype of ALS

ALS often presents with asymmetric muscle weakness, which progressively worsens and spreads through the neuraxis until loss of motor neurons controlling diaphragmatic muscle results in respiratory insufficiency and ultimately death. Other symptoms related to motor neuron degeneration include fasciculation and muscle cramps, spasticity, dysarthria (difficulty speaking), dysphagia (difficulty swallowing) and dyspnea (difficulty breathing) (Mitchell and Borasio, 2007, Hardiman et al., 2011, Kiernan et al., 2011). While the majority of cases are limb onset, 30% of patients initially present with bulbar symptoms (dysarthria, dysphagia and dyspnea) (Logroscino et al., 2010). A small proportion of ALS patients present with overt Frontotemporal Lobar Degeneration (FTLD); however, the incidence of some degree of cognitive involvement (social disinhibition and deficits in emotional processing) has been reported to be as high as 50% (Ringholz et al., 2005). The majority of ALS cases appear sporadic with no known familial inheritance (sALS) while approximately 10% of ALS patients show a family history (fALS) (Byrne et al., 2011). To date, approximately 22 genes have been

identified in fALS, as well as in some sALS, patients (Al-Chalabi et al., 2012, Peters et al., 2015), the most commonly studied, and resembling classical ALS, being Cu/Zn Superoxide Dismutase 1 (SOD1), Fused in Sarcoma/Translated in Liposarcoma (FUS/TLS; focused in this thesis), TAR-DNA Binding Protein 43 (TDP43), and Open Reading Frame 72 on chromosome 9 (C9ORF72) (see Chapter 1.1.4).

1.1.3 Mechanisms of pathogenesis of ALS

A known pathological hallmark of many neurodegenerative diseases is the presence of ubiquitin-positive protein aggregates or inclusions in neuronal cell bodies. In addition to this feature, pathological examination of post-mortem neural tissue from ALS patients reveals abnormal accumulation of intermediate filament proteins such as peripherin (Corbo and Hays, 1992, He and Hays, 2004) and neurofilament protein (Corbo and Hays, 1992, Hardiman et al., 2011) as well as the microtubule stabilizing protein, tau (Strong et al., 2006). FUS and TDP43 positive inclusions can be found in the cytoplasm of motor neurons from affected patients with or without mutations in the genes encoding these proteins (Arai et al., 2006, Neumann et al., 2006, Mackenzie et al., 2007, Deng et al., 2010), the presence of TDP43 inclusions being more common (Janssens and Van Broeckhoven, 2013) (see below).

There is also evidence of excitotoxicity as a major factor for ALS pathogenesis. In many cases of sALS, increased glutamate concentration in the cerebrospinal fluid (Loeb et al., 1994, Shaw et al., 1995) has been detected. This increase is likely due to decreased expression and activity of the glutamate transporter EAAT (Rothstein et al., 1995). The low expression of cytosolic Ca^{2+} binding proteins and the presence of Ca^{2+} permeable AMPA receptors (Celio, 1990, Siklos et al., 1996, Williams et al., 1997, Appel et al., 2001) indicate a preferential susceptibility of motor neurons to glutamate induced-excitotoxicity.

The pathogenesis of ALS can also occur via non-cell autonomous mechanisms; *i.e.*, non-neuronal cells may also be involved in loss of motor neuron function. Upregulation of TLR4 regulated genes has been detected in patients with sALS which could indicate chronic macrophage activation (Engelhardt and Appel, 1990, Zhang et al., 2011). In addition, the blood-spinal cord barrier can be compromised in ALS (Winkler et al., 2013) resulting in infiltration of immune cells at the site of motor neuron degeneration (Kawamata et al., 1992). Microglial activation also was observed before the onset of symptoms in ALS mouse models (Alexianu et al., 2001, Henkel et al., 2006) and the severity of symptoms correlates with microglial activation in the motor cortex of ALS patients (Turner et al., 2004). Finally, alterations in T-cell populations were found in the nervous tissue and blood of ALS patients (Henkel et al., 2013).

Although motor neurons ultimately die, death is preceded by a dysfunctional state. A common, widely studied, neuropathological finding in ALS patients and ALS animal models is loss of the integrity of neuromuscular junctions and retraction of nerve terminals (Fischer et al., 2004, Blijham et al., 2007). In addition, axonal transport is perturbed in ALS indicated by proximal accumulation of mitochondria and lysosomes in the proximal axon (Sasaki and Iwata, 1996a).

Another common, but less studied, feature in ALS is atrophy and retraction of motor neuron dendrites (Nakano and Hirano, 1987, Karpati et al., 1988, Takeda et al., 2014). This process would be expected to result in a loss of central connections and ultimately an inability of motor neurons to respond to inputs from higher order neurons. The mechanisms underlying dendritic attrition are explored in Chapter 4.3 of this thesis.

1.1.4 Genetic Heterogeneity of ALS

Several genes are implicated in ALS. Four genes out of twenty-two identified ALS-related genes make up the majority of familial cases and are most commonly studied: Cu/Zn

Superoxide Dismutase 1 (SOD1), Fused in Sarcoma/ Translated in Liposarcoma (FUS/TLS; the focus of this thesis), TAR-DNA Binding Protein 43 (TDP43), and Open Reading Frame 72 on chromosome 9 (C9ORF72). These genes and their involvement in ALS are outlined below.

SOD1: *SOD1* was the first gene linked to ALS (Rosen, 1993). SOD1 is a ubiquitously expressed, cytosolic antioxidant metalloenzyme that catalyzes the conversion of superoxide into hydrogen peroxide and molecular oxygen (Fridovich, 1995, 1997). Mutations in SOD1 (fALS1) account for approximately 20% of fALS cases. SOD1 mutations promote misfolding and aggregation of the protein leading to a gain of toxic function, which is implicated in pathogenesis rather than a loss of dismutase activity (Borchelt et al., 1994); insoluble, ubiquitin-positive SOD1 inclusions are present in motor neurons of patients with SOD1 mutation, as well as culture and transgenic animal models (Bruijn et al., 1997, Durham et al., 1997, Kato et al., 2000, Stieber et al., 2000, Kato et al., 2001, Chung et al., 2003). These intracellular aggregates are FUS- and TDP43-negative (Keller et al., 2012). Mutations in SOD1 have been linked to a number of pathogenic cascades such as calcium homeostasis dysregulation (Siklos et al., 1996, Roy et al., 1998, Siklos et al., 1998, Jaiswal and Keller, 2009, Tradewell et al., 2011), abnormalities in mitochondrial function (Sasaki and Iwata, 1996b, Borthwick et al., 1999, Bendotti et al., 2001, Tradewell et al., 2011, Vehvilainen et al., 2014), neuronal excitotoxicity (Rothstein et al., 1995, Bruijn et al., 1997, Kruman et al., 1999, Howland et al., 2002), and dysregulation of proteasome function (Kabashi et al., 2004, Cheroni et al., 2005, Kabashi et al., 2008a). Furthermore, recent studies have suggested that misfolding of SOD1 can be propagated in a prion-like fashion, which can be transmitted both intra- and inter-cellularly (Grad et al., 2015).

C9ORF72: Recently, a hexanucleotide repeat expansion in the non-coding region of C9ORF72 was identified in fALS linked to chromosome 9 (DeJesus-Hernandez et al., 2011,

Renton et al., 2011, Daoud et al., 2012, Siuda et al., 2014). This represents the most prevalent cause of fALS (approximately 20-30%) and is responsible for a significant percentage of sALS cases, particularly in Finland (Gijselinck et al., 2012). C9ORF72 contains DENN domains which are commonly found in GDP/GTP exchange factors responsible for activating Rab-GTPases, a class of GTPases that plays a role in vesicular trafficking and fusion (Levine et al., 2013, Farg et al., 2014).

Three main hypotheses for C9ORF72 expansion toxicity are currently being investigated by several groups: 1) loss-of-function due to decreased levels of the protein (DeJesus-Hernandez et al., 2011, Almeida et al., 2013, Belzil et al., 2013a), 2) sequestration of RNA-binding proteins in intranuclear C9ORF72 RNA-foci (DeJesus-Hernandez et al., 2011, Mizielinska et al., 2013, Mori et al., 2013a, Sareen et al., 2013, Xu et al., 2013) or 3) non-ATG mediated RAN translation leading to synthesis of toxic dipeptide repeats (Ash et al., 2013, Cruts et al., 2013, Janssens and Van Broeckhoven, 2013, Mori et al., 2013b, Zu et al., 2013, Gendron et al., 2014). Patients carrying C9ORF72 expansions display a wide variety of clinical symptoms ranging from purely ALS to solely FTLD symptoms. Abnormal accumulation of neuronal cytoplasmic TDP43-positive inclusions are evident in post-mortem tissue of patients with C9ORF72 repeat expansions (Murray et al., 2011) and in a disease mouse model of C9ORF72 (Chew et al., 2015).

***TARDP*:** Cytoplasmic accumulation of ubiquitinated TDP43-positive inclusions has been the pathological hallmark of ALS and FTLD (Arai et al., 2006, Neumann et al., 2006, Mackenzie et al., 2007). In 2008, mutations in the *TARDP* gene encoding TDP-43 were linked to familial ALS type 10 (fALS10) (Kabashi et al., 2008b, Sreedharan et al., 2008). TDP43, like FUS, is an hnRNP shown to have roles in transcription and RNA splicing and export. TDP43 also resides predominantly in the nucleus, but shuttles between the nucleus and the cytoplasm to perform its

various functions.. TDP43 is also hyperphosphorylated in disease states (Hasegawa et al., 2008) and abnormal accumulation of its C-terminal fragment (Neumann et al., 2006) have also been observed and attributed to abnormal alternative splicing of TDP43 (Xiao et al., 2015). How these modifications are involved in disease mechanisms is not yet understood.

***FUS*:** Mutations in the gene encoding FUS (a.k.a. fused in sarcoma/translated in liposarcoma), account for 4-5% of fALS cases known as fALS6 (Kwiatkowski et al., 2009, Vance et al., 2009). FUS is a heterogeneous nuclear ribonucleoprotein (hnRNP, DNA/RNA binding protein), mainly found in the nucleus and synaptic spines. Its various roles in transcription, RNA splicing, microRNA processing, RNA transport and regulation of translation require FUS to shuttle between the nucleus and cytoplasm (Fujii and Takumi, 2005, van Blitterswijk and Landers, 2010). In patients with fALS6, FUS can be retained in the cytoplasm of motor neurons of the ventral horn and frontal cortex in the form of FUS-positive inclusions (Vance et al., 2009, Blair et al., 2010, Hewitt et al., 2010, Tateishi et al., 2010). Interestingly, FUS positive inclusions can be found in both familial and sporadic forms of ALS with no known FUS mutations (an exception is fALS1) suggesting involvement of a common pathway (Deng et al., 2010). Furthermore, in rare cases, ALS presents with juvenile onset (jALS) often with mental retardation (Nelson and Prensky, 1972, Baumer et al., 2010). These more severe cases of ALS also present with FUS mutations and FUS-positive, TDP43-negative cytoplasmic inclusions in motor neurons (Baumer et al., 2010, Conte et al., 2012, Yamashita et al., 2012). Finally, FUS neuronal cytoplasmic inclusions can be found in ubiquitin-positive Frontotemporal Lobar Degeneration (FTLD-U) (Neumann et al., 2009), a neurodegenerative disorder leading to dementia, which has some clinical overlap with ALS (ALS-FTD), that is, ALS patients may present with cognitive deficits and frontotemporal dementia (Mackenzie and Feldman, 2005,

Murphy et al., 2007). Intraneuronal FUS-containing inclusions are also observed in Neuronal Intermediate Filament Disease (NFID) and Basophilic Inclusion Body Disease (BIBD), diseases associated with FTLD and motor neuron disease (Armstrong et al., 2011, Gelpi et al., 2012, Lee et al., 2013). The presence of FUS-positive inclusions in these variants of motor neuron disease (fALS, SALS, jALS, ALS-FTD, NFID and BIBD) illustrates a role in a potential common pathway that FUS might have in the pathological spectrum of motor neurons diseases. The pathogenic cascades that are activated in cells expressing mutant FUS are unclear. This thesis will primarily focus on the role of FUS in ALS pathogenesis.

FUS and TDP43 may function together in common pathways. These proteins share some common RNA targets (Honda et al., 2013); FUS regulates mRNA levels encoding histone deacetylase 6 (HDAC6) in a common biological pathway with TDP-43 (Kim et al., 2010). Both proteins accumulate in stress granules in cell lines (Bosco et al., 2010, Dormann et al., 2010, Gal et al., 2011, Ito et al., 2011, Kino et al., 2011, McDonald et al., 2011, Sama et al., 2013). Double-knockdown of FUS and TDP43 in zebrafish caused a locomotor phenotype that was rescued by overexpression of WT FUS, but not by TDP43 (Kabashi et al., 2010, Kabashi et al., 2011), a result that was recapitulated in *Drosophila* (Wang et al., 2011), which suggests that FUS probably acts downstream of TDP43 in the common pathway. These observations indicate that these two proteins are likely involved in overlapping biochemical pathways, with TDP43 upstream of FUS.

1.2: Importance of heterogeneous ribonucleoprotein particles (hnRNPs)

1.2.1 Importance of hnRNPs in neuronal function and disease

Many types of hnRNPs are important for cell maintenance and synaptic plasticity. With cellular stress, these proteins accumulate in stress granules and processing bodies (P-bodies or

GW-bodies). Stress granules are particles that form under stressful conditions, such as experimental heat-shock, osmotic stress and UV irradiation, and are responsible for stalling translation of housekeeping RNAs until the stressor is removed (Anderson and Kedersha, 2009). Unlike P-bodies and transport granules, stress granules are not transported along microtubules; however, their formation is microtubule-dependent (stress granules disassemble in the presence of a microtubule destabilizing agent) (Kedersha et al., 2005). Stress granule markers include TIA-1/TIAR, G3BP, and Poly-A binding Protein (PABP1) (Kedersha et al., 2005). Both TDP-43 and FUS localize to stress granules in cell lines subjected to stress (Bosco et al., 2010, Dormann et al., 2010, Gal et al., 2011, Ito et al., 2011, Kino et al., 2011, McDonald et al., 2011). In addition, mutant FUS accumulates more readily in stress granules than WT FUS (Bosco et al., 2010). P-bodies are hnRNPs that share some components with stress granules and are responsible for stalled translation and regulated degradation of specific RNAs. The constituent hnRNPs were initially characterized in immunolabelling experiments using autoantibodies from patients with motor and sensory deficits against the GW182 antigen (a component of P-bodies) (Eystathioy et al., 2002, Eystathioy et al., 2003). Other components of P-bodies include decapping enzymes (DCP1 and DCP2), which catalyze the removal of the 5' and 3' RNA cap and Argonaute-2 (Ago2), which acts as a scaffold for P-body proteins and is responsible for nucleation of these particles (Moser and Fritzler, 2010). More recently, it has been shown that both stress granules and p-bodies exhibit liquid-phase properties in mammalian cells with the capability of forming distinct non-membranous bound droplets and fusing with one another (Kroschwald et al., 2015). These properties are also exhibited by mutant FUS granules *in vitro* (Patel et al., 2015). To maintain polarization and respond to synaptic input, neurons need to transport mRNAs to post-synaptic sites to be available for local translation in response to

synaptic activity. This transport of stalled mRNAs to synapses is accomplished via neuronal transport granules. These hnRNPs share components with P-bodies and are specifically identified by Staufen-1 and Fragile-X Mental Retardation Protein (FMRP), a translational repressor that is absent in Fragile-X Mental Retardation Syndrome, the most common form of mental retardation (Barbee et al., 2006, Liu-Yesucevitz et al., 2011). Furthermore, the hnRNP protein, Survival of Motor Neuron (SMN), is required to assemble spliceosomes, is a component of stress granules and also complexes with FMRP (Liu-Yesucevitz et al., 2011). Deletion mutations leading to deficiency of SMN are responsible for Spinal Muscular Atrophy (SMA) (Lefebvre et al., 1995). Mutations in other hnRNP proteins such as Angiogenin and Ataxin-2 cause spinocerebellar ataxia and are associated with increased risk of ALS (Greenway et al., 2006, Corrado et al., 2011). Finally, mutations in TAF15, a member of the FET family of proteins with similarities to FUS have been discovered in patients with ALS and make it prone to aggregation (Couthouis et al., 2011). FUS, TAF15 and EWS, the final member of the FET family of proteins, have been shown to co-aggregate in neural tissue of FTLD-U patients (as well as NIFID and BIBD patients) and not in fALS6 patients which distinguishes FUS pathology in FTLD-U from fALS6 (Neumann et al., 2011). The association of many hnRNPs with neurological diseases, many of which present with motor deficits, illustrates their importance in maintaining neuronal integrity.

1.3: Structure, Function and Trafficking of FUS

1.3.1 FUS Structure and Function

FUS is a 526 amino acid protein belonging to the FET (FUS/ EWS/ TAF15) family of proteins originally discovered in a variety of human sarcomas caused by the gene translocations resulting in fusion of these proteins with oncogenic transcription factors (Kovar, 2011). FUS contains an N-terminal rich in Glutamine, Glycine, Serine, and Tyrosine (QGSY) similar to

transactivation domains of other transcription factors. Adjacent to this region is a Glycine-rich domain which, due to its hydrophobic nature, probably promotes protein-protein and protein-RNA interactions. Together, the region containing these domains (specifically residues 1-239) contains low complexity sequences domains making FUS inherently aggregation prone (determined by an algorithm ranking FUS 15th out of 27, 879 human proteins (Gitler and Shorter, 2011, Kato et al., 2012a); it aggregates spontaneously and becomes insoluble *in vitro* (Sun et al., 2011b)). FUS also has an RNA-Recognition Motif (RRM), responsible for recognition of RNAs, particularly those containing GGUG motifs (Lerga et al., 2001), flanked by two Arginine-Glycine-Glycine (RGG) domains which, along with the RRM motifs, contribute to the physical protein-RNA interaction of FUS, actually mediated by its zinc finger motif (Lerga et al., 2001). FUS binds a vast number of RNA transcripts, mainly in intronic regions; however, mutant FUS binds RNAs mainly at their 3' untranslated regions (UTRs) (Hoell et al., 2011). Knockdown of FUS in neurons leads to alterations in RNA splicing (Nakaya et al., 2013) and, of interest, FUS regulates its own expression levels through skipping of exon 7 of its own mRNA leading to mRNA degradation through the nonsense-mediated decay pathway (Zhou et al., 2013). In addition to regulation of RNA splicing, this hnRNP has also been shown to transport mRNA to dendritic spines of cultured hippocampal neurons, particularly mRNA encoding β-actin and the actin stabilizing protein, Nd1-L, upon stimulation of metabotropic glutamate receptors (Fujii and Takumi, 2005). The general hypothesis regarding FUS-induced toxicity is an increased propensity to accumulate into stress granules (shown in cell lines) which would likely lead to stalled translation of associated RNAs. However, FUS may not accumulate in stress granules in neurons (Shelkovnikova et al., 2013) and through metabolic labelling of newly synthesized proteins, FUS granules were demonstrated to be translationally active in NIH/3T3 cell lines.

More recently, granules containing WT or mutant FUS protein has been shown to exhibit liquid-like properties, which have the potential to transition into a solid state, a transition that is accelerated by ALS-causing mutations in FUS (Patel et al., 2015).

Subcellular trafficking and degradation of FUS are modulated through its methylation and phosphorylation, respectively (Perrotti et al., 2000, Du et al., 2011, Dormann et al., 2012, Tradewell et al., 2012, Yamaguchi and Kitajo, 2012).

1.3.2 Regulation of FUS Nucleocytoplasmic Trafficking

The majority of cases of fALS6 are caused by mutations clustered in the C-terminus of FUS, which encodes a non-classical PY nuclear localization sequence (Gal et al., 2011). This finding is consistent with the most obvious effect of these mutations being abnormal cytosolic accumulation of FUS. Nuclear translocation of FUS is mediated through the nuclear import receptor Transportin (importin β) (Dormann et al., 2010) and its nuclear export, mediated by its nuclear export signal, is dependent on the export receptor Crm1 (Kino et al., 2011). The RGG-rich domains are common among hnRNPs and are subject to arginine methylation, which is known to influence their nuclear-cytoplasmic shuttling. (Liu and Dreyfuss, 1995, Nichols et al., 2000, Passos et al., 2006, Tradewell et al., 2012). In general, during RNA polymerase II transcription, the nascent RNA transcript is coated with hnRNPs, which are then methylated and exported from the nucleus (Yu, 2011); however, in some cases, arginine methylation may also act as a signal for nuclear import as is the case for the RNA binding protein Sam68 (Cote et al., 2003). Several groups have shown through mass spectrometry that FUS contains asymmetric dimethylated arginine residues (defined below) (Boisvert et al., 2003, Rappsilber et al., 2003). Recently, we have shown that arginine methylation of FUS RGG domains regulates its nucleocytoplasmic shuttling and inhibition of methylation maintained WT and mutant FUS in the

nucleus of cultured motor neurons (Tradewell et al., 2012). These findings were confirmed by other groups (Du et al., 2011, Dormann et al., 2012, Yamaguchi and Kitajo, 2012, Scaramuzzino et al., 2013) and Dormann *et al.* reported that arginine methylation of FUS modulates its interaction with Transportin (Dormann et al., 2012).

1.3.3 Arginine Methylation

Arginine is a positively charged residue with guanidine nitrogen atoms that are subject to the addition of methyl groups. Arginine methylation is a post-translational modification known to play a role in transcription, RNA trafficking and affect protein-protein/ protein-RNA interactions. This modification is catalyzed by a family of enzymes called Protein Arginine Methyltransferases (PRMTs). All PRMTs catalyze the addition of a single methyl group, using S-adenosylmethionine as a methyl donor, to an arginine nitrogen atom forming monomethylarginine (MMA) (Bedford and Clarke, 2009, Nicholson et al., 2009). Class 1 PRMTs (PRMTs 1, 2, 3, 4, 6 and 8) are capable of adding a second methyl group onto the same nitrogen atom forming asymmetric dimethylarginine (ADMA). Class 2 PRMTs (PRMTs 5, 7, 9) add a second methyl group to the other nitrogen atom forming symmetric dimethylarginine (SDMA). MMA, ADMA and SDMA all have different functional outcomes and can either promote protein-protein or protein-RNA interactions or act to hinder these interactions by invoking steric hindrance upon the modified protein (Bedford and Clarke, 2009, Nicholson et al., 2009). The mechanisms which regulate arginine methylation are not well understood. Arginine-Glycine rich motifs (RGG) are the preferred substrate for most PRMTs; however, isolated arginines outside of RGG motifs can also be methylated. PRMT4 and PRMT5 also show a preference for proline-glycine-methionine (PGM) motifs (Cheng et al., 2007). To date, only one arginine demethylase, JMJD6, has been identified and specifically demethylates arginine 3 of histone 4 (H4R3) (Chang et al., 2007). Cells can potentially regulate arginine methylation by

deimination of the arginine residue by peptidyl arginine deiminases (Bicker and Thompson, 2013). This process converts arginine residues to citrulline, which cannot be methylated by PRMTs.

Our lab and others have shown that the class 1 PRMT, PRMT1, interacts with and methylates FUS and this post-translational modification regulates its nucleocytoplasmic trafficking (Du et al., 2011, Dormann et al., 2012, Tradewell et al., 2012, Yamaguchi and Kitajo, 2012, Scaramuzzino et al., 2013). When carrying out our study, we observed a shift in the distribution of PRMT1 in motor neurons paralleling mutant FUS, i.e., a more cytoplasmic (less nuclear) distribution of PRMT1 in neurons with cytoplasmic retention of FUS. Thus, we hypothesized that cytoplasmic mislocalization of mutant FUS would result in loss of methylation and therefore function of PRMT1's nuclear substrates, contributing to motor neuron dysfunction. To test this hypothesis, we chose to investigate methylation of histone 4 arginine 3 (H4R3) as a major nuclear substrate of PRMT1 regulating transcription. This study is reported in Chapter 4.2.

1.4: Importance of Epigenetics in Neuronal Function

1.4.1 Epigenetics

Cells in the human body display a variety of specialized functions despite having the same genomic DNA sequence. These cell type differences are partly mediated through changes in gene expression during development and involve epigenetic mechanisms which include, but are not limited to, DNA methylation, histone post-translational modification, chromatin remodeling, and RNA processing. The combination of these processes results in a certain transcriptomic profile that governs differentiation, maintenance of cell specialization and adaptation to changes in environment.

1.4.2 Histone Modifications as Regulators of Transcription

Histone proteins form nucleosome core particles that package DNA into a compact structure and can thereby regulate its accessibility. Each assembled nucleosome comprises an octamer containing two copies of each core histone (H2A, H2B, H3 and H4). The flexible N-terminal tails of core histones are susceptible to post-translational modifications that include methylation, acetylation, phosphorylation, ubiquitination, and others (Cheung et al., 2000, Khan and Krishnamurthy, 2005). These modifications can alter interactions between core histone components and thereby influence DNA binding, the higher-order structure of chromatin, transcription factor binding, or access to the transcriptional machinery. Histone modifications can also act in a combinatorial manner, influencing additional post-translational modifications on the same or other histones (Lee et al., 2010). Such combinations of these modifications may serve important regulatory functions to coordinate changes in gene expression at specific loci across the genome in response to different cellular states.

There is strong evidence for alterations in histone modifications playing a role in various neurological disorders. For example, a trinucleotide expansion in the first intron of the frataxin (*FXN*) gene, which causes Friedreich ataxia, is accompanied by hypoacetylation of H3 and H4 in regions close to the repeat expansion leading to a suppression of transcription of the *FXN* gene (Herman et al., 2006, Greene et al., 2007). Furthermore, chromatin immunoprecipitation experiments have revealed hypoacetylation of H3 and H4 along exon 1 of the FMR1 locus encoding the fragile-X mental retardation protein (FMRP) in cells carrying the pathogenic trinucleotide expansion which causes a Fragile-X Syndrome, a common form of mental retardation (Coffee et al., 2002, Eiges et al., 2007, Kumari and Usdin, 2010). There is evidence of altered gene expression in motor neurons of individuals with ALS (Bergeron et al., 1994, Jiang et al., 2005, Campos-Melo et al., 2013); however, it is unclear whether these occur as a

result of transcriptional dysregulation through alterations in histone modifications and the role it might play in motor neuron dysfunction in ALS. There is evidence in alterations of histone modifications in ALS. H3 acetylation and expression of the histone acetylatransferase CREB-binding protein (CBP) were decreased specifically in motor neurons of the SOD1 G85R ALS mouse model (Rouaux et al., 2003). Hypoacetylation of H3 has also been detected in blood leukocytes from ALS patients compared to controls (Cudkowicz et al., 2009). Increased acetylation of H4 was detected in ALS spinal cord homogenates compared to controls but there was no distinction of cell type (Liu et al., 2013). Increases in histone 3 lysine trimethylation have also been detected in blood and brain tissue from ALS patients with C9ORF72 pathogenic expanded repeats compared to controls or individuals with non-pathogenic repeats (Belzil et al., 2013b) and is thought to contribute to reduced C9ORF72 expression.

Histone deacetylase inhibitors have been considered for treatment of neurodegenerative diseases including ALS, specifically valproic acid, which showed no effect on survival and disease progression in ALS patients (Piepers et al., 2009) and sodium phenylbutyrate, which is under phase 2 trial, showed tolerability and increase in H4 acetylation in ALS patient blood leukocytes (Cudkowicz et al., 2009).

During our study characterizing the influence of FUS methylation on its subcellular distribution, we observed nuclear depletion of PRMT1 in neurons expressing mutant FUS. Among its many substrates, PRMT1 catalyzes ADMA of arginine 3 of histone 4 (H4R3), which can facilitate binding of CBP and cofactors to the nucleosome and catalyze lysine acetylation of H4 at positions 5, 8, 12, and 16 and H3 at positions 9 and 14 (Strahl et al., 2001, Wang et al., 2001). These histone acetylation marks are associated with the formation of active chromatin. In contrast, loss of H4R3 ADMA is accompanied by the formation of repressive heterochromatin

(Huang et al., 2005). H4R3 may also be symmetrically methylated by PRMT5 (Zhao et al., 2009). *In situ* analysis of murine developing cortex indicated that SDMA of H4R3 is the predominant form of methylated H4R3 in neural progenitors whereas H4R3 ADMA occurs in later stages of neural development (Chittka, 2010), indicating that this post-translational modification could be particularly important for neuronal development and function.

1.4.3 Importance of Chromatin Remodeling Complexes in Neuronal Function

The neuronal Brg1-associated factor (nBAF) complex is composed of 15 BAF subunits and the DNA-helicase, Brg1. During neuronal differentiation, BAF53a, BAF45a,d and SS18 subunits in neural progenitors are exchanged for BAF53b, BAF 45b,c and CREST respectively (Lessard et al., 2007, Yoo et al., 2009, Staahl et al., 2013). During mitotic exit, neural progenitors express miR-9/9* and miR-124, which repress expression of BAF53a through degradation of its mRNA after binding their corresponding targeting sites (MREs) within the 3'UTR (Yoo et al., 2009). Expression of these miRNAs in fibroblasts converts them into neurons and their inhibition in developing cortical neurons leads to defects in dendritic branching (Yoo et al., 2009, Giusti et al., 2014). Neurons deficient in BAF53b were defective in activity-dependent dendritic outgrowth (Wu et al., 2007) and BAF53b knockout mice exhibited memory loss associated with deficits in synaptic plasticity (Vogel-Ciernia et al., 2013). Knockdown of either BAF45a or BAF53a reduced proliferation of neural progenitor cells, as indicated by reduced BrdU incorporation (Wu et al., 2007). Mutations in BAF subunits are associated with autism spectrum disorders, the most common of which, Coffin-Siris Syndrome associated with microencephaly, has been linked to mutations in BAF250A, BAF250B, Brg1 and BAF47 (Halgren et al., 2012, Neale et al., 2012, Tsurusaki et al., 2012). Though these are developmental disorders, the role of the BAF complex in adult onset neurodegenerative diseases has only recently been revealed. *de novo* mutations in CREST were discovered in ALS trios (individuals

with ALS with unaffected parents) (Chesi et al., 2013). Expression of these variants in primary cortical neurons induced activity-dependent dendritic growth defects (Chesi et al., 2013). This same study showed through co-immunoprecipitation techniques that FUS interacts with CREST and multiple BAF subunits. Concurrent studies in our lab also identified Brg1 as a FUS-interacting partner, prompting us to investigate nBAF complexes in our models of ALS as well as the link to the dendritic attrition characteristic of the disease, given the role of these chromatin remodeling complexes in establishing and maintaining dendrites during development.

Chapter 2: Hypothesis and Rationale

2.1: Rationale

The Durham lab, in collaboration with the lab of Dr. Stéphane Richard, developed a murine dissociated spinal cord culture model of fALS6 in which plasmids encoding WT or ALS-linked mutant FUS are expressed in motor neurons, the cell type most vulnerable in the disease (Tradewell et al., 2012). Unlike motor neurons expressing mutant SOD1, neurons expressing mutant FUS have a comparable viability over the course of the experiment to those expressing WT FUS or control neurons injected with an inert fluorescent marker, although they exhibit morphological changes. Of note, dendrites appear thinner and less branched. As in fALS spinal cord and culture models using cell lines, a higher percentage of motor neurons in our fALS6 primary culture model have diminished nuclear FUS and abnormal accumulation of FUS-positive cytoplasmic inclusions. We demonstrated that FUS interacts with and is methylated by PRMT1 and that methylation of FUS is required for its export to the cytoplasm (Tradewell et al., 2012). During this study, double immunolabelling of neurons expressing FLAG-tagged WT or mutant FUS with anti-FLAG and with anti-PRMT1 revealed nuclear depletion of PRMT1 in neurons with cytoplasmic accumulation of FUS. This depletion of nuclear PRMT1 would be expected to lead to reductions in methylation of nuclear substrates, many of which are transcriptional regulators, such as H4R3, a major nuclear substrate of PRMT1 with downstream consequences to transcription. Thus, changes in the distribution of FUS may not only alter its own functions, but that of its binding partners as well.

Thus, having demonstrated significant consequences to PRMT1 function (see Chapter 4.2), we hypothesized that loss of function of FUS binding partners could contribute to neuronal dysfunction in ALS. In relation to the changes in dendritic morphology observed in neurons expressing mutant FUS, we identified the DNA-helicase SMARCA4 (Brg1) in FUS immunoprecipitates from Vsc4.1 cells (resulting from the fusion ventral spinal cord cells and

neuroblastoma) (Das et al., 2005) indicating that it was a potential FUS-binding partner. Brg1 stood out being a major subunit of the nBAF chromatin remodeling complex that regulates neuronal differentiation and dendritic morphology. At the same time, Chesi *et al.* reported interactions between FUS and members of the nBAF chromatin remodeling complex including CREST and Brg1 (Chesi et al., 2013). In particular, they identified variants in the gene encoding CREST associated with ALS in ALS trios (Chesi et al., 2013). These results suggested that the changes in dendritic morphology observed in neurons expressing mutant FUS could be due to changes in epigenetic programs brought about by dysregulation of the nBAF complex.

2.2: Hypothesis and Specific Aims

Hypothesis:
Cytoplasmic accumulation of FUS leads to loss of function of its binding partners with consequences to transcriptional regulation underlying dendritic architecture.

Specific Aims:

1) To further characterize the fALS6 culture model with particular focus on FUS mislocalization and dendritic attrition.

2) To assess the consequences of PRMT1 mislocalization in fALS6 culture model

3) To explore the consequences of FUS mislocalization on nBAF complex composition and function in relation to dendritic attrition in fALS6 culture model.

4) To determine pathways of toxicity identified in the fALS6 (FUS) culture model are common to models of other types of fALS.

Experimental models: In order to address the hypothesis and specific aims, experiments were performed using a primary murine motor neuron culture model (see Materials and Methods). Motor neurons are the cell type most vulnerable to the disease and display neuronal characteristics such as expression of nBAF subunits and highly branching dendrites which are

evaluated in this thesis. Furthermore, several characteristics of the disease have previously been replicated in other culture models of ALS using this cell type (Durham et al., 1997, Roy et al., 1998, Kabashi et al., 2010, Tradewell et al., 2011, Tradewell et al., 2012).

Chapter 3: Materials and Methods

3.1: Dissociated Spinal Cord-Dorsal Root Ganglion (DRG) Cultures

Dissociated spinal cord-DRG cultures are prepared from embryonic day 13 (E13) CD1 mouse embryos. Spinal cords with attached DRGs are harvested and placed in a 60mm dish containing 1ml of dissecting medium (40g/L Sucrose, 1g/L Dextrose, 2.4g/L HEPES dissolved in 1X Dulbecco's PBS). The tissue is cut into small pieces with a scalpel, followed by addition of 2ml dissecting medium and 300µl of 10X trypsin and incubation at 37ºC for 30 min. The sample is then transferred to plating medium (modified N3 supplemented medium (composition below) with 1% Penicillin/Streptomycin/Neomycin and 1% FBS to neutralize the trypsin) and triturated using a Pasteur pipette to dissociate the cells. Cells are plated in multiwell culture dishes containing 18mm glass coverslips coated with Poly-D-lysine and Matrigel basement membrane matrix (Corning Incorporated, NY, USA). Cell plating density is 375,000/well for 12-well plates and 950,000/well for 6-well plates. Cells are maintained at 37ºC in 5% CO_2 in modified N3 medium (insulin 10µg/ml, apo-transferrin 200µg/ml, BSA 10µg/ml, putrescine 32µg/ml, selenium 26ηg/ml, triiodothyronine 20ηg/ml, hydrocortisone 9.1ηg/ml, progesterone 13ηg/ml) plus 1.5% horse serum. When the cultures reach confluency (day 4-6 post-plating), they are treated with 1.4 µg/ml cytosine-β-D-arabinofuranoside for 3 days to stop mitosis of non-neuronal cells. Cultures are fed twice weekly by replacing half of the medium with antibiotic-free N3 medium.

3.2: Identification of Motor Neurons in culture

Experiments are performed on spinal cord-DRG cultures between 3-8 weeks after dissociation. At this stage motor neurons are distinguishable from other neuronal cell types and can be morphologically identified (Roy et al., 1998). Motor neurons have much larger cell bodies (>20µm) and highly-branching dendrites. These neurons also express choline acetyltransferase , glutamate receptors and the characteristic neurofilament network (Durham, 1992).

3.3: Gene Transfer by Intranuclear Microinjection

Motor neurons in long term culture are not transfectable using lipophilic agents; hence microinjection is used to introduce plasmid DNA directly into the nucleus (Durham et al., 1997). Although viral vectors can be used for gene transfer, microinjection presents certain advantages in our culture model such as very high efficiency of gene transfer (over 90%) and high flexibility to co-express multiple plasmids. Injectate is prepared by diluting plasmid DNA in a solution of 20mg/ml 70kDa Dextran in 50% Tris-EDTA (TE). In cases where injection markers are necessary 70kDa dextran conjugated to fluorescent isothiocyanate (FITC; Invitrogen Life Technologies, Burlington,ON) is used in the injectate. The injectate is then clarified by centrifugation at 15,000xg for 15 min (Eppendorf 5804). To prepare the injection needle, 3 inch, 1 mm diameter quick fill glass capillaries (World Precision Instruments, Sarasota, FL) are pulled to a fine tip using a Narishige PN-3 microelectrode puller (Narishige International INC., NY, USA). Prior to microinjection, coverslips are placed in a dish containing warm Eagle's Minimum Essential Medium (EMEM; Invitrogen Life Technologies) lacking bicarbonate, supplemented with 5g/L glucose, and pH adjusted to 7.4 (injection buffer). The dish is placed on the stage of a Zeiss Axiovert 35 microscope (Carl Zeiss Microscopy, LLC, USA) and microinjection is accomplished at 400X magnification using an Eppendorf 5246 (or Femtojet transjector) and an Eppendorf 5171 micromanipulator (Eppendorf, Hamburg, Germany). After injection, the coverslips are placed in a solution of 0.75% Gentamicin in culture medium to prevent bacterial growth and cultures are incubated at 37^{o}C in 4% CO_2 until the cells are analyzed for the experiment. Cells are analyzed a minimum of 16 hrs post-injection to ensure that no motor neurons that are lethally damaged by the microinjection procedure are included in the experiment.

3.4: Expression Plasmids

Expression plasmids encoding Flag-tagged WT and mutant FUS were produced by the Richard lab (McGill University, Lady Davis Institute) by amplifying human FUS cDNA using the following forward and reverse primers:

Forward: 5^1-GGC AAG CTT CCA CCA TGG ATT ACA AGG ATG ACG ACG ATA AGG CCT CAA ACG ATT ATA CCC AAC-3^1

Reverse: 5^1-GGC CTC GAG TTA ATA CGG CCT CTC CCT GCG ATC C-3^1 (FUS^{WT}), 5^1-GGC CTC GAG TTA ATA CGG CCT CTC CCT GCC ATC CTG TCT GTG C-3^1 (FUS^{R521G}), or 5^1-GGC CTC GAG TTA ATA CGG CCT CTC CCT GTG ATC CTG TCT GTG C-3^1 (FUS^{R521H}).

DNA fragments were then digested using HindIII and XhoI restriction enzymes and inserted in pcDNA3.1 vector. For microinjection, FUS-FLAG pcDNA3.0 plasmids were diluted in injectate at 20ηg/μl. eGFP-tagged WT and R521H FUS encoding plasmids were generated by digesting the plasmids described above with HindIII and XhoI restriction enzymes and inserting FUS encoding transcripts into the HindIII and SalI compatible site of the peGFPC1 (Clonetech) vector. peGFPC1-FUS plasmids were injected at 20ηg/μl.

TDP43 plasmids were generated by the Rouleau lab and used in our previous collaborative study (Kabashi et al., 2010).

In order to overexpress Brg1 or disrupt its function, pBJ5-Brg1 and pBJ5-Brg1 DN plasmids, a gift from Jerry Crabtree (Addgene #17873 and #17874) were injected at 20ng/μl. Brg1 and scramble shRNA expressing plasmids (pSuper-Brg1 and pSuper-scramble) were a kind gift from Dr. Betty Moran (Rutgers University, New Jersey) and were injected at 30ng/μl.

To assess how mutant or WT human FUS affects protein expression through effects on mRNA transcripts, 3'UTR reporter expression plasmids for the mRNA of interest were created

by inserting double stranded DNA fragments (G-blocks, IDT) into BglII and EcoR1 sites of the dsRed-sensor vector (a kind gift from Lynn Hudson, Addgene # 22743), downstream of the dsRed coding sequence and injected at 5ng/µl for Scramble 1, Scramble 2 and Brg1 3'UTR and 1ng/µl for BAF53a 3'UTR.

3.5: Immunocytochemistry and Immunohistochemistry

Cultured cells were fixed in 3% paraformaldehyde (PFA) in PBS for 10 min, permeabilized in 0.5% NP-40 for 1 min and fixed once more for 2 min. Cells were then blocked in 5% horse serum in PBS for 30 min. Incubations in primary and secondary antibodies were for 30 min, followed by 3 X 5 min washes in PBS. Coverslips were mounted on microscope slides using DAKO mounting medium (Agilent Technologies).

FUS^{WT} and FUS^{R495X} transgenic mice and non-transgenic littermates (in collaboration with L. Hayward, U. Massachusetts Medical School, Worchester, MA) were perfused with 4% PFA in PBS for 30 min. Samples of brain and spinal cord were stored in 4% PFA at 4ºC. Immunolabelling was carried out on 4 µm sections from paraffin blocks. Antigen retrieval was performed by boiling tissues for 10 min with BD Retrievagen A pH 6.0 (Cat#550524). Tissue sections were incubated with primary antibody overnight at 4^{o}C followed by incubation in AlexaFluor-conjugated secondary antibody, then mounted in Prolong gold antifade reagent with DAPI (Life Technologies).

For human spinal cord, and mice used for the post-mortem interval study, tissues were fixed in 10% neutral buffered formalin, embedded in paraffin and cut in 4 µm sections. As postmortem changes can affect the ability to detect proteins by immunohistochemistry, a study to mimic postmortem interval was carried out in mice to validate the efficacy of antibodies. Adult C57Bl6 (approximately 12 months old) were euthanized by ketamine/xylazine intraperitoneal

injection. Tissues were either perfusion-fixed in place with 4% PFA or immersion-fixed after excision in 10% neutral buffered formalin immediately or with post-mortem interval. Antigen retrieval in human and mouse tissue sections was performed by boiling in sodium citrate buffer. Tissues were blocked in 5% BSA + 0.03% TritonX-100 in PBS for 1 hr at RT. Samples were then incubated with primary antibody overnight at 4ºC followed by biotinylated secondary antibody. Labelling was visualized using Vectastain Elite ABC kit (PK-6100, Vector Laboratories) using diaminobenzidine as substrate and ImmPACT DAB peroxidase substrate kit (SK-4105, Vector Laboratories).

3.6: Imaging

Images were viewed using a Zeiss Observer Z1 microscope (Carl Zeiss Microscopy) equipped with a Hamamatsu ORCA-ER cooled CD camera (Hamamatsu, Japan). Filter sets 02, 13 and 00 were used for epifluorescence microscopy (Carl Zeiss Microscopy). Images were acquired and analyzed with Zeiss Axiovision software.

Long term time-lapse imaging of FUS inclusion formation was carried out in an Olympus VivaView incubator microscope (Olympus, ON, Canada). Neurons were injected with eGFP-FUS^{R521H} expression plasmid and were imaged every 15 min from days 4-6 post-injection.

3.7: Analysis of Histone Post-translational Modifications

Histones were extracted from spinal cord-DRG cultures according to a modified protocol (Shechter et al., 2007). All reagents were pre-chilled on ice. Cells were washed in PBS, harvested into microfuge tubes and pelleted by centrifugation at 2800xg. To obtain nuclear and cytoplasmic fractions, the pellets were pipetted vigorously in 0.1% NP40 in PBS, then nuclei were pelleted by centrifugation at 2800xg. Nuclear pellets were dissolved in 0.4 N HCl and incubated on ice for 1.5 hrs. Acid-insoluble proteins were precipitated by centrifugation at 15,000xg. The supernatant was collected and histones were precipitated by addition of

trichloroacetic acid to a final concentration of 30% and incubated on ice for 1.5 hrs. Proteins were pelleted at 16,000xg for 10 min and pellets were washed twice with ice-cold acetone. After air drying, pellets were dissolved in Laemmli buffer. Samples were separated by 15% SDS-PAGE and transferred to nitrocellulose membrane. Consistent loading of histone proteins was verified by Coomassie-staining of sister gels. Nitrocellulose membranes were blocked in 5% skim milk in Tris-buffered saline (TBS) and probed with primary antibody against acetylated histone 3 K9/14 and asymmetrically dimethylated histone 4 R3) and horseradish peroxidase (HRP)-conjugated secondary antibodies in 5% skim milk in TBS with 3 X 15 min washes with TBST. Optical density of bands was performed using NIH Image J software. For AMI-1 (7,7′-Carbonylbis(azanediyl)bis(4-hydroxynaphthalene-2-sulfonic acid) treatments, levels of histone 3 acetylation in samples from treated cultures were normalized to untreated control indicated by Western blot, and normalized once more to amount loaded compared to control indicated by Coomassie staining.

For measurement of histone modifications *in situ*, immunofluorescence was performed using H3K9/K14Ac or H4R3me and the mean fluorescence pixel intensity from both antibodies was measured by tracing the area of the nucleus using the outline spline function and the mean fluorescence intensity of the region of interest was recorded using the Zeiss Axiovision software.

3.8: Measuring Transcriptional Activity by Bromouridine (BrU) Incorporation

Cultures were incubated in 5 mM BrU in culture medium for 2 hrs at 37^{o}C. Cells were incubated in 3% PFA in PBS for 15 min at 37^{o}C and incorporation was detected by immunocytochemistry with anti-BrdU antibody (this antibody also labels BrU).

3.9: Analysis of Dendritic Morphology

Motor neurons were injected with mCherry-encoding vector to visualize entire cell morphology and images were taken at 100X (Axiovert, Carl Zeiss). Images were exported to 8-bit .tif images and the cell body and dendrites were traced using the semi-automated ImageJ tracing plugin, NeuronJ (http://www.imagescience.org/meijering/software/neuronj/). Branching points were designated using NeuronStudio (CNIC, Mount Sinai School of Medicine) and measurements of dendritic morphology were performed with Bonfire (Bonnie Firestein, Rutgers University) using the resulting .swc file.

3.10: Antibodies and Reagents

Antibodies used for this study were: Mouse Anti-FLAG M2 (Sigma F1804, 1:400), rabbit anti-FLAG (Sigma F2555, 1:50), mouse anti-FUS (Santa-Cruz sc-47711, 1:200), rabbit anti-FUS (Proteintech 11570-1-AP, 1:400), rabbit anti-PRMT1 (Abcam ab73246, 1:400), mouse anti-synaptophysin (Santa-Cruz sc-12737, 1:400), rabbit antibody to asymmetrically dimethylated H4R3 (Active Motif 39705, 1:400 ICC, 1:500 WB), rabbit anti-acetylated H3K9/K14 (Cell Signaling 9677, 1:400 ICC, 1:1000 WB), mouse anti-MAP2 (Novus Biologicals NBP1-92711, 1:400), mouse anti-BrdU (Sigma SAB4700630), rabbit anti-Brg1 (Proteintech 21634-1-AP, 1:600), rabbit anti-BAF53b (Abcam ab140642, 1:400), rabbit anti-CREST (Proteintech 12439-1-AP, 1:800), anti-mouse Cy2 (Rockland, 610-711-124,1:300); Cy3 (Jackson, 715-165-150, 1:300), anti-rabbit Cy2; Cy3 (Jackson, 711-225-152; 711-165-152, 1:300), anti-rabbit HRP (Jackson, 111-035-045, 1:2500), AMI-1 (Santa Cruz sc-205928), 5-Bromouridine (Sigma 851087), TUNEL assay (Promega G3250), PFI-3 (Cayman Chemical Co., 15267).

Chapter 4: Results

4.1: Characterization of fALS6 culture model

4.1.1 Characterization of fALS6 model

In our previous study, we established a primary culture model of fALS6 by expressing mutant or WT human FUS in motor neurons of dissociated murine spinal cord cultures by intranuclear microinjection of plasmid expression vectors (Tradewell et al., 2012). Motor neurons overexpressing mutant human FUS (R521 mutations), and to a lesser extent FUS^{WT}, presented with granular cytoplasmic inclusions within 3 days (Fig. 1B, C), the preponderance of which co-localized with the RNA-marker SYTO RNA Select (Tradewell et al., 2012). Over a longer time course mutant FUS formed filamentous and skein-like inclusions which developed 6-7 days post-injection, reminiscent of the neuronal cytoplasmic inclusions observed in ALS spinal cord (Fig. 1F, G). Dendrites with skein-like inclusions also appeared atrophic (Fig. 1D, E).

In order to observe the kinetics of FUS inclusion formation, live cell imaging of neurons expressing eGFP-tagged mutant FUS, using an Olympus VivaView incubator microscope, confirmed that large globular and filamentous inclusions formed as a result of growth and fusion of smaller aggregates. Time-lapse imaging of neurons expressing eGFP-FUS^{R521H}, or eGFP-FUS^{WT}, carried out between days 4-7 post-injection showed diffuse accumulation of FUS within the cytoplasm followed by a sudden coalescence into small granules throughout the neuron (see Tibshirani et al., 2015). These inclusions were transported anterogradely and retrogradely in dendrites, fused, and in some neurons lined up and fused into linear inclusions in dendrites parallel to the cytoskeleton. In some motor neurons, ring-like FUS-positive inclusions were observed mainly in the perikarya (Fig. 1F). Consistent with previous studies, inclusions were apparent when either mutant or WT FUS accumulated in the cytoplasm, modeling inclusions that occur in fALS6 and sALS.

In contrast to human FUS^{WT}, the FUS^{R521H} and FUS^{P525L} mutants, the truncation mutant FUS^{495X} rarely formed inclusions when over-expressed in motor neurons, but did accumulate in the cytoplasm (not shown).

To determine if endogenous mouse FUS co-distributed with ectopically expressed human FUS, FLAG-FUS^{R521H} was expressed in motor neurons and cultures were co-labelled with anti-FLAG and anti-FUS (antibody 11570-1-AP) to visualize both human FUS and total FUS in the same neurons. When ectopic human FUS was completely cytoplasmic, we observed no nuclear signal from the anti-FUS antibody (Fig. 1H-K), confirmed by a scan of fluorescence intensity through a plane of the cell including the nucleus showing similar patterns of fluorescence between the two antibodies (Fig. 1L). These observations suggest that endogenous FUS was also depleted from the nucleus with ectopically expressed human FUS.

4.1.2 Evaluation of mFUS toxicity in motor neurons

In neurons over-expressing human FUS in which FUS was exclusively cytoplasmic, Hoechst staining was highly condensed (see Fig. 1, 2, 3, 4); however, unlike the fALS1, neurons expressing mutant FUS were negative for TUNEL staining at three days post-injection (Fig. 1M), indicating that apoptosis does not occur in these neurons within the time frame of the experiment. Furthermore, neurons expressing mutant FUS had a comparable viability curve to WT FUS expressing neurons or injection controls (Tradewell unpublished data).

A common feature of ALS is dendritic atrophy and in motor neurons (Nakano and Hirano, 1987, Karpati et al., 1988, Takeda et al., 2014). In FUS R521C transgenic mice, dendritic attrition in spinal motor neurons was evident (Qiu et al., 2014). Similar dendritic attrition were observed in the FUS R521G transgenic mouse (Sephton et al., 2014) and in our primary motor neuron culture model of fALS6. We compared dendritic morphology in cultured motor neurons expressing WT or mutant FUS along with mCherry to visualize cell morphology.

Neurons were imaged on day 3 post-injection for Sholl analysis as described by Kutzing *et al.* (see Materials and Methods). Indeed, there was a significant decrease in dendritic complexity in neurons expressing mutant FUS compared to WT or empty vector indicated by Sholl analysis (Fig. 1N). Dendritic branching was further categorized according to Root, Intermediate and Terminal branches. These Sholl curves indicate that the attrition observed in mutant FUS-expressing neurons was at the level of intermediate and terminal branches, not root branches or primary branches (Fig. 1O). There were also significant decreases in the number of both terminal and branch points, in the average number of processes per neuron and in total cable length in neurons expressing mutant FUS, a measure of total dendritic output (Fig. 1P).

4.2: Consequences of PRMT1 mislocalization in the fALS6 culture model

4.2.1 Nuclear depletion of PRMT1 in neurons with cytoplasmic FUS

ADMA of FUS by PRMT1 regulates its subcellular localization and inhibition of PRMT1 activity retains WT or mutant FUS in the nucleus. Having noted redistribution of PRMT1 with FUS in motor neurons in those experiments (see Rationale; Chapter 2.1), their co-distribution was evaluated quantitatively in the present study by double-label immunocytochemistry with anti-PRMT1 and anti-FLAG in neurons microinjected with constructs encoding FLAG-tagged WT or mutant (R521H, P525L, R495X) human FUS. The normal distribution of the endogenous murine proteins was evaluated in uninjected neurons. FUS and PRMT1 distribution was classified as either essentially nuclear, exclusively cytoplasmic or distributed between both compartments, as illustrated in Supplementary Figure S1A. The microinjection procedure had no effect on distribution of PRMT1 (Supplementary Figure S1B). The nuclear/cytoplasmic distribution of PRMT1 was congruent not only with endogenous FUS in control cultures, but with ectopically expressed WT or mutant human FUS. Expression of human WT or ALS-linked mutants significantly shifted PRMT1 distribution to either mostly nuclear in neurons expressing FUS^{WT}, or mostly cytoplasmic in neurons expressing mutant FUS (Fig. 2A-C). The greater redistribution of FUS and PRMT1 to the cytoplasm in neurons expressing FUS^{P525L} was consistent with the juvenile onset and rapid disease progression in patients with this mutation relative to the milder phenotype of R521 mutations. Although there was a significant shift in FUS/PRMT1 to the cytoplasm in neurons expressing FUS^{R495X}, the concordance of their distribution was not as high as with other mutants. In no neurons was FUS^{R495X} exclusively nuclear, yet 29% had exclusively nuclear PRMT1. Despite missing the C-terminus containing a nuclear localization sequence, this mutant was capable of entering the nucleus, as 17% of

neurons had both nuclear and cytoplasmic protein labelled by anti-FLAG, in agreement with Bosco et al. (2010).

PRMT1 was not recruited to FUS inclusions. Even when PRMT1 was depleted from nuclei along with FUS, it was not detected in granular FUS inclusions of WT or mutant human FUS on day 3 post-injection nor in vermiform or skein-like inclusions on day 6 post-injection, indicating that PRMT1 does not maintain association with aggregated FUS (Fig. 2D,E).

A major function of FUS is transport of specific mRNAs to dendritic spines. Presence of FUS at synapses has been demonstrated in cultured hippocampal neurons and human and mouse brain. Similarly, double-label of spinal cord cultures with antibodies to FUS (11570-1-AP) and synaptophysin revealed endogenous FUS at dendritic spines of motor neurons (Fig. 2F), while PRMT1 was not (Fig. 2G).

To further examine the co-distribution of PRMT1 with endogenous FUS, cultures at two stages of development were double-labelled with anti-FUS and anti-PRMT1: at 2 weeks *in vitro* when FUS is almost exclusively nuclear, and at 4 weeks when motor neurons have developed dendritic spines and a greater proportion of motor neurons contain cytoplasmic FUS at a point in time. Distribution of FUS and PRMT1 was categorized as in Supplementary Figure 1A ; *i.e.*, nuclear, exclusively cytoplasmic or distributed between both compartments. As in Fig. 2A, the distribution of PRMT1 paralleled FUS in both 2 and 4 week old cultures, both being more cytoplasmic at 4 weeks *in vitro* compared to 2 weeks (Fig. 2H).

Endogenous FUS can also accumulate in the cytoplasm under specific cellular stress, notably sorbitol-induced hyperosmotic stress (Sama et al., 2013). To determine if PRMT1 also would redistribute with cytoplasmic FUS with added stress, cultures were treated with 0.4M sorbitol for 2 hrs and subsequently double-labelled with anti-FUS and anti-PRMT1. Treatment

with sorbitol did indeed significantly shift both FUS and PRMT1 from the nucleus to the cytoplasm (Fig. 2I).

In summary, PRMT1 distributed with FUS in motor neurons under both physiological conditions and under conditions of stress that result in cytoplasmic accumulation/nuclear depletion of FUS, including osmotic stress and expression of ALS-causing FUS mutants.

4.2.2 Nuclear depletion of PRMT1 reduces asymmetric arginine dimethylation of histone 4

Next we tested the hypothesis that depletion of PRMT1 from the nucleus in neurons with mislocalized FUS would result in hypomethylation of PRMT1's nuclear substrates, using H4R3 as a representative substrate. PRMT1 is the major methyltransferase catalyzing asymmetric dimethylation of H4R3, a key regulator of transcription. The milder R521H mutant was used in these experiments in order to evaluate neurons with nuclear, cytoplasmic or combined nuclear/cytoplasmic distribution of FUS, the severe mutants being almost exclusively cytoplasmic. Methylation of H4R3 was evaluated by indirect immunocytochemistry with an antibody specifically recognizing asymmetrically methylated H4R3 (H4R3Me2) (Fig. 3A) and quantified as pixel intensity of epifluorescence in motor neuron nuclei (Fig. 3B). This antibody recognizes asymmetrically, but not symmetrically methylated H4R3 (Sun et al., 2011a). H4R3 ADMA was significantly decreased in motor neurons with predominantly cytoplasmic WT or R521H FLAG-FUS compared to neurons with nuclear FUS, 3 days after plasmid injection (Fig. 3B).

Decrease in H4R3 methylation has been associated with the formation of repressive heterochromatin. Interestingly, chromatin was not as condensed in neurons of control cultures that exhibited both nuclear depletion of endogenous FUS and PRMT1 (Supplementary Figure S1A). Thus, the severe chromatin condensation is not an obligate consequence of cytosolic accumulation of FUS, particularly under physiological conditions.

4.2.3 H3K9/K14 Acetylation is decreased in motor neurons with cytoplasmic FUS

Acetylation of lysine residues of histones is a well characterized post-translational modification, which plays a role in transcription by weakening the association between positively charged lysine residues and negatively charged DNA; this results in loosened organization of chromatin, allowing access to transcriptional machinery (Marks and Xu, 2009). Furthermore, histone modifications can act in a combinatorial manner, for example, H4R3 ADMA by PRMT1 results in H4 and H3 acetylation (Wang et al., 2001). We hypothesized that decreased H4R3 ADMA associated with redistribution of FUS and PRMT1 to the cytoplasm would result in decreased H3 acetylation at lysine residues 9 and 14 (H3K9/K14). Acetylation of these residues was detected using antibody recognizing only the acetylated form and quantified as pixel density of epifluorescence of antibody labelling 3 days following microinjection of motor neurons with constructs encoding WT or R521H FLAG-FUS. H3 acetylation was significantly decreased when FUS was cytoplasmic (either WT or R521H) compared to when FUS was nuclear (Fig. 4A,B).

Similar changes in histone marks were observed in spinal cord cultures treated with the PRMT inhibitor AMI-1, which preferentially, although not exclusively, inhibits PRMT1 (Cheng et al., 2004). Histones were extracted via acid-solubilization (see Chapter 3.7) from control cultures and cultures treated with 20 μM AMI-1 for 24, 48 and 72 hrs. Western blots of purified histones were probed with antibodies to asymmetrically dimethylated H4R3 and acetylated H3K9/K14. H3K9/K14 acetylation was significantly reduced in cultures treated with AMI-1 for 24 hrs compared to untreated cultures (Fig. 4C). This decreased H3K9/K14 acetylation was not maintained in cultures treated longer than 24 hrs, suggesting desensitization to the compound's effect. Decreases in both H4R3me and H3K9/K14Ac were confirmed *in situ* by comparing

fluorescence intensity of antibody labelling in nuclei of neurons treated with AMI-1 and control (Fig. 4D).

We confirmed that decreased H3K9/K14 acetylation was downstream of decreased H4R3 methylation. Inhibiting histone deacetylase (HDAC) activity prevented the decrease in H3K9/K14 acetylation associated with loss of nuclear FUS/PRMT1, but not the decrease in H4R3 ADMA. Cultures were treated with 7.5 μM Vorinostat (SAHA) or vehicle for 48 hrs, beginning 24 hrs post-injection of motor neurons with FLAG-FUS^{R521H} construct. In neurons with depletion of nuclear FUS, H4R3 ADMA was decreased (Fig. 4F), but H3K9/K14 acetylation was maintained and even increased in cultures treated with SAHA (Fig. 4E).

4.2.4 Transcriptional activity is decreased in neurons with cytoplasmic FUS

Such reductions in histone ADMA and acetylation would be expected to have consequences on the transcriptional activity of the cell. Because of the wide-ranging effects of FUS on gene transcription and RNA splicing, overall transcriptional activity was assessed in neurons with nuclear or cytoplasmic FUS/PRMT1 by employing a 5-bromouridine (BrU) incorporation assay to detect newly synthesized RNA. Indeed, BrU incorporation within the nucleus, measured as intensity of anti-BrdU immunolabelling, was significantly less in neurons with cytoplasmic endogenous FUS, compared to neurons with predominantly nuclear FUS (Fig. 5A). Inhibiting PRMT activity with AMI-1 also reduced BrU incorporation, even in neurons with nuclear FUS (Fig. 5B), indicating that loss of PRMT1 function did indeed contribute to the decrease in transcription with loss of nuclear FUS.

Unfortunately, the BrU assay was not meaningful in neurons over-expressing human FUS from plasmid DNA because of high background resulting from transcription of FUS from the

plasmid CMV promoter. However, these data do demonstrate the importance of FUS localization in transcriptional regulation under normal conditions through its effect on PRMT1 function.

Decreases in transcriptional activity would be expected to lead to consequences to neuronal physiology, notably dendritic and synaptic maintenance which requires the continued delivery of translationally repressed mRNAs to be translated locally. We thus hypothesized that maintenance of H3K9/K14Ac would maintain transcriptional activity and prevent mutant FUS induced dendritic attrition. Neurons expressing mutant FUS were treated with the HDAC inhibitor SAHA for three days. Treatment with SAHA prevented both the decrease in H3K9/K14Ac (Fig. 4E) and dendritic attrition in neurons expressing mutant FUS as indicated by Sholl analysis. Notably, treatment of control neurons injected with pcDNA3-empty vector with SAHA did not significantly increase dendritic branching compared to vehicle treated neurons (Fig. 6).

4.2.5 Coincident distribution of PRMT1 with WT or mutant FUS in murine spinal motor neurons *in situ*

PRMT1 distribution also was evaluated in a transgenic mouse model in collaboration with the Hayward lab (University of Massachusetts Medical School) (Fig. 6). Mice harboring WT or R495X human FUS transgenes were established by cloning cDNAs into MoPrP.Xho (ATCC #JHU-2) containing the promoter, 5'-intronic and 3'-untranslated sequences of the murine prion protein (PrP) gene (Lawrence Hayward, personal communication). R495X lines, including the line PX78 used in this study had 11-15 transgene copies and 3-5 fold FUS overexpression. While mice from the mutant FUS transgenic lines display no obvious weakness, abnormalities were detected by electromyography (EMG), including fibrillation potentials, muscle denervation and reduction in motor unit number estimation (MUNE) at 8-12 months. These abnormalities did not occur in mice from lines expressing nuclear human FUS^{WT} (lines

PWT17 or PWT52, limited to 3 transgene copies, <2-fold FUS overexpression). Non-transgenic littermates served as controls.

The distribution of FUS and PRMT1 assessed by double-label immunocytochemistry is shown in Fig. 7. Human FUS^{WT} (Fig. 7D) was mostly nuclear, similar to endogenous FUS in non-transgenic littermates (Fig. 7A). A higher burden of cytoplasmic FUS^{R495X} was observed in the perikarya of motor neurons in the anterior horn of the spinal cord (Fig. 7G, J), indicating a shift in the equilibrium of the mutant toward the cytoplasm in addition to its presence in the nucleus. Most neurons had a mixture of nuclear and cytoplasmic labelling, but the amount of cytoplasmic mutant FUS was variable as can be seen by comparing Fig. 7G and Fig. 7J. No inclusions were identified by FUS immunohistochemistry (or by ubiquitin or p62 inclusion markers; data not shown). Like FUS, PRMT1 was predominantly nuclear in cross-sections of spinal cord from non-transgenic (Fig. 7B) and FUS^{WT} transgenic (Fig. 7E) mice, but cytoplasmic labelling was detected in neurons in sections from FUS^{R495X} mice (Fig. 7H and K) in amounts relative to FUS.

4.2.6 Post-mortem interval affects subcellular distribution of PRMT1

Cytoplasmic FUS inclusions have also been observed in spinal motor neurons in sporadic ALS. However, in control experiments using archived autopsied spinal cord tissue from three individuals dying of non-neurological causes (collaboration with the Strong lab, Western University), we noticed that rather than the predominantly nuclear anti-PRMT1 labelling expected in motor neurons, labelling was mostly cytoplasmic (Fig. 8A). Thus, we investigated the possibility that PRMT1 is lost from nuclei postmortem. This hypothesis was investigated in mice by fixing lumbar spinal cord immediately following euthanasia or after a postmortem interval of 6 hrs, considered to be a short postmortem interval for processing of human autopsy tissue. Cross-sections of spinal cord immunolabelled with antibody to PRMT1 or FUS are

illustrated in Fig. 8B. PRMT1 was depleted from the nucleus of motor neurons as early as 6 hrs postmortem, despite persistence of nuclear FUS. Even following immediate immersion in formalin fixative, preservation of PRMT1 distribution was variable compared to perfusion fixation (as in Fig. 7) or cryopreservation (data not shown). Thus, PRMT1 is labile postmortem, obviating reliable studies with archived human autopsy specimens.

4.3: Exploring other mechanisms of dendritic attrition in fALS6 model

4.3.1 Nuclear Depletion of Brg1 with cytoplasmic accumulation of FUS

Having identified altered function of the FUS-interacting partner PRMT1, we looked for other important FUS-interactors whose function could also be perturbed as a result of FUS cytoplasmic accumulation. In a list of FUS-interactors identified by mass spectrometry of anti-FUS immunoprecipitate from Vsc4.1 cells (see Hypothesis and Rationale) we identified Brg1 as an interacting partner of FUS. An observation also made by Chesi *et al.* (Chesi et al., 2013).

To determine whether Brg1 nuclear depletion occurs due to cytoplasmic accumulation of FUS, motor neurons were microinjected with plasmids encoding either WT or mutant FUS bearing ALS-causing mutations. Indeed, cytoplasmic distribution of WT or mutant FUS was sufficient to induce a significant nuclear depletion of Brg1 in motor neurons (Fig. 9A) as indicated by average fluorescence intensity of Brg1 antibody labelling in the nucleus (Fig. 9B). Unlike PRMT1, Brg1 did not redistribute with FUS to the cytoplasm, but rather its expression seemed reduced in neurons with cytoplasmic FUS (Fig. 9A).

4.3.2 Brg1 function is required for maintenance of dendritic morphology

Brg1 is the main ATP-dependent DNA helicase responsible for unwinding chromatin to allow access for transcriptional machinery and is thus essential for nBAF complex function. In order to determine whether Brg1 is required for maintenance of dendritic morphology in motor

neurons, we examined the dendritic architecture in neurons in which Brg1 function was prevented either through genetic manipulation or pharmacological inhibition (Fig. 9C). Neurons, expressing either shRNA specific for Brg1 or a dominant-negative mutant of Brg1 (K798R) showed significant dendritic attrition compared to control neurons (Fig. 9E,F). In addition, treatment of cultures with PFI-3, an inhibitor targeting Brg1 and its homologous partner Brm (Cayman Chemical 15267), for 72 hrs did not deplete nuclear Brg1 (data not shown), but did significantly reduce dendritic branching in a dose-dependent manner (Fig. 9D,G). These data suggest that Brg1 activity is required to maintain dendritic branching in motor neurons and that the dendritic attrition observed in neurons expressing mutant FUS is caused by nuclear depletion of Brg1 leading a loss of Brg1 function.

4.3.3 Overexpression of Brg1 prevents dendritic attrition caused by mutant FUS

We hypothesized that reintroduction of Brg1 in motor neurons expressing either mutant FUS or TDP43 would maintain the dendritic architecture in these neurons. Double immunolabel of Brg1 and FLAG in neurons expressing R521G FUS with or without overexpression of human Brg1 indicated that overexpression of Brg1 was sufficient to maintain Brg1 in the nucleus despite cytoplasmic accumulation of FUS (data not shown). Dendrite morphology was quantified by Sholl analysis in neurons expressing R521G FUS either alone or coexpressed with human Brg1 for 72 hrs. Indeed, co-expression of Brg1 with mutant FUS completely prevented the dendritic attrition (Fig. 10A), the Sholl curve being similar to neurons expressing mCherry alone (Fig. 10B). The number of branch and terminal points as well as total cable length were also significantly higher in this condition compared to when the mutant was expressed alone (Fig. 10B). Thus, restoring expression of Brg1 is sufficient to preserve dendrite morphology in neurons expressing mutant FUS. The data support that restoring Brg1 function in the presence of mutant FUS is sufficient in preventing dendritic attrition.

4.3.4 Post-transcriptional regulation of Brg1 protein levels in neurons with cytoplasmic FUS

Absence of Brg1 protein could result from various mechanisms ranging from altered transcription to accelerated protein degradation. Our experiments involving Brg1 co-overexpression indicated that plasmid-derived Brg1 is stably maintained in the nucleus despite the presence of cytoplasmic FUS. Three possibilities could contribute to this difference: 1) plasmid-derived Brg1 transcription is under control of the constitutive promoter CMV, 2) Defects in splicing of endogenous Brg1 RNA would not occur with RNA derived from the Brg1cDNA, and finally 3) negative regulation of endogenous Brg1 is mediated through its 3'UTR, which is not present on plasmid-derived Brg1 transcripts.

This last possibility was the easiest to test in our culture model using a dsRed reporter plasmid with the Brg1 3'UTR downstream of the coding sequence. If Brg1 protein levels are being negatively affected through its 3'UTR when FUS accumulates in the cytoplasm, then decreased dsRed fluorescence in neurons expressing mutant FUS would be expected. Neurons were injected with either WT or P525L FUS plus dsRed-Brg1 3'UTR plasmids and the amount of dsRed expression was measured as fluorescence intensity. At two days post-injection, little to no dsRed was detected in neurons expressing mutant FUS compared to easily visualized dsRed epifluorescence in neurons expressing WT FUS (Fig. 11B,C). This difference in dsRed expression was not detected with expression of dsRed with scramble 3'UTR sequence, indicating the suppression of dsRed expression by mutant FUS was mediated through the Brg1 3'UTR. dsRed expression is a measure of protein expression; thus, though the reduced expression of Brg1 in the presence of mutant FUS could be mediated through its 3'UTR, we cannot determine whether this effect is mediated through decreased mRNA stability or protein translation.

4.3.5 Status of other nBAF subunits with cytoplasmic accumulation of FUS

We next sought to determine whether other subunits of the nBAF complex were dysregulated in addition to Brg1. We assessed the expression of BAF53b and CREST, both of which are necessary for neuronal differentiation and have been shown to be involved in activity-dependent dendritic outgrowth (Wu et al., 2007, Staahl et al., 2013). In the culture model, fluorescence intensity measurements of nuclear antibody labelling indicated a significant decrease in BAF53b expression with nuclear depletion/cytoplasmic accumulation of either WT or mutant FUS (Fig. 12A,B). Depletion of BAF53b also occurred in motor neurons of ALS autopsy specimens (see below Chapter 4.3.6).

Expression of BAF53b is suppressed by BAF53a, the protein present in neural progenitor BAF complexes; thus, an interesting possibility for loss of BAF53b expression would be re-expression of BAF53a as a result of de-repression of its mRNA through regulation of its 3'UTR. To address this possibility, a BAF53a 3'UTR dsRed reporter plasmid was constructed (as described for the Brg1 3'UTR above) and was coexpressed with WT or mutant (P525L) FUS. Indeed, dsRed expression was high in neurons expressing mutant cytoplasmic FUS, but not in neurons expressing WT FUS (Fig. 12C), indicating de-repression of BAF53a expression.

We also evaluated the presence of the CREST subunit, which is also important for nBAF function, is upregulated during neuronal differentiation, and has been shown to be mutated in certain cases of ALS (Chesi et al., 2013). Indeed, CREST was depleted from the nucleus of neurons with cytoplasmic FUS in the culture model (Fig. 12A,B) and in motor neurons of cases of fALS and sALS (Fig. 13). Thus, critical subunits of the nBAF complex are downregulated in neurons with cytoplasmic FUS, but ectopic expression of Brg1 alone was sufficient to mitigate the effect on dendritic architecture.

4.3.6 Brg1, BAF53b and CREST are depleted in motor neurons from ALS patients

In order to test the relevance of nBAF subunit depletion in culture models of ALS, Brg1, BAF53b and CREST expression was evaluated by immunohistochemistry in cross-sections of spinal cord from ALS and control autopsy cases (Fig. 13). In addition to familial ALS due to TDP43/FUS mutations, cytoplasmic inclusions of TDP43 in particular are found in other cases of ALS, including sporadic disease. To assess any relationship of nBAF subunit expression with TDP pathology, serial sections were labelled with BAF subunit and TDP43 antibodies. Brg1, BAF53b, and CREST were significantly depleted from the nuclei of ALS patients with C9ORF72 expansion, fALS patients carrying the A4V SOD1 mutation and of sALS patients with no known mutations, compared to control individuals dying from non-neurological causes (Fig. 13). Interestingly, Brg1, BAF53b and CREST were depleted in motor neurons regardless of the presence or absence of TDP43 cytoplasmic inclusions (Fig. 14). The presence of FUS inclusions in autopsy tissue is rarer and more difficult to observe than TDP43 inclusions and was not ascertained in this post-mortem study.

4.4: Determine overlapping pathological pathways between fALS6 and fALS10 models

4.4.1 Decreased H3K9/K14 acetylation with cytoplasmic accumulation of TDP43

Decreased H3K9/K14 acetylation was a primary end point in FUS-mediated toxicity in motor neurons (see Chapter 4.2.3) and is expected to have consequences to gene expression. In order to determine whether decrease histone 3 acetylation was a shared pathway with cytoplasmic accumulation of FUS and TDP43, neurons were injected with FLAG-tagged WT or mutant TDP43 encoding plasmids and double immunolabelled with H3K9/K14Ac and FLAG antibody. Indeed, neurons that had cytoplasmic accumulation of either WT or G348C TDP43

had a marked decrease in H3K9/K14Ac (Fig. 15A) as measured by decreased fluorescence intensity of H3K9/14 antibody labelling (Fig. 15A, B).

4.4.2 nBAF subunit depletion in neurons with cytoplasmic accumulation of TDP43

Our observation that nBAF subunits are depleted in ALS patient motor neurons regardless of the causative genetic mutation made it very likely that nBAF subunits would also be depleted in our fALS10 model (note, we did not have samples from a fALS10 autopsy specimen to test). Motor neurons were microinjected with plasmids encoding WT or mutant TDP43 and immunolabelled with anti-FLAG and anti-Brg1, anti-BAF53b, or anti-CREST (Fig. 16A). Indeed motor neurons expressing WT or mutant TDP43 showed a decrease in Brg1, BAF53b and CREST when either WT or mutant protein accumulated in the cytoplasm by day 3 post-injection as indicated by decreases in antibody fluorescence intensity (Fig. 16B). These results indicate that nBAF subunit depletion is a shared pathogenic pathway between FUS and TDP43.

4.4.3 Dendritic Attrition occurs in neurons expressing mutant TDP43

TDP43 has many parallel functions with FUS. In *Drosophila*, overexpression of WT TDP43 increased dendritic branching, an effect not observed with expression of mutant TDP43. (Lu et al., 2009). Thus, alterations in dendritic morphology could be a common pathway shared by TDP43 and FUS leading to motor neuron dysfunction. To determine whether mutant TDP43 expressing neurons also exhibit dendritic branching abnormalities in our culture model, we compared dendritic morphologies of cultured motor neurons expressing WT and mutant TDP43. Marked decrease in dendritic branching was measured in motor neurons expressing mutant TDP43, but not WT TDP43, compared to control neurons expressing mCherry (Fig. 17A). These results are different than those described by Lu *et al.*, which could reflect differences in

experimental system. Like mutant FUS expressing neurons, this decrease in dendritic complexity was due to loss of intermediate and terminal branches indicated by the root, intermediate, terminal categorization in Sholl analysis (Supplementary Figure S3). Dendritic attrition induced by mutant TDP43 could be prevented by the same interventions as in the fALS model. Firstly, dendritic attrition was prevented by treatment of neurons expressing mutant TDP43 with 7.5μM SAHA for three days (Fig. 17B). Secondly, co-overexpression of Brg1 along with mutant TDP43 prevented mutant TDP43-induced dendritic attrition in motor neurons. Thus, common pathways affected by different genes could be targeted by common interventions.

Chapter 5: Discussion and Future Directions

5.1: Moving onwards with a culture model of fALS6

The majority of fALS6 patients present with mutations at the C-terminal region of FUS containing the nuclear localization sequence (Lagier-Tourenne and Cleveland, 2009). Cytoplasmic inclusions containing FUS have been observed in motor neurons of fALS and sALS patients (Deng et al., 2010), implicating altered trafficking and distribution of this hnRNP more generally in ALS pathogenesis. Furthermore, the degree to which ALS-linked FUS mutants accumulate in the cytoplasm of cultured cells generally correlates with severity of disease in patients (Bosco et al., 2010, Dormann et al., 2010). In addition, FUS plays a role in parallel cellular functions with TDP43 and TDP43 cytoplasmic accumulation is also a common pathological finding in ALS (Neumann et al., 2006, Mackenzie et al., 2007, Mackenzie et al., 2010, Kabashi et al., 2011, Kryndushkin et al., 2011, Lattante et al., 2013). Thus, determining the mechanisms of toxicity manifested by cytosolic accumulation of these normally nuclear proteins could allow further insight to be gained of this complex disease.

To this end, we developed a primary culture model of fALS6 to determine the negative consequences of FUS cytoplasmic accumulation. Reminiscent of neuropathological findings (Kwiatkowski et al., 2009, Vance et al., 2009, Deng et al., 2010), FUS accumulated in the cytoplasm in the form of granular, linear and skein-like inclusions (Fig. 1A-G). Time-lapse imaging showed that these large inclusions formed by fusion of small inclusions, or growth into longer linear inclusions (see Tibshirani et al., 2015). These results support the observations made by Patel *et al*, which demonstrate that FUS granules have fluid like properties with the ability to fuse and, with time, grow long filamentous structures from these granules *in vitro* (Patel et al., 2015). The presence of mutant FUS in the cytoplasm, and depletion from the nucleus, led to the complete depletion of endogenously expressed FUS in the nucleus (Fig. 1K,L). The effect observed could potentially be due to the sequestration of endogenous FUS in mutant FUS

inclusions as FUS is known to be prone to self-association via its low complexity sequences (Sun et al., 2011b, Kato et al., 2012b). Alternatively, FUS has been shown to regulate its own expression via alternative splicing of its own mRNA subjecting its own mRNA to the nonsense-mediated degradation pathway (Zhou et al., 2013). Thus, overexpression of FUS could lead to a suppression of endogenously expressed FUS through this pathway and actually represent total FUS.

In addition to the R521C/G/H and P525L mutants that were examined in culture, the truncation mutant R495X was investigated in both cultured motor neurons and transgenic mice (Bosco et al., 2010, Waibel et al., 2013). Cytoplasmic FUS was increased in motor neurons expressing FUS^{R495X}, both in the culture model and in transgenic mice, yet significant levels were retained in the nucleus (This mutant was both nuclear and cytoplasmic in over 40% of neurons in the culture model and almost all spinal motor neurons in the transgenic mice) (Fig 2B and Fig. 7). Thus, despite missing the nuclear localization sequence in the deleted C-terminus, FUS^{R495X} can be imported into the nucleus, as previously reported by Bosco *et al*. (Bosco et al., 2010).

Neurons expressing mutant FUS did not undergo apoptosis (Fig. 1M) and had a viability curve comparable to WT FUS overexpression controls during the period of the experiment. However, mutant FUS-expressing neurons did undergo significant dendritic retraction (Fig. 1N-P), a common neuropathological finding in ALS (Nakano and Hirano, 1987, Karpati et al., 1988, Takeda et al., 2014), which could represent an early manifestation of mutant FUS toxicity and lead to significant loss of vital connections with higher order neurons and other neurons along the neuraxis leading to motor neuron dysfunction. Time-lapse imaging of neurons expressing mutant FUS indicated that the dendritic attrition observed is truly due to dendritic retraction

rather than a failure of neurons to develop dendrites (data not shown). Similar dendritic attrition occurred in motor neurons expressing mutant TDP43, although some loss of viability was observed over the same time period in this model (Kabashi et al., 2010).

Conversely, motor neurons expressing mutant SOD1 have mostly died during this time period (Durham et al., 1997, Roy et al., 1998, Tradewell et al., 2011, Cha et al., 2014, Tran et al., 2014) reflecting that motor neuron physiology can be altered through multiple and distinct pathways. Indeed, our lab has shown that dysregulation of calcium homeostasis is a major factor contributing to mutant SOD1 toxicity (Roy et al., 1998, Tradewell et al., 2011), but does not occur in neurons expressing mutant FUS or TDP43 (Tran et al., 2014). Of note, dendritic attrition was also observed in our culture model of fALS1 (data not shown), indicating that despite differences in disease mechanisms, dendritic attrition is a common outcome. Since loss of motor neurons occurs much more slowly in the FUS (fALS6) and TDP43 (ALS10) culture models, they provide a good opportunity to study pre-lethal mechanisms of motor neuron dysfunction.

5.2: Evidence for transcriptional dysregulation through changes in histone marks

We previously reported that asymmetric arginine dimethylation (ADMA) of FUS by PRMT1 is a strong regulator of FUS nucleocytoplasmic shuttling and that both WT and FUS mutants interact with PRMT1 (Tradewell et al., 2012), findings also reported by other labs (Du et al., 2011, Dormann et al., 2012, Yamaguchi and Kitajo, 2012, Scaramuzzino et al., 2013). In the present study, we further developed the primary culture model in which WT or mutant human FUS is expressed in motor neurons of dissociated spinal cord cultures (Tradewell et al., 2012)

and investigated how the interaction of PRMT1 and FUS might lead to loss of nuclear function of PRMT1 and contribute to toxicity.

Using primary spinal cord cultures, we demonstrated that nuclear depletion of FUS correlated with a loss of PRMT1 function in the nucleus, leading to downregulation of transcription through loss of major histone modifications. PRMT1 was depleted from the nucleus of cultured motor neurons with cytoplasmic endogenous FUS or ectopically expressed mutant (R521H, R521G, P525L or R495X) or WT human FUS (Fig. 2). Although there was a definite and statistically significant shift in PRMT1 localization to the cytoplasm in motor neurons expressing FUS^{R495X}, nuclear depletion of PRMT1 was not as complete as in cultured neurons expressing FUS^{R521H} or FUS^{P525L}. This could be influenced by the continued presence of nuclear FUS in neurons expressing FUS^{R495X}.

The mechanism underlying loss of nuclear PRMT1 is unclear. PRMT1 does not necessarily maintain association with FUS even though ADMA by PRMT1 is important for FUS trafficking and the two proteins can be co-immunoprecipitated (Du et al., 2011, Tradewell et al., 2012, Yamaguchi and Kitajo, 2012, Scaramuzzino et al., 2013). PRMT1 was clearly not recruited to synapses with endogenous FUS (Fig. 2G), nor was it associated with cytoplasmic inclusions of WT or mutant human FUS in motor neurons (Fig. 2D,E). In contrast, others have reported that some PRMT1 was associated with inclusions of truncated FUS, as well as being diffusely cytoplasmic, and in stress granules in oxidatively challenged SH-SY5Y cells (Yamaguchi and Kitajo, 2012). In addition, PRMT1 and PRMT8 accumulated in inclusion bodies in COS cells expressing FUS mutants (Scaramuzzino et al., 2013). There are 10 known alternatively spliced PRMT1 isoforms, only one of which, PRMT1v2, contains a nuclear export

signal (Goulet et al., 2007). Shifting the proportion of alternatively spliced variants to PRMT1v2 cannot be excluded as an alternative explanation for the observed loss of nuclear PRMT1.

Redistribution of PRMT1 observed in the culture model was validated *in vivo* in mice. PRMT1 was predominantly nuclear in spinal motor neurons of non-transgenic mice and transgenic mice carrying the human FUS^{WT} transgene, but both nuclear and cytoplasmic in FUS^{R495X} transgenic mice, similar to the distribution of FUS (Fig. 7). This pattern was consistent with observations in cultured motor neurons (this study) and HEK-293 cells (Bosco et al. (2010) (*i.e.*, increased cytoplasmic FUS/PRMT1, but considerable retention in the nucleus) and with the very mild phenotype of these mice, only detected by EMG.

Unfortunately, we could not reliably assess the distribution of PRMT1 in human tissue, or whether it is mislocalized to the cytoplasm in neurons of ALS patients. By immunohistochemistry, PRMT1 was cytoplasmic in spinal motor neurons in the archived control tissue tested (spinal cord from individuals dying of non-neurological causes). A study in mice comparing PRMT1 distribution with time of processing demonstrated that postmortem interval before tissue fixation is the most likely reason for its cytoplasmic distribution in control autopsy tissue (Fig. 8). Best results were obtained using perfusion fixation with paraformaldehyde or cryopreservation; distribution of PRMT1 was compromised even with immediate immersion fixation in formalin or paraformaldehyde. Similarly, endogenous PRMT1 was not retained in the nuclear fraction upon subcellular fractionation of cultured cells (Tibshirani, unpublished data) suggesting that interaction with its substrates is transient or labile. Loss of nuclear PRMT1 under these circumstances could be explained by compromised integrity of the nuclear membrane leading to leakage of small, soluble proteins such as PRMT1 into the cytoplasm and/or loss of energy-dependent protein interactions (Boisvert et al., 2003). Although isoform switching to

PRMT1v2 is a possibility in living cells, it seems unlikely postmortem. These experiments stress the importance of determining postmortem effects on cellular processes being investigated in such specimens.

Decreased H4R3Me2 and H3K9/K14Ac resulted from nuclear depletion of FUS and PRMT1 (Fig. 3, 4A,B). The normal function of FUS includes recruiting HDAC1 to sites of induced DNA damage and this process is perturbed in cells expressing mutant FUS (Wang et al., 2013). However, we observed decreased H3K9/K14Ac when endogenous FUS or either WT or R521H FUS were depleted from the nucleus, indicating this decrease was inherent upon the localization of FUS rather than brought on by a functional consequence of the mutation.

Decreased H4R3Me2 and H3K9/K14Ac had consequences on transcriptional activity. BrU-incorporation into RNA was reduced in motor neurons with cytoplasmic endogenous FUS/PRMT1 compared to those with nuclear FUS/PRMT1, indicating this was a normal physiological process with FUS trafficking (Fig. 5). The data are more than correlative. Reduction of PRMT1 expression has physiological consequences to motor neurons that relate to the ALS phenotype. These include reduction in mitochondrial size (Tradewell et al., 2012) and dendritic branching (Supplementary Figure S2).

Overall, the data indicate that PRMT1 redistribution could be a normal consequence of FUS localization. This conclusion is supported by the coincidence of FUS and PRMT1 localization in motor neurons of developing spinal cord cultures and those subjected to osmotic shock by treatment with sorbitol, both conditions associated with increased cytoplasmic distribution of endogenous FUS. It is possible that reducing the neuron's transcriptional activity while FUS delivers its cargo mRNAs to synapses could be an adaptation to prevent the production of excessive RNAs until the return of FUS to the nucleus. Regardless, should

depression in transcription be sustained, as in pathological retention of FUS brought on by mutation or long term stress, consequences for neuronal function would be expected, particularly related to synaptic and dendritic maintenance. A difference between redistribution of endogenous FUS and ectopically expressed human FUS was the condensation of chromatin in the latter (Fig. 1J, 3A, 4A, 12A). This could reflect a difference in trafficking kinetics, a hypothesis being investigated, or other consequences of disrupted nuclear function of FUS. Regardless, chromatin condensation was not associated with apoptosis (neurons were not TUNEL-positive, Fig. 1M).

In summary, our results point to a sustained loss of nuclear PRMT1 function as a contributing mechanism of mutant FUS toxicity in ALS. Loss of nuclear PRMT1 correlated with cytoplasmic mislocalization of FUS and was associated with changes in histone marks linked to transcriptional inhibition. The extent to which this repression is general or affects particular gene families remains to be determined. Given that FUS itself can affect transcription of a large number of genes by binding to RNA polymerase (Schwartz et al., 2012), its redistribution to the cytoplasm could, through a physiological process, influence transcription both directly and indirectly through PRMT1. Although cycling of PRMT1 between the nucleus and the cytoplasm is a normal physiological process, sustained loss of nuclear PRMT1 would be expected to have significant consequences on neuronal function in the context of pathological cytoplasmic FUS accumulation in ALS.

5.3: Dysregulation of chromatin remodeling complexes: A common pathway in ALS?

5.3.1 nBAF subunit depletion

Following our observations with nuclear PRMT1 depletion in our fALS6 culture model, we investigated the possibility that other FUS-interacting partners residing in the nucleus were

mislocalized. To further investigate this possibility and other epigenetic mechanisms of dendritic attrition, we evaluated the localization of another FUS-interacting partner identified by our lab and others, Brg1, the main DNA-helicase found in the nBAF chromatin remodeling complex responsible for neuronal differentiation and activity-dependent outgrowth. Interestingly, unlike PRMT1, Brg1 was depleted from the nucleus rather than mislocalized to the cytoplasm in neurons with cytoplasmic FUS (Fig. 9A,B). Again, this depletion was observed with cytoplasmic accumulation of either WT or mutant FUS, suggesting once again that this observation is a manifestation dependent on FUS localization, which is magnified by its aberrant retention in the cytoplasm, with downstream consequences to dendritic morphology.

Genetic or pharmacological knock-down of Brg1 function indicated that Brg1 is required for maintenance of motor neuron dendritic morphology (Fig. 9C-E). On the other hand, other groups reported that cortical neurons with knockdown of nBAF function (either knockdown of key nBAF subunits or by expression of CREST with ALS-associated mutations) did not exhibit dendritic retraction under normal conditions but, rather showed a defect in dendritic outgrowth upon depolarization with KCl treatment (Wu et al., 2007, Chesi et al., 2013). The difference from our results could be due to differences in cell type, intrinsic activity or stage of development. Motor neurons are tonically active, generating trains of action potentials, which could reflect different requirements for Brg1. Motor neurons in our culture model have reached a more advanced state of maturation including highly developed dendritic branches, whereas cortical and hippocampal cultures used in the other studies were much younger (approximately 5 days *in vitro*) and the ability to extend dendrites was being evaluated. Thus, neurons could have different requirements for nBAF function at different developmental stages or at different basal activity levels.

nBAF subunit depletion was not restricted to Brg1 in our fALS6 culture model. Indeed we observed depletion of other critical nBAF subunits, BAF53b and CREST, shown to be required for neuronal differentiation and dendritic outgrowth (Wu et al., 2007, Yoo et al., 2009, Staahl et al., 2013, Vogel-Ciernia et al., 2013). Co-overexpression of Brg1 completely prevented mutant FUS-induced dendritic attrition in motor neurons on day 3 post-injection (Fig. 10). This result was surprising since Brg1 overexpression did not prevent decreases in H3K9/K14 acetylation, a major substrate for the bromodomains of Brg1 (Shen et al., 2007), nor did it prevent depletion of BAF53b and CREST on day 3 (data not shown). Thus, though Brg1 is being overexpressed, the nBAF complex is not expected to function without H3K9/K14 acetylation or the presence of these nBAF subunits. We therefore hypothesize that the effect of Brg1 overexpression on the rescue of mFUS dendritic attrition is due to the build-up of pro-dendritic factors before depletion of H3Ac, BAF53b and CREST. Indeed, evaluation of neuronal dendritic morphology in motor neurons co-expressing Brg1 and mutant FUS on day 6 post-injection (3 days after observed decreases in H3Ac and nBAF subunits) demonstrated severe dendritic retraction comparable to neurons expressing mutant FUS alone. Thus, in order to maintain dendritic morphology, neurons must maintain expression of all components of the nBAF complex.

5.3.2 Mechanisms of nBAF subunit depletion

Initially we chose to study Brg1 because we (and others) had identified it as a FUS-interacting partner and we hypothesized that its distribution would be altered with the expression of mutant FUS, like PRMT1. However, the results suggest changes in the expression of Brg1 as a response to loss of nuclear FUS and or its cytoplasmic retention rather than a shift in Brg1 distribution because it is bound to FUS.

Unlike endogenously expressed Brg1, plasmid-derived Brg1 was stably maintained in the nucleus despite the presence of cytoplasmic FUS. While investigating explanations for this difference we observed that mutant FUS, but not WT FUS, represses the expression of mRNA transcripts containing Brg1 specific 3'UTRs (Fig. 11), suggesting a post-transcriptional regulatory mechanism for mutant FUS induced Brg1 depletion. It is yet unknown whether this decrease in protein expression is due to sustained repression of translation or whether Brg1 3'UTR containing transcripts are targeted for degradation. *In situ* hybridization experiments, RNA live imaging and metabolic labelling experiments are in progress in a collaborative study to address this question. It is not yet clear how Brg1 and FUS work together in the nucleus to modulate gene expression patterns.

In non-neuronal cells, BAF53b expression is thought to be repressed by BAF53a expression. In neuronal cells, miR9/9* and miR124 are expressed and bind to BAF53a 3'UTR and target it's mRNA for degradation (Yoo et al., 2009). Using the same reporter system, we observed that de-repression of BAF53a 3'UTR containing RNA transcripts occurs in neurons expressing mutant FUS, but not in neurons expressing WT FUS (Fig. 12C). A subject for future study would be to determine if this effect is due to miR9/9* and miR124 being downregulated with expression of mutant FUS. De-repression of BAF53a expression is a potential mechanism for BAF53b depletion and is an interesting observation for two reasons: 1) FUS could influence nBAF subunit depletion both directly, as is the case for Brg1, and indirectly as could be the case for BAF53b through re-expression of BAF53a, 2) If BAF53a is in fact re-expressed in neurons, this finding could suggest that the nBAF subunit composition is shifting towards an immature composition observed in neural progenitor cells and that neurons expressing mutant FUS could be de-differentiating or at least losing their neuronal identity. Unfortunately, due to an

unavailability of antibodies that recognize BAF53a and not BAF53b we could not confirm our findings by assessing protein levels of BAF53a. Further investigation on the nBAF subunit composition and expression of neuronal markers in mutant FUS expressing neurons is needed to address these questions.

5.3.3 Common pathways in ALS revealed

The genetic heterogeneity of ALS has imposed challenges in identifying a common pathological pathway leading to motor neuron dysfunction. Multiple mutations in nBAF subunits are linked to autism spectrum disorders which are disorders linked to improper development and formation of dendrites (Halgren et al., 2012, Neale et al., 2012, Tsurusaki et al., 2012). nBAF complex dysfunction was not yet implicated in adult onset disease until the discovery of CREST mutations in ALS trios (Chesi et al., 2013). In evaluating the expression of nBAF subunits in ALS autopsy tissue to validate our findings in culture, we observed that dysregulation of the nBAF complex could potentially be a common disease pathway in ALS. We observed depletion of Brg1, BAF53b and CREST in motor neurons of ALS patients, but not in non-neurological controls (Fig. 13). This observed depletion was irrespective of patient genotype as depletion was observed in patients with C9ORF72 expansions, SOD1 A4V and sALS patients with no known ALS-causing mutations. Depletion of nBAF subunits occurred in neurons with or without TDP43 pathology as neurons with nuclear TDP43 still demonstrated loss of nBAF subunits (Fig. 14). It is possible that some TDP43 pathology is unable to be detected due to hidden antigens in the pathological aggregates. Another possibility is that motor neurons present in ALS patients activate stress response pathways that bypass the requirement for TDP43 cytoplasmic accumulation and lead to depletion of these subunits. The continued presence of nuclear TDP43 in some neurons also demonstrates that nBAF subunit depletion is likely specific and not due to a general suppression of protein expression. In conclusion nBAF complex dysregulation is a

convergent mechanism in ALS that could potentially be targeted for therapeutic intervention; however, the fact that the nBAF complex requires the presence of all subunits in order to function and that the depletion of these subunits could be mechanistically different between subunits presents quite a challenge to this effect.

5.4: Identifying shared pathways between FUS and TDP43

Cytosolic accumulation of TDP43 is another common finding in ALS and FTLD. In addition, FUS and TDP43 have overlapping functions in several pathways involving RNA regulation (Lagier-Tourenne and Cleveland, 2009). For example, FUS and TDP43 both regulate HDAC6 mRNA levels (Kim et al., 2010). In a zebrafish animal model, WT FUS rescued the motor phenotype observed in a TDP43 knock-out but not vice-versa, demonstrating that FUS could potentially act downstream of TDP43 (Kabashi et al., 2011). Dendritic branching defects have also been observed in *Drosophila* neurons overexpressing mutant but not WT TDP43 (Lu et al., 2009). Indeed, expression of mutant TDP43 in motor neurons led to a significant reduction in dendritic branching compared to WT expressing neurons (Fig. 17A) similar to neurons in our fALS6 model.

Like in our fALS6 model, cytosolic accumulation of TDP43 led to depletion of Brg1, BAF53b and CREST (Fig. 16) and re-introduction of Brg1 prevented the dendritic attrition observed (Fig. 17B), which suggests a common pathway of nBAF complex dysregulation between FUS and TDP43. In addition, decreases in H3 acetylation with cytoplasmic accumulation of TDP43 (Fig. 15) also occurred suggesting that transcriptional repression by alterations in histone modifications is another common pathway between these two hnRNPs. Whether this decrease in H3 acetylation is a result of shifting the distribution of PRMT1 directly is unknown. PRMT1 does not methylate TDP43; however, PRMT1 can be immunoprecipitated

with TDP43 (Finelli et al., 2015). Alternatively TDP43 directly interacts with FUS (Kim et al., 2010, Kryndushkin et al., 2011) and could influence PRMT1 localization indirectly through altering the localization of FUS. Regardless, the data point to histone hypoacetylation as a common factor in fALS6 and fALS10 pathogenesis that could be targeted with epigenetic drugs to maintain transcription.

5.5: Conclusion

This thesis reveals multiple lines of evidence for epigenetic consequences of FUS mislocalization. Retraction of dendrites, a major phenotype of neurons in our culture model as well as in ALS patients would be expected to lead to lost connections with higher order neurons and loss of motor neuron connectivity in the neural network for motor control. Underlying dendritic attrition, many levels of epigenetic consequences of FUS mislocalization are operating including alterations of histone modifications, dysfunction of nBAF chromatin remodeling complexes and sequence-specific repression and de-repression of protein expression through post-transcriptional regulation of mRNA transcripts. The combination of all of these changes illustrates the multiple points of regulation that FUS has on the transcriptomic profile of the cell with effects on cell fate. Some of these consequences are also apparent in other culture models of ALS and ALS patients giving broader implication to our findings. Thus, it is imperative that these mechanisms be taken into account when evaluating therapeutics for the disease whose mechanism of action is to alter gene expression in motor neurons in an effort to upregulate the expression of prosurvival genes.

Figures

Figure 1. Mutant human FUS forms granular, linear and skein-like neuronal cytoplasmic inclusions and depletes nuclear endogenous FUS.

(**A** to **G**) Immunolabelling of cultured motor neurons with anti-FLAG antibody on Day 3 (**A-C**) or Day 6-7 (**D** to **G**) after intranuclear microinjection of indicated plasmids. Arrows in A to C point to motor neuron nuclei. Mutant FUS was retained in the cytoplasm in the form of granular inclusions on Day 3 post-injection (**A-C**), and formed linear, donut, and skein-like inclusions by 6 days, as illustrated in the neurons shown in (**D** to **G**). (**E**) 3D reconstruction of skein-like inclusions of eGFP-FUS from (**D**). (**H** to **K**) Double-label of a motor neuron expressing FLAG-FUS^{R521H} with anti-FLAG and anti-FUS to visualize both human and total FUS. Endogenous FUS is visible in the nuclei of background cells, but not in the motor neuron with only cytoplasmic FLAG labelling. (**L**) Fluorescence intensity profiles of anti-FLAG, anti-FUS and Hoechst labelling from profile line drawn on the motor neuron in **K**, demonstrating co-distribution of FLAG and FUS labelling, and thus human FUS with endogenous FUS. Scale bar = 20 µm. (**M**) TUNEL assay was performed on neurons injected with FUSR521H plasmid. Neurons with cytoplasmic FUS and condensed chromatin were not positive for TUNEL staining indicating intact DNA. Treatment of cultures with DNAse was used as a positive control; negative control was no treatment. Scale bar = 20 µm. (**N**) Total sholl analysis comparing dendritic branching of neurons expressing either WT, mutant FUS or pcDNA3 empty vector on Day 3 post-injection. "S.D." indicates a significant difference ($p<0.05$) between mutant FUS and empty vector control. (**O**) Categorization of sholl curve shown in M, into Root, Intermediate and Terminal segments. "S.D." indicates a significant difference ($p<0.05$, Welch's t-test) between mutant FUS and empty vector control. (**P**) Further characterization of dendritic morphology. *** indicates significant difference compared to empty vector control ($p<0.001$, Student's t-test).

Figure 1.

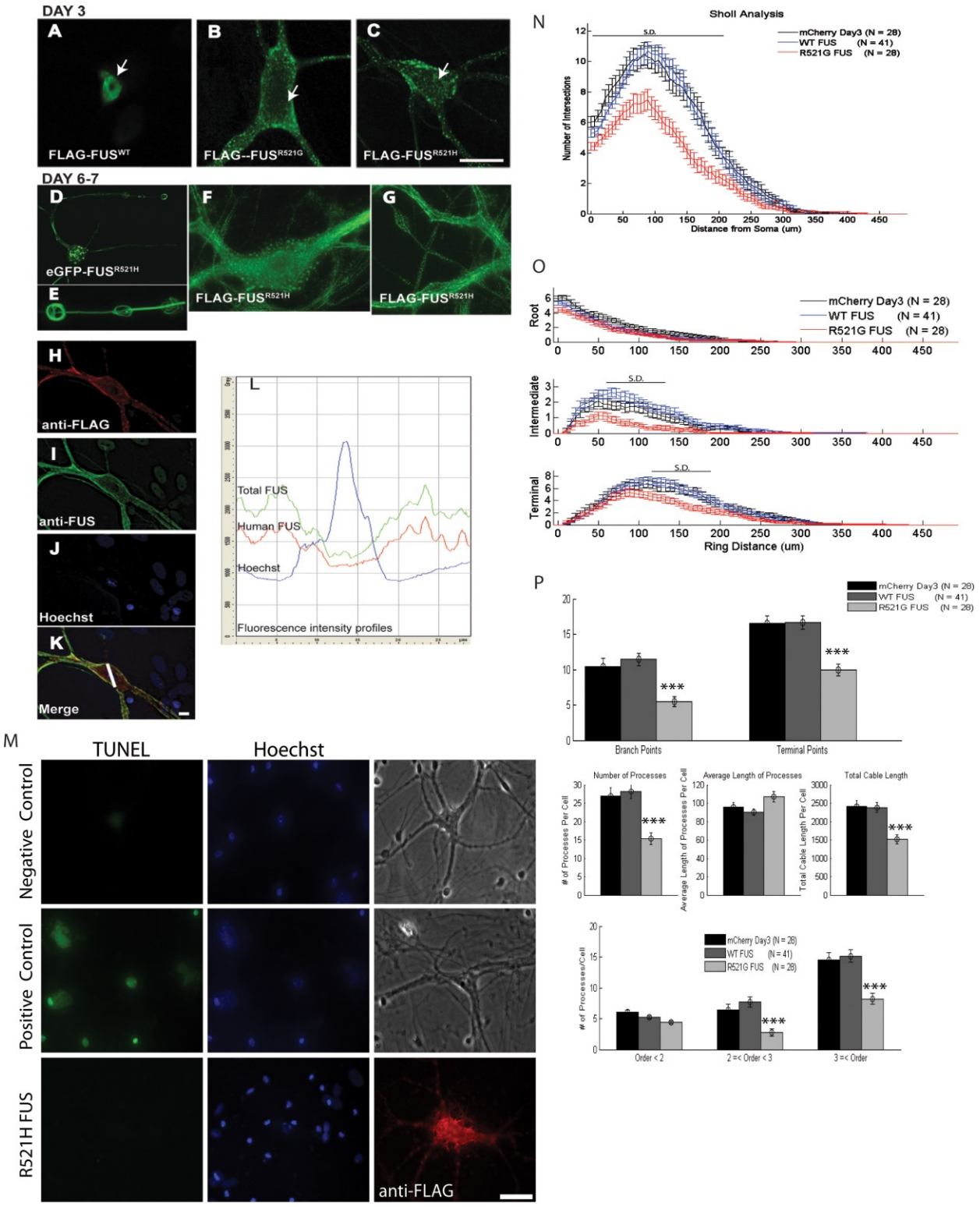
DAY 3
A
FLAG-FUS^WT
B
FLAG--FUS^R521G
C
FLAG-FUS^R521H
DAY 6-7
D
eGFP-FUS^R521H
E
F
FLAG-FUS^R521H
G
FLAG-FUS^R521H
H
anti-FLAG
I
anti-FUS
J
Hoechst
K
Merge
L
Total FUS
Human FUS
Hoechst
Fluorescence intensity profiles
N
Sholl Analysis
S.D.
mCherry Day3 (N = 28)
WT FUS (N = 41)
R521G FUS (N = 28)
Number of Intersections
Distance from Soma (um)
O
Root
Intermediate
Terminal
Ring Distance (um)
P
Branch Points
Terminal Points
Number of Processes
Average Length of Processes
Total Cable Length
# of Processes/Cell
Order < 2
2 =< Order < 3
3 =< Order
M
TUNEL
Hoechst
Negative Control
Positive Control
R521H FUS
anti-FLAG

Figure 2. Co-distribution of PRMT1 and FUS.

(**A**) Double-label of cultured motor neurons with antibodies to FUS and PRMT1. Distribution of PRMT1 mimicked that of endogenous, WT and mutant human FUS. Arrows point to motor neurons. Scale bar = 50 µm. (**B** and **C**) Quantitation of FUS and PRMT1 localization in neurons either uninjected (n=6 cultures 17-62 neurons per culture) or injected with indicated FUS plasmids (n=3 cultures per condition, 11-77 neurons per culture). Asterisks indicate significant shift in distribution from the nucleus to cytoplasm compared to endogenous proteins in uninjected neurons *p<0.05, **p<0.01, ***p<0.001; t-test. (**D** and **E**) PRMT1 was not recruited to mutant FUS granular, linear and skein-like inclusions. Scale bars = 50 µm and 20 µm, respectively. (**F** and **G**) Co-labelling of either FUS or PRMT1 with synaptophysin. Neurons with cytoplasmic PRMT1/FUS were selected to determine whether cytoplasmic PRMT1 is recruited to synapses. Large arrows in **F** point to two dendrites emerging from the cell body to the left. Endogenous FUS, but not PRMT1 was recruited to synapses. Arrow heads point to some areas of FUS/synaptophysin colocalization. Scale bar = 10 µm. (**H**) Quantification of endogenous FUS and PRMT1 localization in cultured motor neurons at two stages of development of spinal cord cultures. Asterisks indicate significantly different distribution at 4 compared to 2 weeks, **p<0.01, ***p<0.001; (t-test, n=3 per condition, 30-256 neurons per culture). More neurons have cytoplasmic FUS/PRMT1 as they develop and establish synaptic connections. (**I**) Quantification of endogenous FUS and PRMT1 localization in motor neurons in control cultures or cultures treated with 0.4 M sorbitol for 2 hrs showing significant redistribution of both proteins from the nucleus to the cytoplasm with osmotic stress. Asterisks indicate significant difference compared to control, *p<0.05, **p<0.01, ***p<0.001; (t-test, n=3 per condition, 28-58 neurons per culture).

Figure 2.

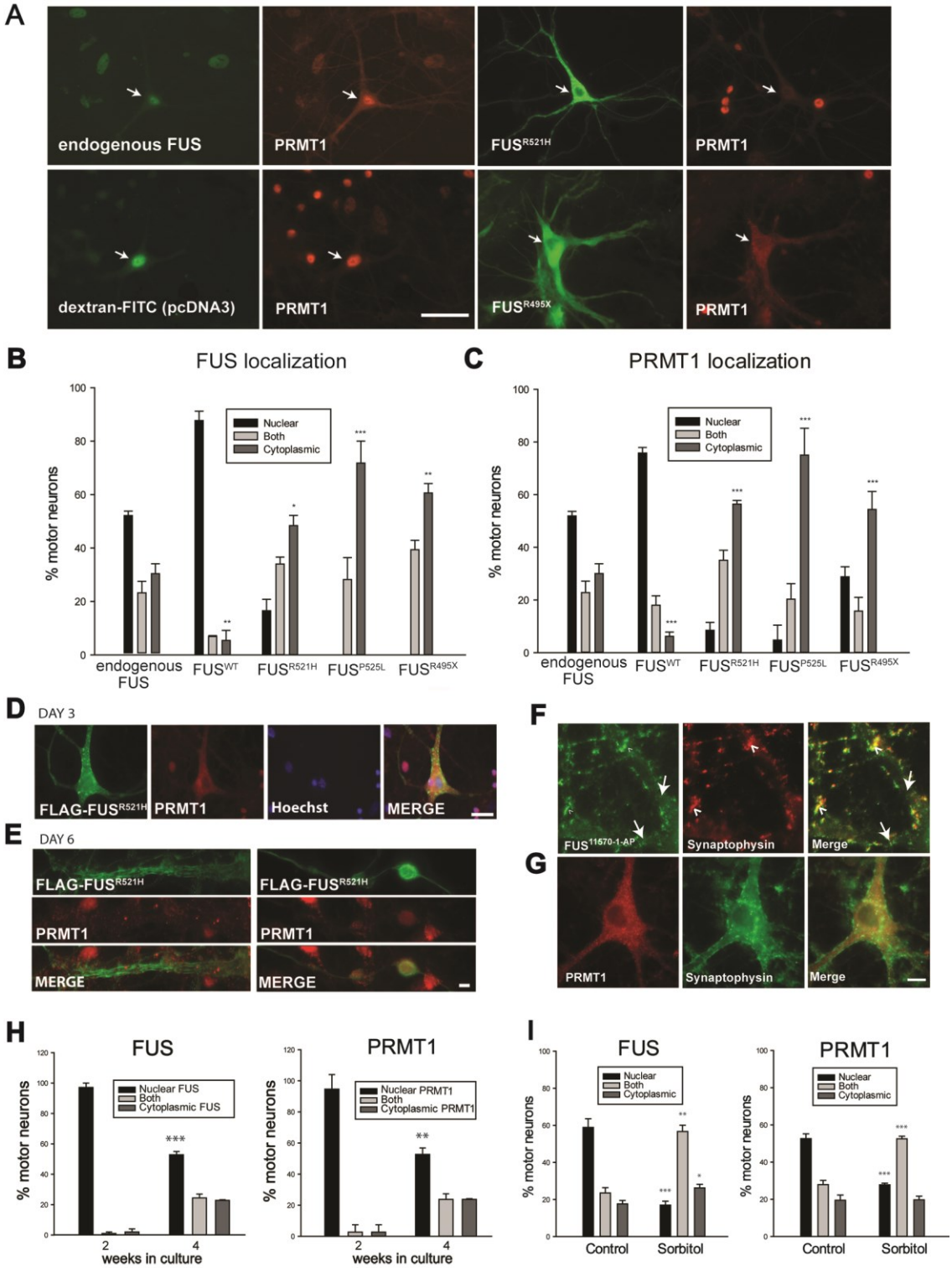
A
endogenous FUS
PRMT1
FUSR521H
PRMT1
dextran-FITC (pcDNA3)
PRMT1
FUSR495X
PRMT1
B
FUS localization
% motor neurons
Nuclear
Both
Cytoplasmic
endogenous FUS
FUSWT
FUSR521H
FUSP525L
FUSR495X
C
PRMT1 localization
% motor neurons
Nuclear
Both
Cytoplasmic
endogenous FUS
FUSWT
FUSR521H
FUSP525L
FUSR495X
D
DAY 3
FLAG-FUSR521H
PRMT1
Hoechst
MERGE
E
DAY 6
FLAG-FUSR521H
PRMT1
MERGE
FLAG-FUSR521H
PRMT1
MERGE
F
FUS11670-1-AP
Synaptophysin
Merge
G
PRMT1
Synaptophysin
Merge
H
FUS
% motor neurons
Nuclear FUS
Both
Cytoplasmic FUS
2
4
weeks in culture
PRMT1
% motor neurons
Nuclear PRMT1
Both
Cytoplasmic PRMT1
2
4
weeks in culture
I
FUS
% motor neurons
Nuclear
Both
Cytoplasmic
Control
Sorbitol
PRMT1
% motor neurons
Nuclear
Both
Cytoplasmic
Control
Sorbitol

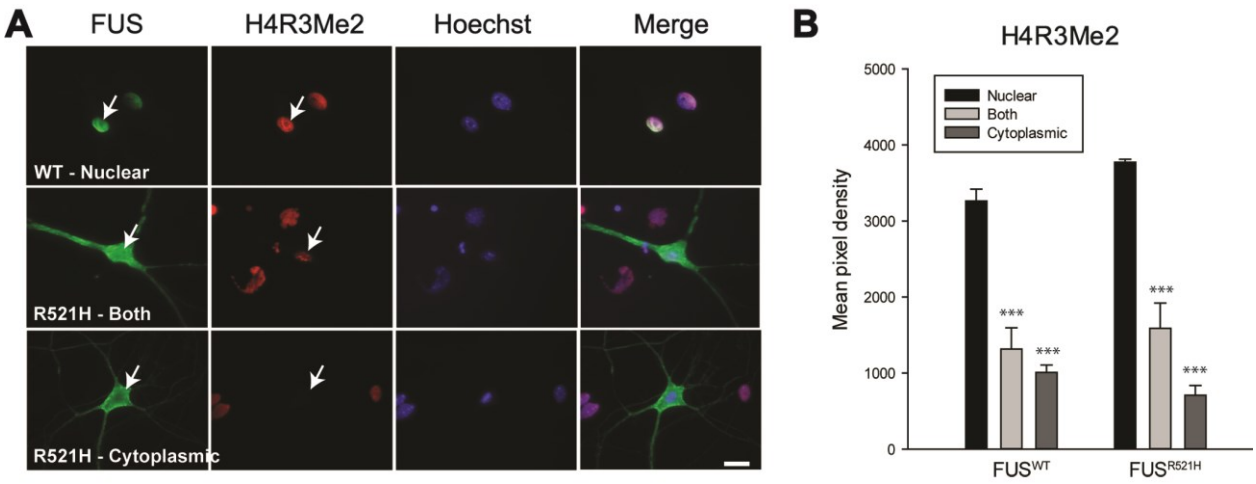

Figure 3. Decreased H4R3 ADMA in motor neurons with cytoplasmic FUS.

(**A**) Double-labelling of motor neurons expressing either WT or mutant FUS, with antibodies to FLAG and asymmetrically dimethylated H4R3 (H4R3Me2). Arrows point to motor neuron nuclei. (**B**) Mean fluorescence intensity of H4R3Me2 antibody labelling corresponding to localization of FUS. Presented are means ± S.E.M. of data collected in n=38 neurons expressing FUS^{WT} and n=18 neurons expressing FUS^{R521H}. ***significantly different from distribution when FUS was nuclear, $p<0.001$; t-test. Scale bar = 20µm.

Figure 4. H3K9/K14 acetylation is decreased in neurons with cytoplasmic FUS, downstream of H4R3 methylation.

(**A**) Double-labelling of motor neurons, expressing either WT or mutant FUS, with antibodies to FLAG and acetylated H3K9/K14 (H3K9/K14Ac) demonstrating decreased H3K9/K14 acetylation in neurons with cytoplasmic FUS. Arrows point to motor neuron nuclei. Presented are means ± S.E.M. of data collected in n=43 neurons expressing WT FUS and n=32 neurons expressing R521H FUS. (**B**) Mean fluorescence intensity of H3K9/K14Ac labelling corresponding to localization of FUS. Asterisks indicate significantly different compared to neurons with nuclear FUS, (***$p<0.001$, Student's t-test). (**C**) Western blot of purified histones from cultures treated with 20 μM AMI-1 (PRMT inhibitor), demonstrating a significant decrease in H3 acetylation, indicated by densitometric measurements of H3K9/K14Ac bands (n=3 per condition), at 24 hrs of treatment. Coomassie stained sister gel shows consistent levels of histone proteins among treatment groups. Asterisks indicate significantly different compared to untreated cultures, (*$p<0.05$, Student's t-test). (**D**) Reduction in H4R3Me2 and H3K9/K14Ac in motor neurons after 24 hrs exposure to 20 μM AMI-1 (**$p<0.01$, Student's t-test), presented as mean fluorescence intensity ± S.E.M. of antibody labelling in nuclei of motor neurons with nuclear FUS. (**E** and **F**) Mean fluorescence intensity of H3K9/K14Ac and H4R3Me2 labelling of neurons expressing R521H-FUS in control cultures (vehicle treated) or cultures treated with the HDAC inhibitor, SAHA. SAHA significantly preserved H3 acetylation, but did not prevent decreases in H4R3 methylation in neurons with cytoplasmic FUS. Asterisks indicate significantly different compared to vehicle treated (***$p<0.001$, Student's t-test); number of neurons evaluated is indicated on the graphs).

Figure 4.

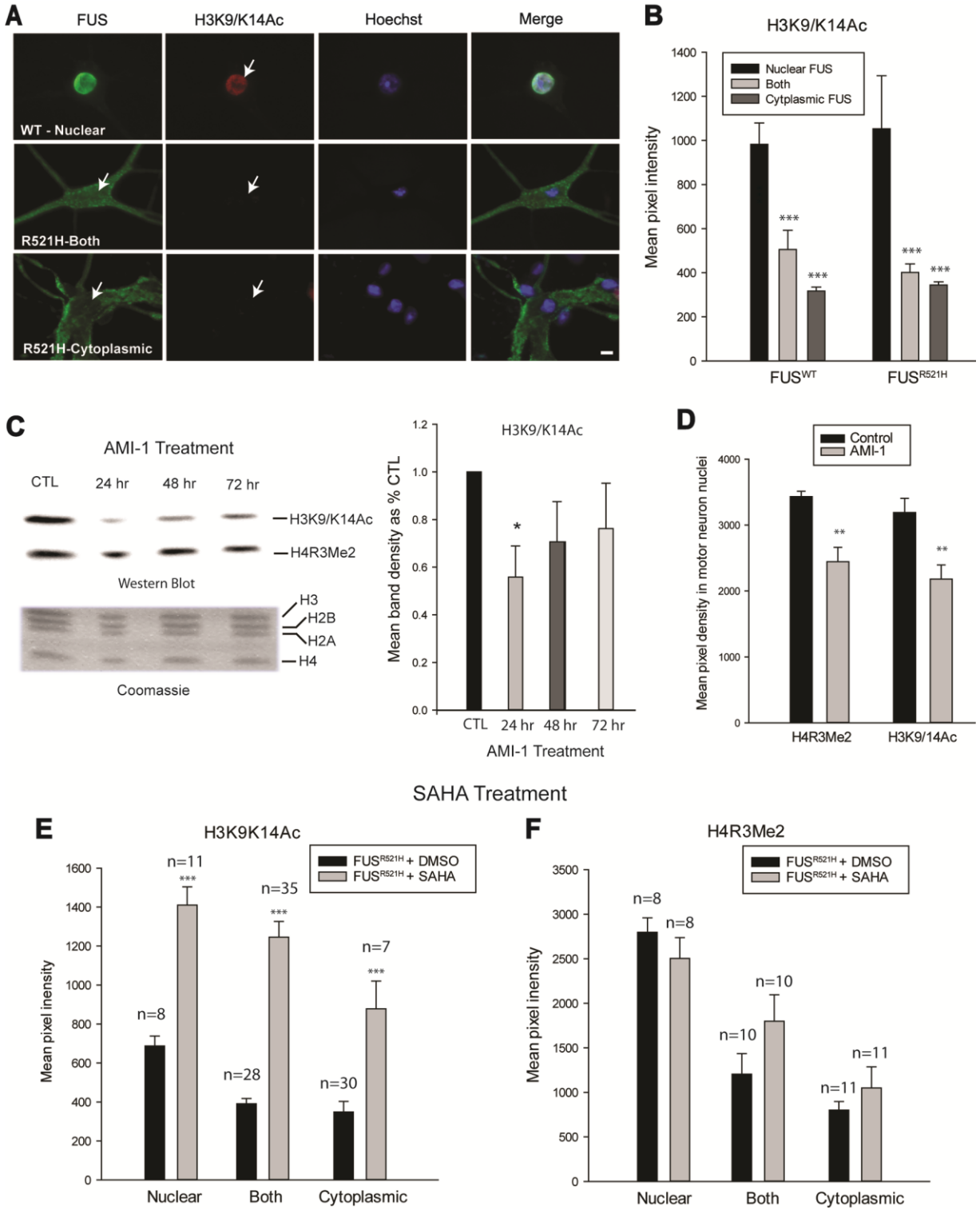
A
FUS
H3K9/K14Ac
Hoechst
Merge
WT - Nuclear
R521H-Both
R521H-Cytoplasmic
B
H3K9/K14Ac
Nuclear FUS
Both
Cytplasmic FUS
Mean pixel intensity
FUSWT
FUSR521H
C
AMI-1 Treatment
CTL
24 hr
48 hr
72 hr
H3K9/K14Ac
H4R3Me2
Western Blot
H3
H2B
H2A
H4
Coomassie
H3K9/K14Ac
Mean band density as % CTL
AMI-1 Treatment
D
Control
AMI-1
Mean pixel density in motor neuron nuclei
H4R3Me2
H3K9/14Ac
SAHA Treatment
E
H3K9K14Ac
FUSR521H + DMSO
FUSR521H + SAHA
Mean pixel inensity
n=8
n=11
n=28
n=35
n=30
n=7
Nuclear
Both
Cytoplasmic
F
H4R3Me2
FUSR521H + DMSO
FUSR521H + SAHA
Mean pixel inensity
n=8
n=8
n=10
n=10
n=11
n=11
Nuclear
Both
Cytoplasmic

Figure 5. RNA synthesis is decreased in neurons with cytoplasmic FUS and following inhibition of PRMT activity by AMI-1.

(**A**) Mean fluorescence intensity of anti-BrdU antibody labelling of neurons incubated with 5 mM BrU for 2 hrs to assess BrU incorporation in newly synthesized RNA. Transcriptional activity was reduced in neurons with cytoplasmic FUS (n=14) compared to those with nuclear FUS (n=12). (**B**) Transcriptional activity was also reduced in neurons with nuclear FUS treated with AMI-1 (n=9) compared to untreated (n=13). (*p<0.05, ***p<0.001, Student's t-test).

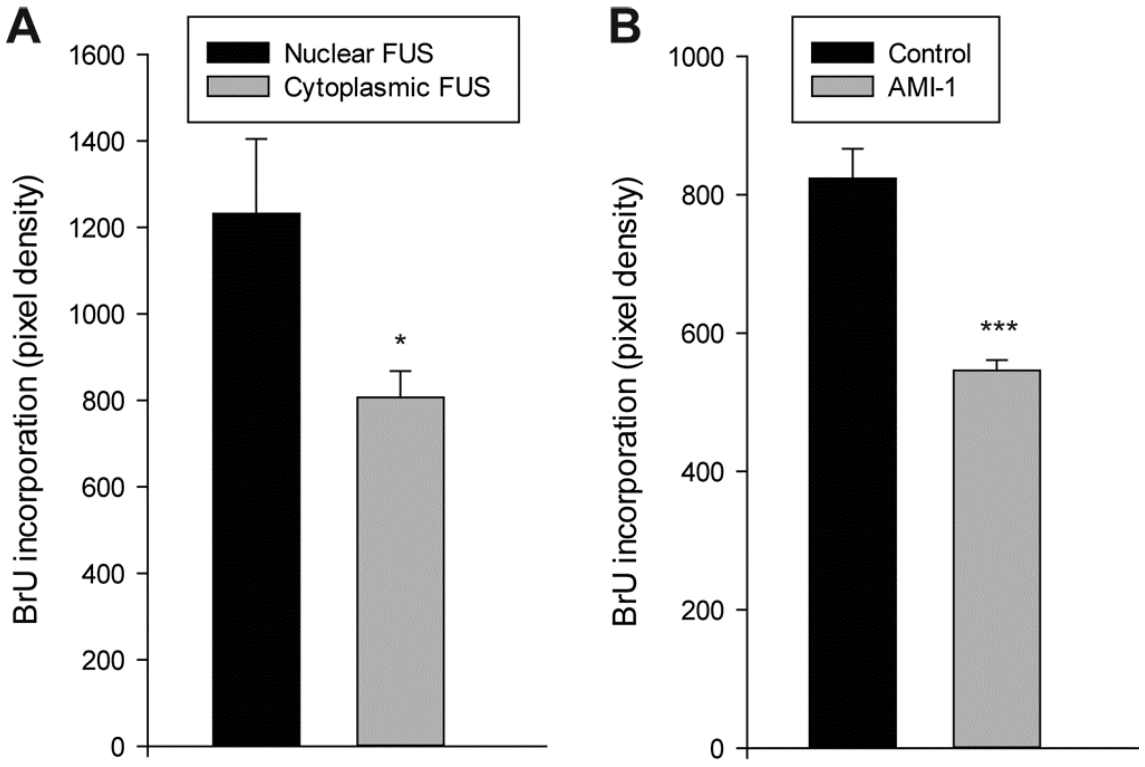

Figure 6. Treatment with SAHA prevents dendritic attrition in neurons expressing mutant FUS.

Dendritic morphology measurements of neurons expressing mutant FUS +/- 7.5μM SAHA on day 3 post-injection. mCherry + pcDNA3 was used as an injection control. Presented are means ± S.E.M. of the data. "S.D." indicates significant difference between R521G DMSO and mCherry DMSO. ($p<0.05$; Welch's t-test). Asterisks indicate significant difference between R521G DMSO and mCherry DMSO (***$p<0.001$; Student's t-test).

Figure 6.

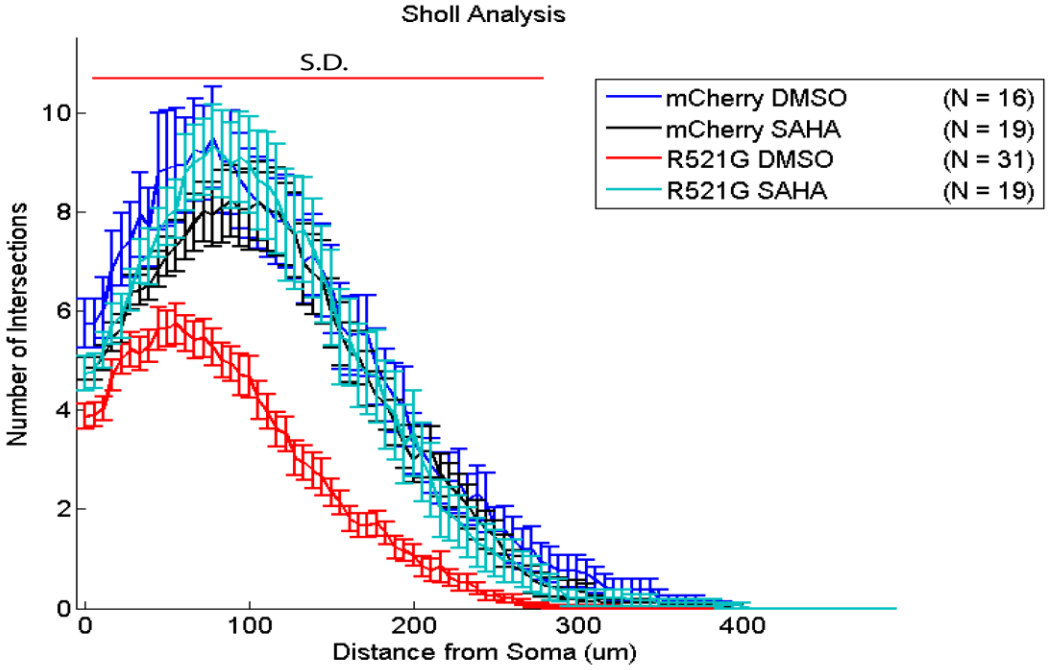
Sholl Analysis
S.D.
mCherry DMSO (N = 16)
mCherry SAHA (N = 19)
R521G DMSO (N = 31)
R521G SAHA (N = 19)
Number of Intersections
Distance from Soma (um)
0
2
4
6
8
10
0
100
200
300
400

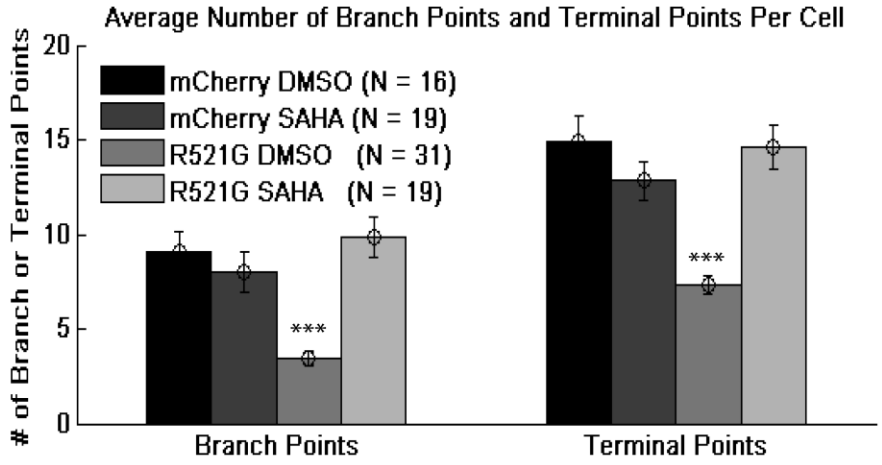
Average Number of Branch Points and Terminal Points Per Cell
mCherry DMSO (N = 16)
mCherry SAHA (N = 19)
R521G DMSO (N = 31)
R521G SAHA (N = 19)
# of Branch or Terminal Points
Branch Points
Terminal Points
***
***
0
5
10
15
20

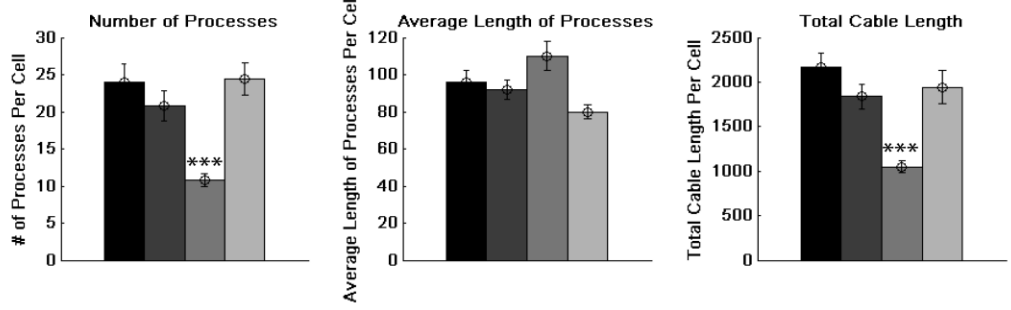
Number of Processes
# of Processes Per Cell
***
Average Length of Processes
Average Length of Processes Per Cel
Total Cable Length
Total Cable Length Per Cell
***

Figure 7. Co-distribution of PRMT1 with FUS in murine spinal motor neurons *in situ* in non-transgenic, and WT and mutant FUS transgenic mice.

Double immunolabelling of cross-sections of spinal cord from non-transgenic mice (**A** to **C**: 154 days old, line PX78 littermate), FUS^{WT} transgenic mice (**D** to **E**: 163 days old, line PWT17) and FUS^{495X} transgenic mice (**F** to **I:** 154 days old, line PX78; **J** to **L**: 378 days old, line PX78) with mouse anti-FUS (sc-47711) and rabbit anti-PRMT1. PRMT1 distribution paralleled FUS, being nuclear in motor neurons of non-transgenic mice and FUS^{WT} transgenics, but to varying degrees cytoplasmic as well as nuclear in neurons of FUS^{R495X} mice. Scale bar = 20 μm.

Figure 7.

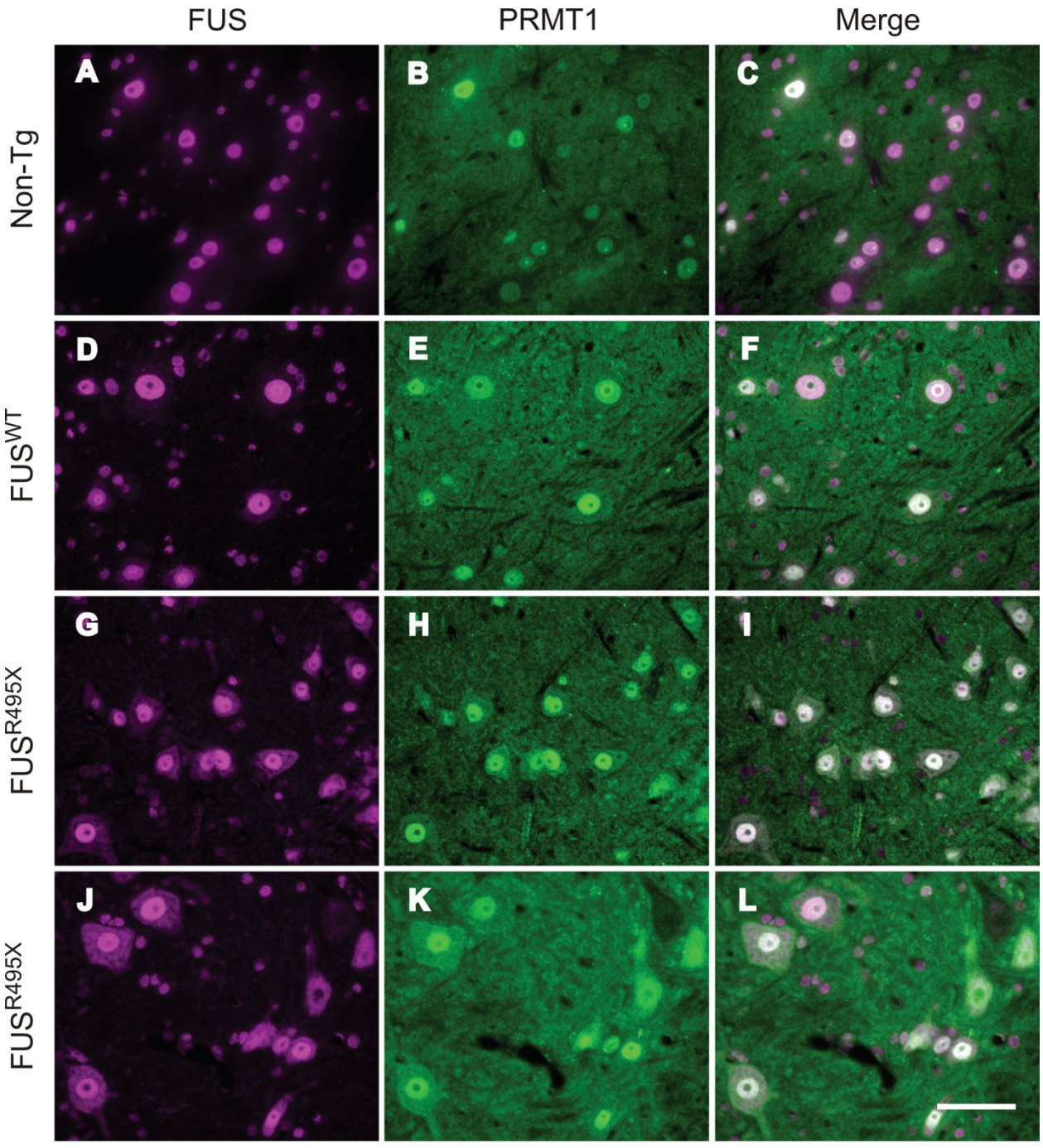
FUS
PRMT1
Merge
Non-Tg
FUSWT
FUSR495X
FUSR495X
A
B
C
D
E
F
G
H
I
J
K
L

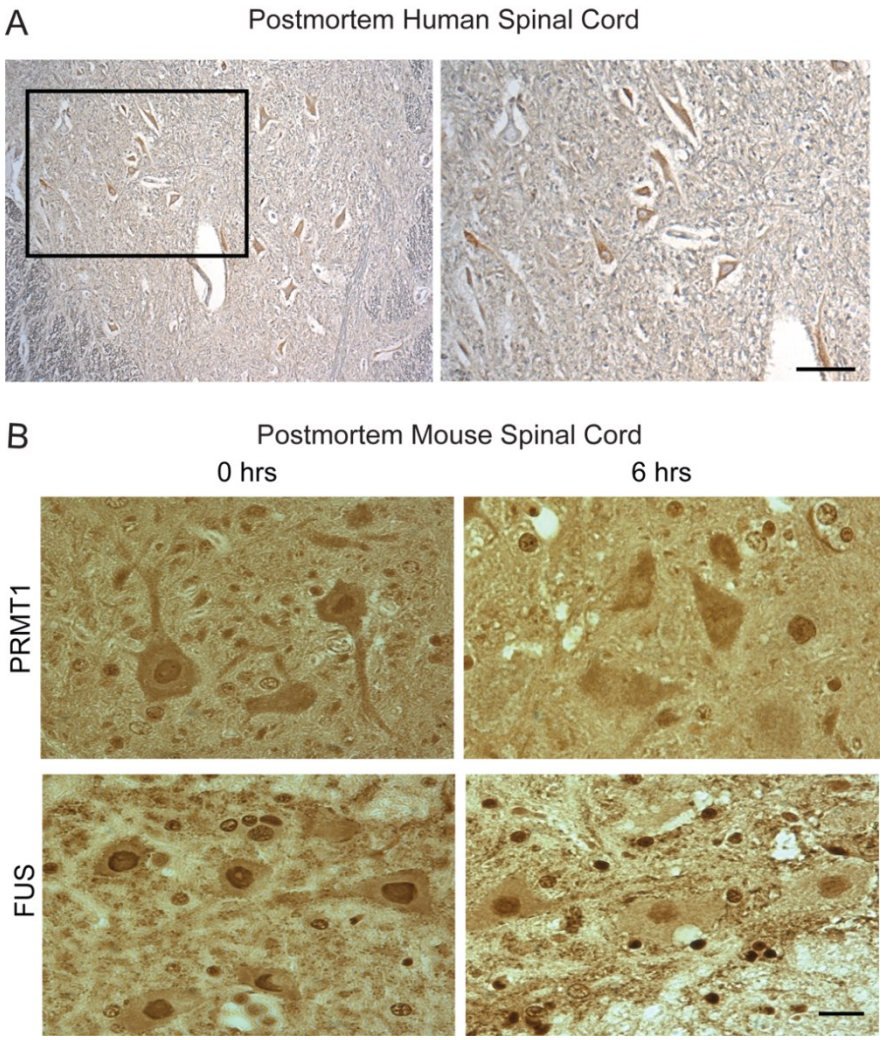

Figure 8. PRMT1 is depleted from the nucleus in archived autopsied human spinal cord and in mouse spinal cord fixed after postmortem interval.

(**A**) Cross section of postmortem spinal cord from a non-neurological control case (immersion fixed and paraffin embedded after excision) immunolabelled with antibody to PRMT1 and counterstained with hematoxylin. Note that PRMT1 is cytoplasmic rather than the expected nuclear distribution. Image to the right is a higher magnification of the boxed area in the left image. (**B**) Mouse spinal cord was excised and fixed by immersion in buffered neutral formalin immediately either after euthanasia or 6 hrs postmortem. Cross-sections from paraffin embedded tissue were labelled with antibody to PRMT1 or FUS. Note that the loss of nuclear PRMT1 with postmortem interval, despite persistence of nuclear FUS. Scale bar = 20 µm.

Figure 9: Brg1 is depleted in neurons expressing mutant FUS and is required for maintenance of dendritic branching.

(A) Double immunolabel of neurons expressing WT or mutant FUS on day 3 post-injection with anti-FLAG/anti-Brg1 antibodies. Arrow head points to nuclei depleted of Brg1. Scale bar = 20μm (**B**) Quantitation of fluorescence intensity from the Brg1 antibody in the nucleus of neurons expressing either WT or mutant FUS. Presented are means ± S.E. of the data. Asterisks indicate significant difference compared to WT nuclear FUS. *p<0.05, **p<0.01, ***p<0.001; (t-test). (**C**) Representative images of neurons expressing mCherry either alone or in the presence of PFI-3 or Brg1 shRNA expression. Scale bar = 30μm. (**D**) Sholl curves of neurons treated with vehicle or varying concentrations of PFI-3. Presented are means ± S.E.M. of the data. "S.D." indicates significant difference compared to vehicle treated neurons (p<0.05, Welch's t-test). (**E**) Sholl curve of neurons expressing mCherry either in the absence or presence of Brg1 shRNA or dominant-negative Brg1. Presented are means ± S.E.M. of the data. "S.D." indicates significant difference compared to mCherry or scramble shRNA (p<0.05; Welch's t-test). (**F-G**) Quantitation of other measures of dendritic morphology. Presented are means ± S.E.M. of the data. Asterisks indicate significant difference compared to respective controls (*** <0.001, t-test).

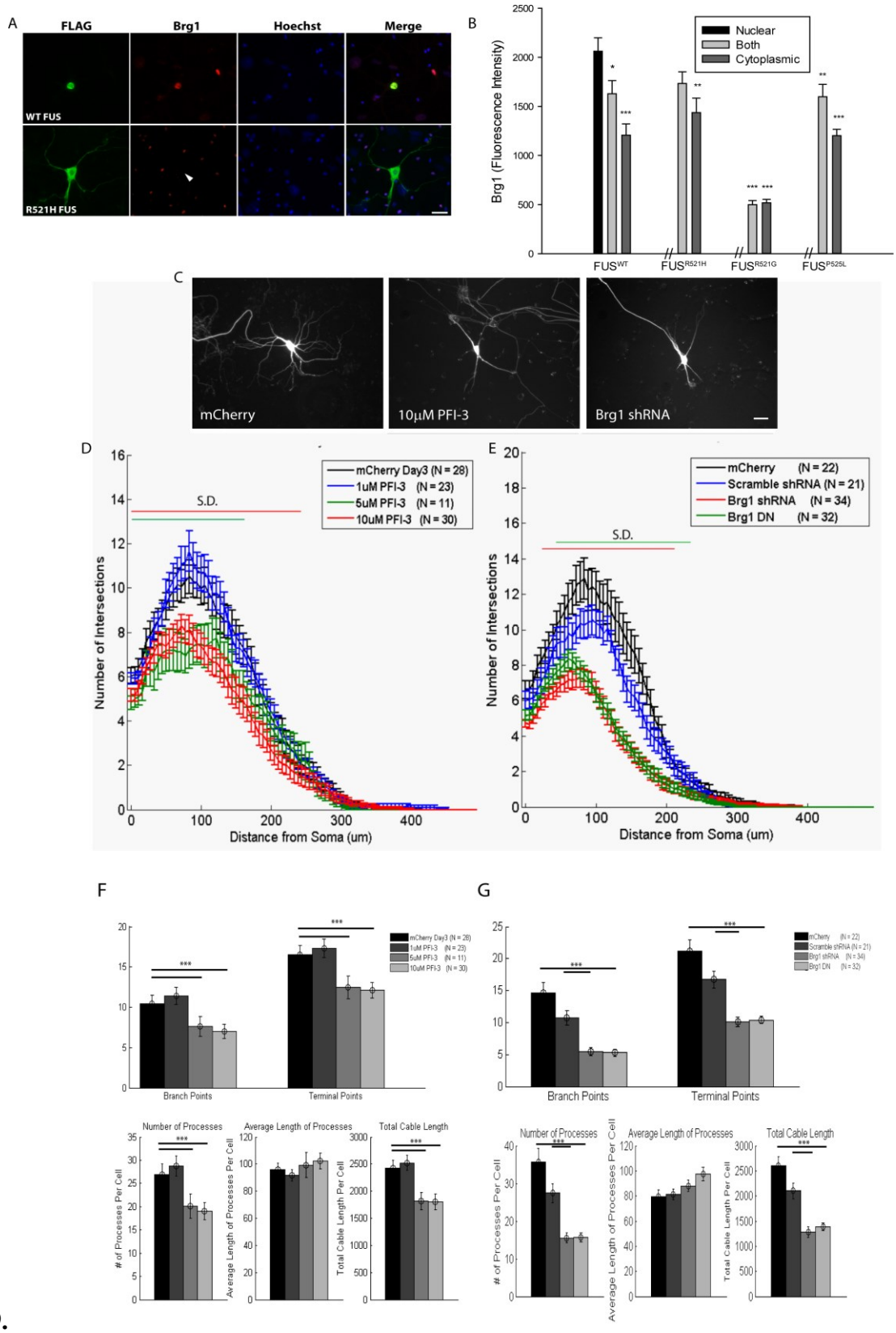
A
FLAG
Brg1
Hoechst
Merge
WT FUS
R521H FUS
B
Brg1 (Fluorescence Intensity)
Nuclear
Both
Cytoplasmic
FUS^WT
FUS^R521H
FUS^R521G
FUS^P525L
C
mCherry
10μM PFI-3
Brg1 shRNA
D
mCherry Day3 (N = 28)
1uM PFI-3 (N = 23)
5uM PFI-3 (N = 11)
10uM PFI-3 (N = 30)
S.D.
Number of Intersections
Distance from Soma (um)
E
mCherry (N = 22)
Scramble shRNA (N = 21)
Brg1 shRNA (N = 34)
Brg1 DN (N = 32)
S.D.
Number of Intersections
Distance from Soma (um)
F
Branch Points
Terminal Points
Number of Processes
Average Length of Processes
Total Cable Length
# of Processes Per Cell
Average Length of Processes Per Cell
Total Cable Length Per Cell
G
Branch Points
Terminal Points
Number of Processes
Average Length of Processes
Total Cable Length
# of Processes Per Cell
Average Length of Processes Per Cell
Total Cable Length Per Cell

Figure 9.

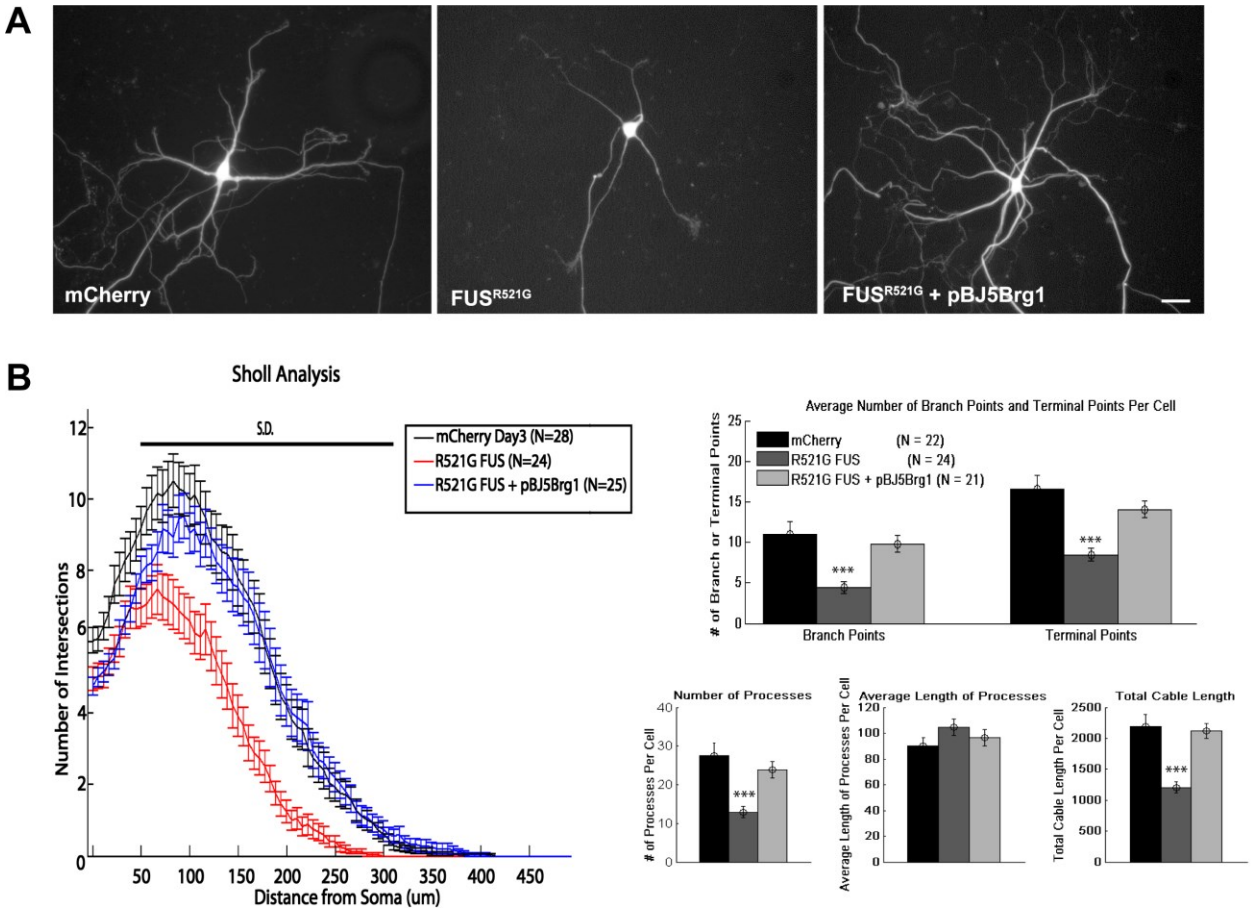

Figure 10. Co-overexpression of Brg1 prevents mutant FUS dendritic attrition

(**A**) Representative images of neurons expressing mCherry along with pcDNA3 empty vector or mutant FUS +/- Brg1 overexpression. Scale bar= 30μm (**B**) Measurements of dendritic morphology representing branching patterns of neurons from A. Presented are means ± S.E.M. of the data. "S.D." indicates a significant difference compared to mCherry/pcDNA3 empty vector ($p<0.05$, Welch's t-test). Asterisks indicate a significant difference compared to mCherry/pcDNA3 empty vector (***$p<0.001$, t-test).

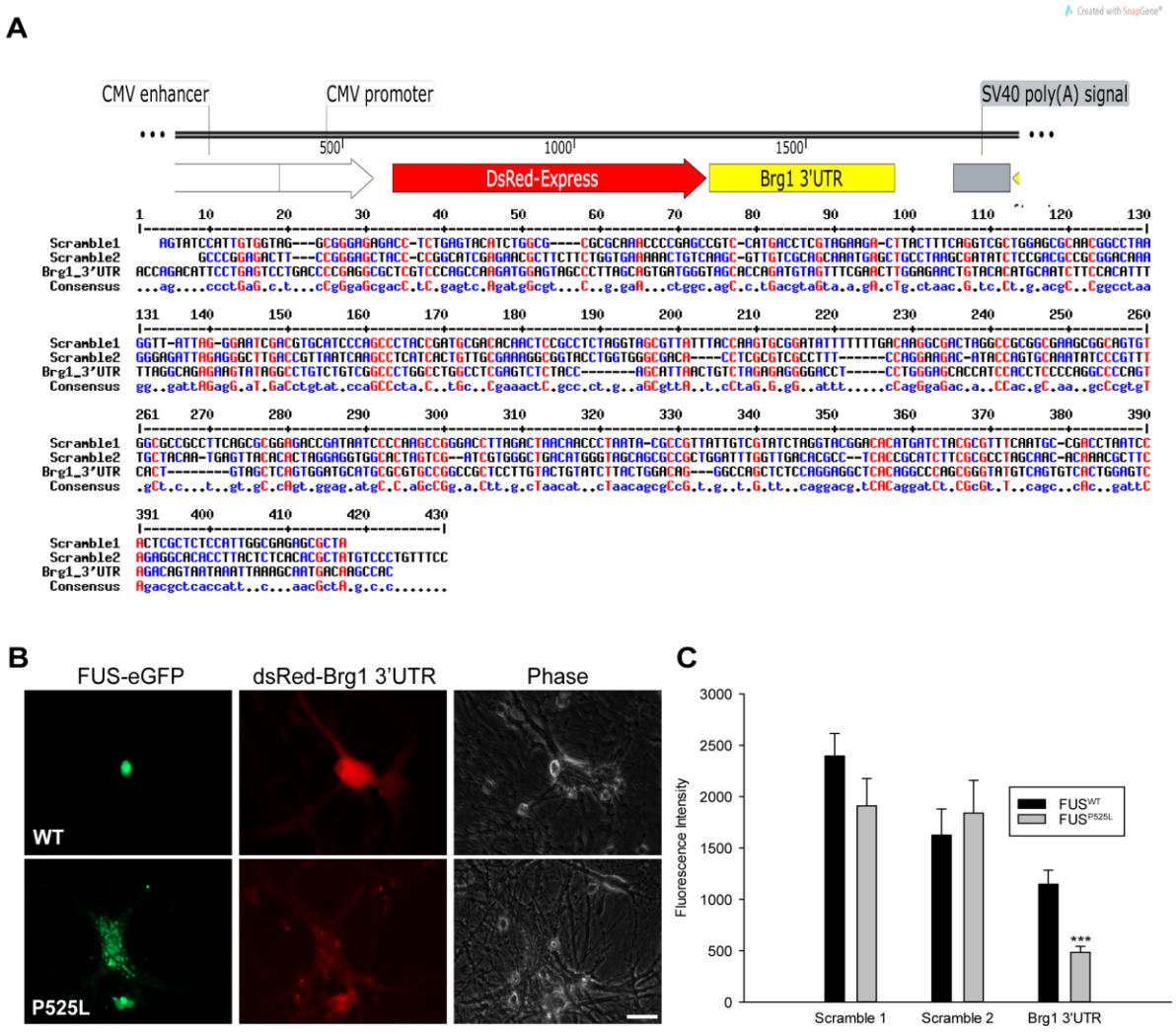

Figure 11. mFUS regulates expression of Brg1 3'UTR containing transcripts

(**A**) Plasmid map of dsRed-Brg1 3'UTR reporter expression system and multiple sequence alignment of scramble and Brg13'UTR sequences used (Multiple sequence alignment with hierarchical clustering, F. CORPET, 1988, Nucl. Acids Res., 16 (22), 10881-10890). (**B**) Representative images of motor neurons expressing dsRed-Brg1 3'UTR along with either WT or mutant eGFP-tagged FUS 2 days post-injection. Scale bar = 20µm (**C**) Fluorescence intensity of dsRed from cell bodies of neurons expressing dsRed-3'UTR (scramble or Brg1) with WT or mutant eGFP-tagged FUS. Asterisks indicate significant difference compared to WT FUS (*** $p<0.001$; t-test).

Figure 12. BAF53b and CREST are also depleted in mFUS containing neurons.

(**A**) Double immunolabel of neurons expressing WT or mutant FUS with anti-FLAG and either anti-BAF53b and anti-CREST antibodies on day 3 post-injection. Outline shows nuclei depleted of nBAF subunits. Scale bar = 20μm. (**B**) Fluorescence intensity of anti-BAF53b or anti-CREST antibodies from the nucleus of neurons expressing WT or mutant FUS on day 3 post-injection. Asterisks indicate significant difference compared to WT nuclear FUS (** $p<0.01$, ***$p<0.001$). (**C**) Representative images of neurons expressing dsRed-BAF53a 3'UTR along with WT or mutant eGFP-tagged FUS on day 2 post-injection. Quantitation of dsRed fluorescence intensity from the cell bodies of these neurons is shown. Asterisks indicate significant difference compared to WT (*** $p<0.001$).

Figure 12.

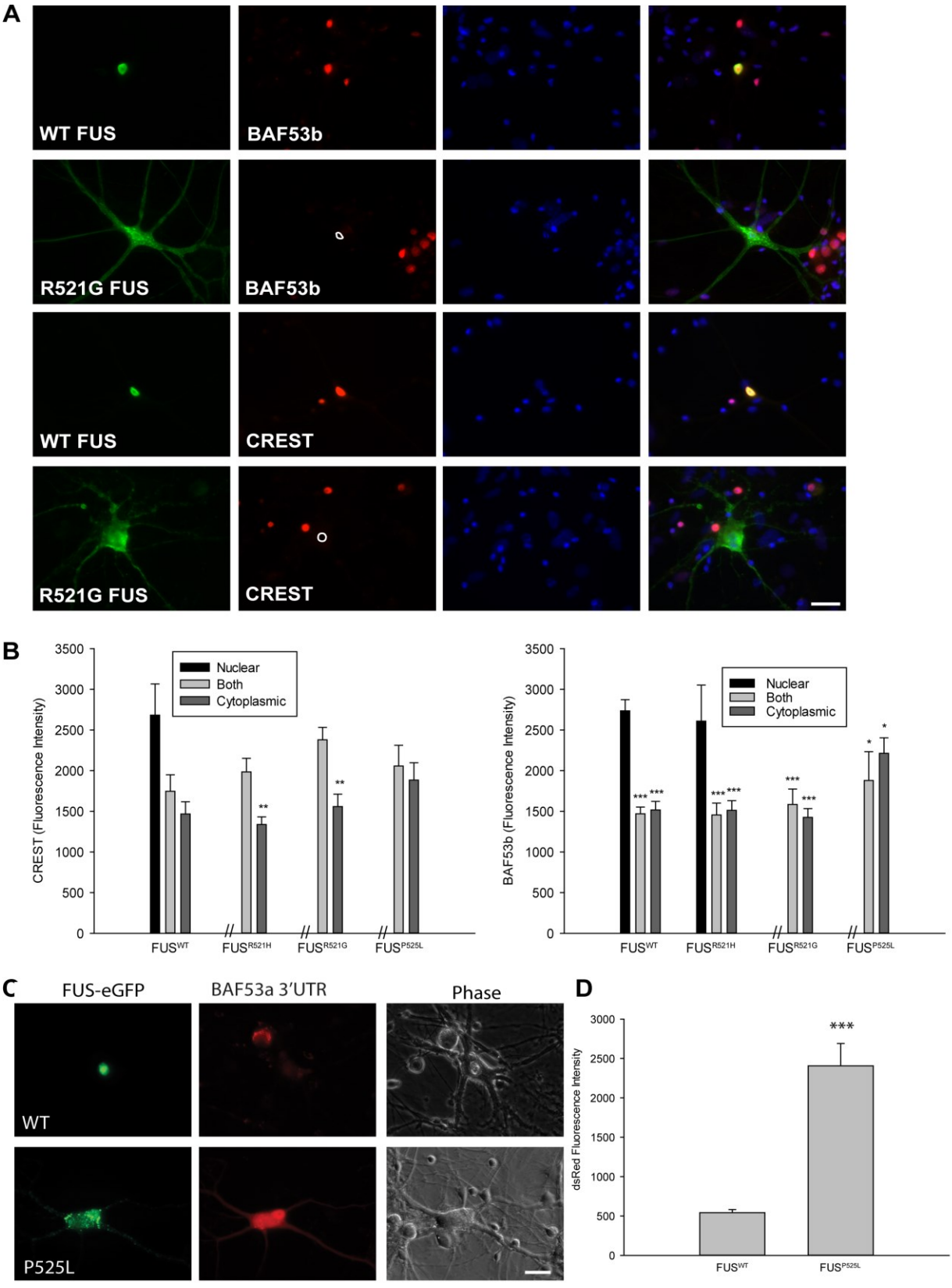
A
WT FUS
BAF53b
R521G FUS
BAF53b
WT FUS
CREST
R521G FUS
CREST
B
CREST (Fluorescence Intensity)
Nuclear
Both
Cytoplasmic
FUSWT
FUSR521H
FUSR521G
FUSP525L
BAF53b (Fluorescence Intensity)
C
FUS-eGFP
BAF53a 3'UTR
Phase
WT
P525L
D
dsRed Fluorescence Intensity
FUSWT
FUSP525L

Figure 13. nBAF subunits are depleted in ALS autopsy tissue

Immunohistochemistry on control and ALS (fALS C9, sALS or A4V SOD1) human spinal cord using antibody to (**A**) Brg1, (**B**) BAF53b or (**C**) CREST. SMI32 antibody was used as a neuronal marker, motor neurons being strongly labelled. Arrow heads point to neuronal nuclei depleted of nBAF subunits. Scale bar = 16μm

Figure 13.

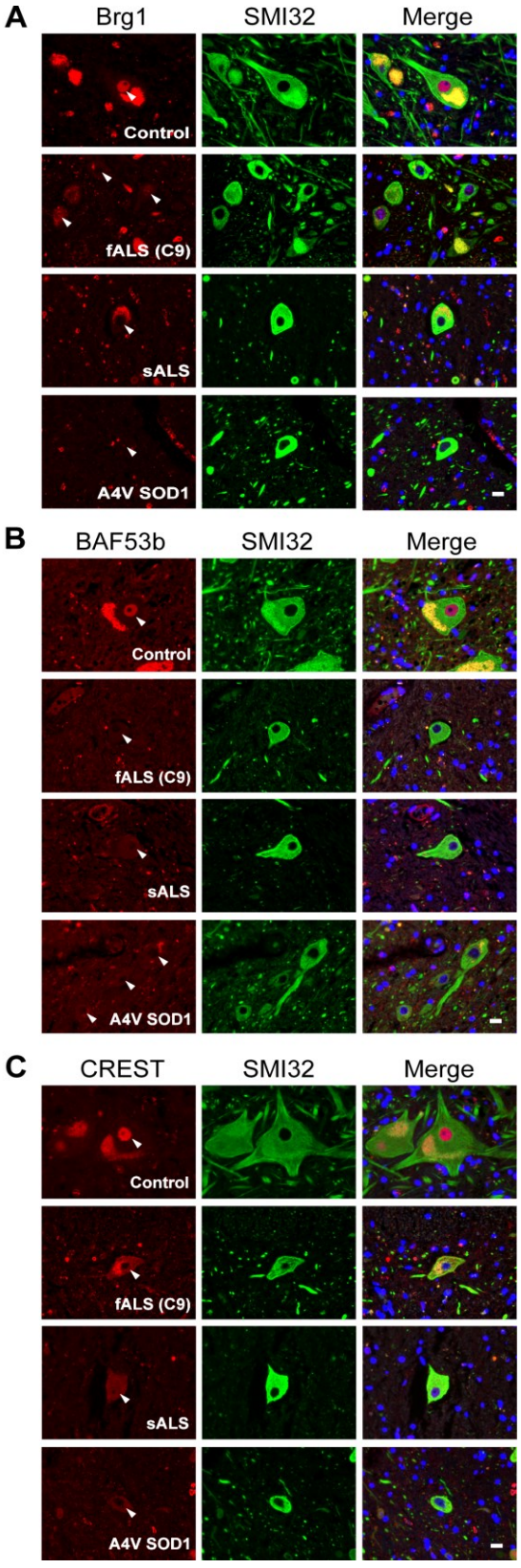
A
Brg1
SMI32
Merge
Control
fALS (C9)
sALS
A4V SOD1
B
BAF53b
SMI32
Merge
Control
fALS (C9)
sALS
A4V SOD1
C
CREST
SMI32
Merge
Control
fALS (C9)
sALS
A4V SOD1

Figure 14. nBAF subunit depletion is independent of TDP43 inclusions in ALS patient autopsy tissue.

Immunohistochemistry was performed on control and ALS (sALS) human autopsy spinal cord using (A) anti-Brg1, (B) anti-BAF53b and (C) anti-CREST antibodies. SMI32 was used as a neuronal marker. Serial sections were also labelled with anti-TDP43 to observe presence of nuclear TDP43 or TDP43 positive inclusions. For each nBAF subunit, a neuron with or without TDP43 cytoplasmic inclusions is shown to illustrate that expression of nBAF subunits is reduced in neurons regardless of TDP43-positive inclusions. Scale bar = 16μm

Figure 14.

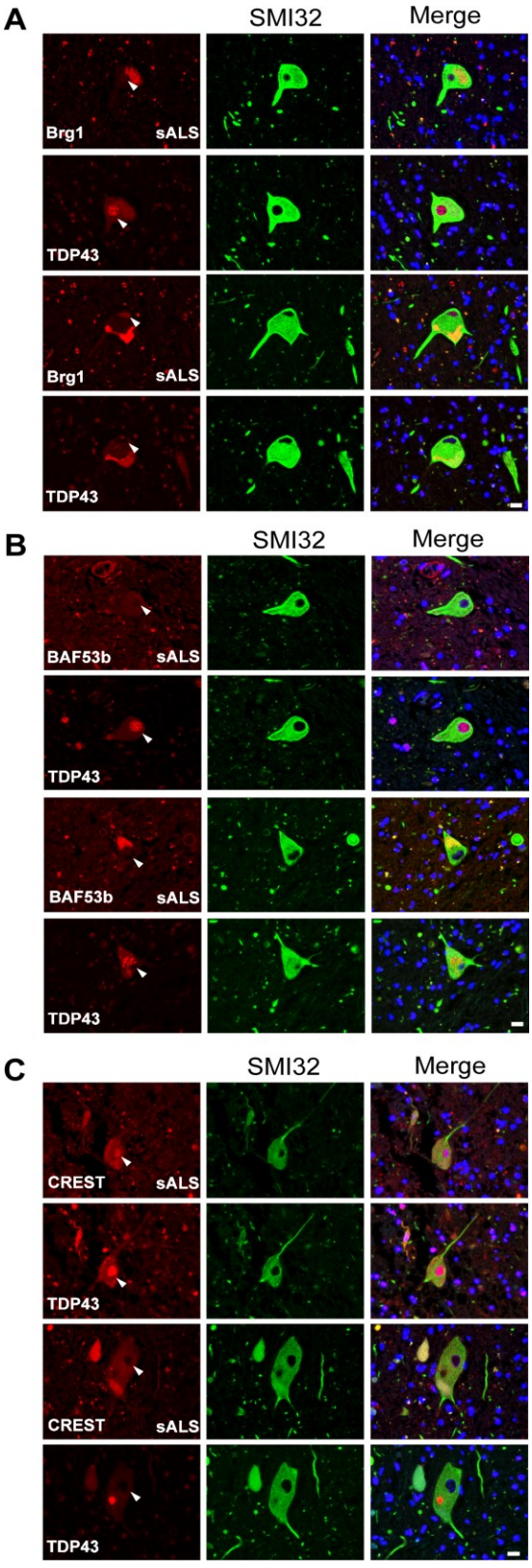
A
SMI32
Merge
Brg1
sALS
TDP43
Brg1
sALS
TDP43
B
SMI32
Merge
BAF53b
sALS
TDP43
BAF53b
sALS
TDP43
C
SMI32
Merge
CREST
sALS
TDP43
CREST
sALS
TDP43

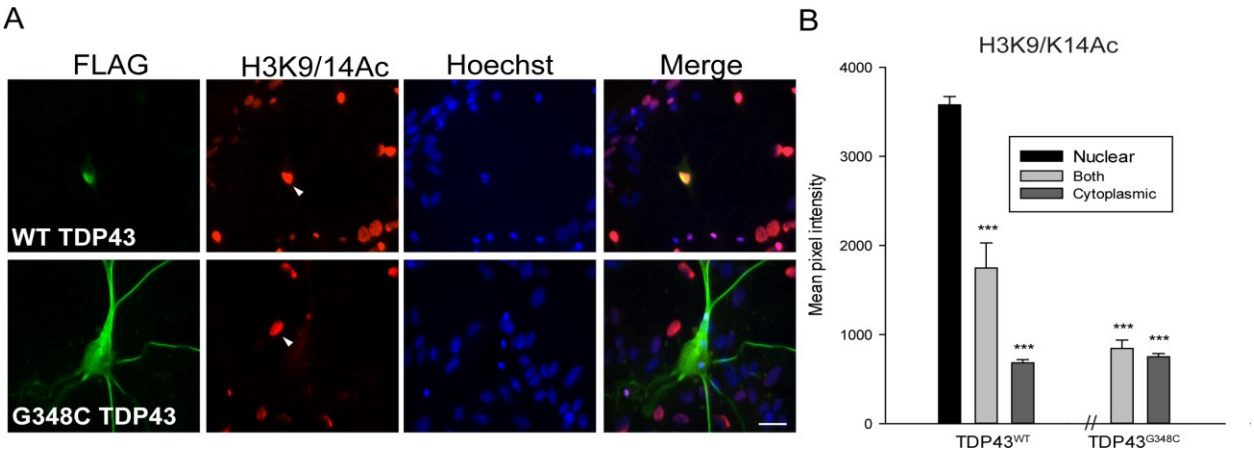

Figure 15. Decreased H3K9/14Ac in neurons with cytoplasmic TDP43.

(**A**) Double-labelling of motor neurons expressing either WT or mutant TDP43, with antibodies to FLAG and acetylated histone 3 (H3K9/14Ac) on day 3 post-injection. (**B**) Mean fluorescence intensity of H3K9/14Ac antibody labelling corresponding to localization of TDP43. Presented are means ± S.E.M. of data collected in n=36 neurons expressing $TDP43^{WT}$ and n=27 neurons expressing $TDP43^{G348C}$. Asterisks indicate significant difference compared to nuclear WT TDP43 (***$p<0.001$; t-test). Scale bar = 20 µm

Figure 16. nBAF subunit depletion in neurons with cytoplasmic TDP43.

(A) Double immunolabelling of neurons expressing WT or mutant TDP43 with anti-FLAG and anti-Brg1, anti-BAF53b or anti-CREST on day 3 post-injection. Scale bar = 20μm. (**B**) Fluorescence intensity measurements from nBAF subunit antibodies in the area of the nucleus of neurons expressing WT or mutant FUS. Presented are means ± S.E.M. of data. Asterisks indicate significant difference compared to nuclear WT TDP43 (*$p<0.05$, **$p<0.01$, ***$p<0.001$; t-test).

Figure 16.

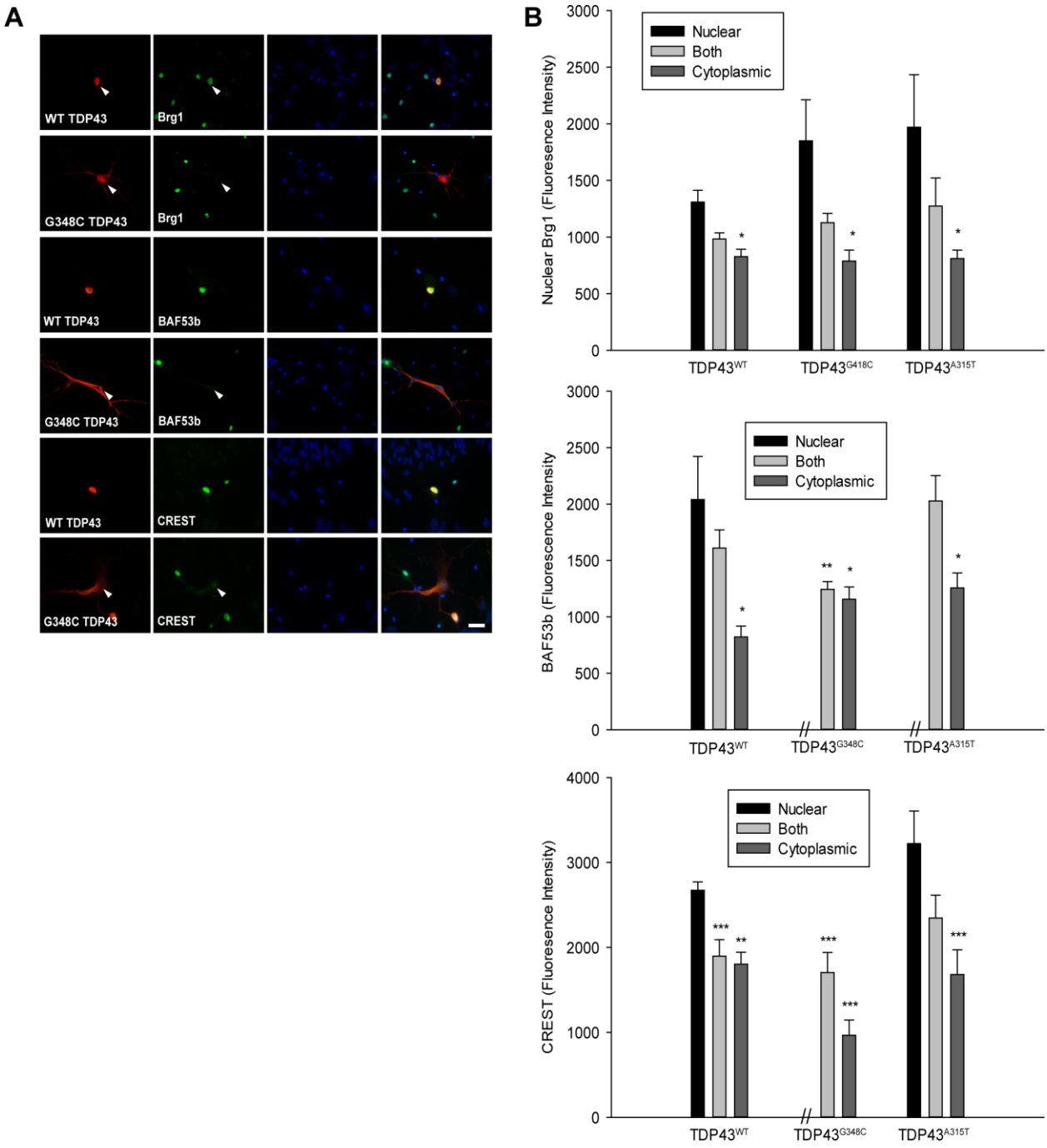
A
WT TDP43
Brg1
G348C TDP43
Brg1
WT TDP43
BAF53b
G348C TDP43
BAF53b
WT TDP43
CREST
G348C TDP43
CREST
B
Nuclear
Both
Cytoplasmic
Nuclear Brg1 (Fluoresence Intensity)
TDP43WT
TDP43G418C
TDP43A315T
BAF53b (Fluorescence Intensity)
TDP43G348C
CREST (Fluoresence Intensity)

Figure 17. Mutant TDP43-induced dendritic attrition can be prevented by Brg1 overexpression and SAHA treatment

(**A**) Measurements of dendritic morphology of neurons expressing WT or mutant TDP43 for three days. Asterisks indicate significant difference compared to mCherry control (***$p<0.001$; Welch's t-test). (**B**) Measurements of dendritic morphology of neurons expressing mutant TDP43 +/- human Brg1. "S.D." indicates significance compared to mCherry control ($p<0.05$, Welch's t-test). Asterisks indicate significant difference compared to mCherry control. (**C**) Measurements of dendritic morphology of neurons expressing mutant TDP43 +/- SAHA treatment. For all analyses, mCherry + pcDNA3 vector was used as an injection control. "S.D." indicates significant difference between mutant FUS DMSO and mCherry DMSO ($p<0.05$, Welch's t-test). Asterisks indicate significant difference between mutant FUS DMSO and mCherry DMSO (***$p<0.001$; t-test).

Figure 17.

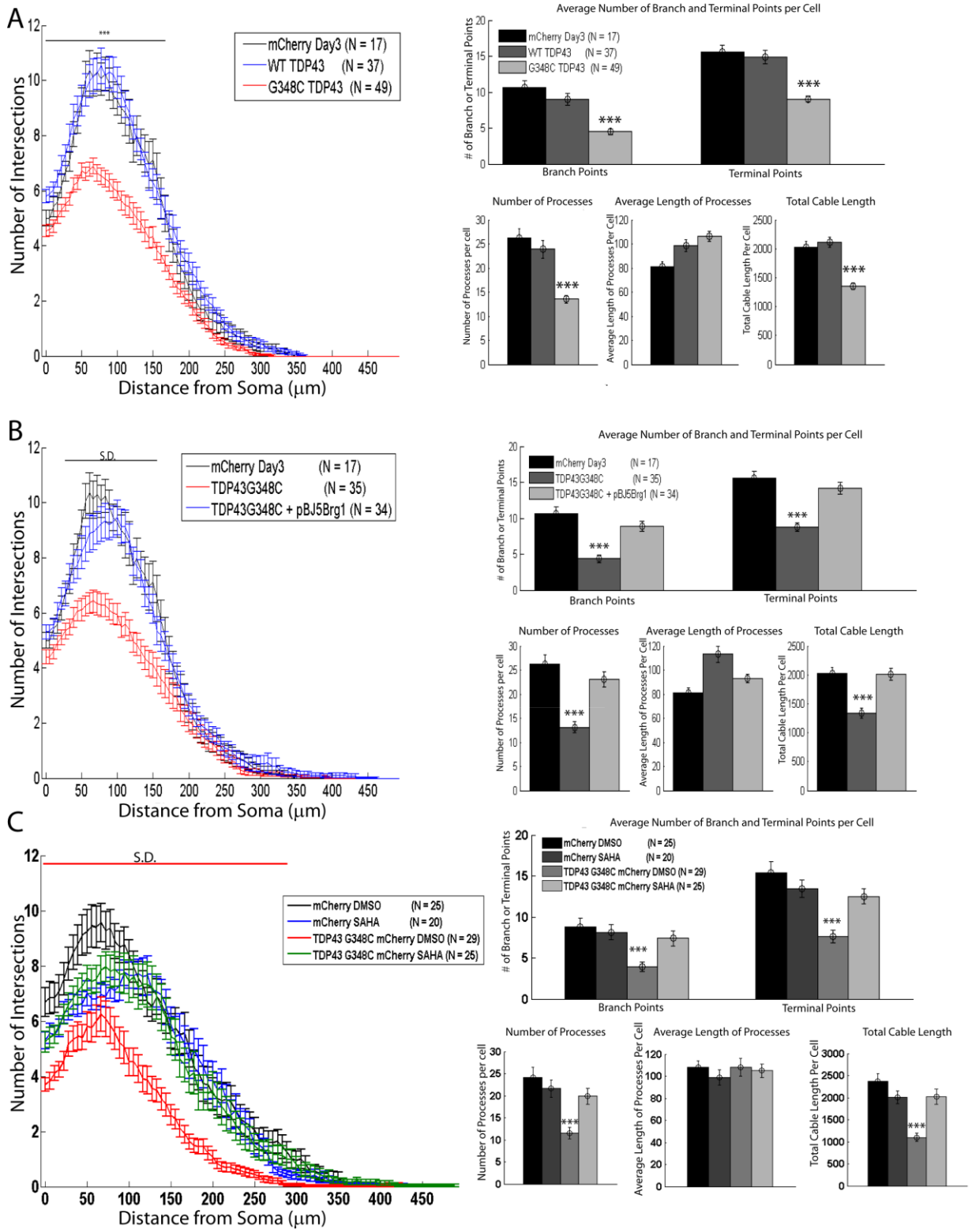
A
B
C
Number of Intersections
Distance from Soma (μm)
S.D.
mCherry Day3 (N = 17)
WT TDP43 (N = 37)
G348C TDP43 (N = 49)
TDP43G348C (N = 35)
TDP43G348C + pBJ5Brg1 (N = 34)
mCherry DMSO (N = 25)
mCherry SAHA (N = 20)
TDP43 G348C mCherry DMSO (N = 29)
TDP43 G348C mCherry SAHA (N = 25)
Average Number of Branch and Terminal Points per Cell
# of Branch or Terminal Points
Branch Points
Terminal Points
Number of Processes
Number of Processes per cell
Average Length of Processes
Average Length of Processes Per Cell
Total Cable Length
Total Cable Length Per Cell
***

References:

Al-Chalabi A, Jones A, Troakes C, King A, Al-Sarraj S, van den Berg LH (2012) The genetics and neuropathology of amyotrophic lateral sclerosis. Acta Neuropathol 124:339-352.

Alexianu ME, Kozovska M, Appel SH (2001) Immune reactivity in a mouse model of familial ALS correlates with disease progression. Neurology 57:1282-1289.

Almeida S, Gascon E, Tran H, Chou HJ, Gendron TF, Degroot S, Tapper AR, Sellier C, Charlet-Berguerand N, Karydas A, Seeley WW, Boxer AL, Petrucelli L, Miller BL, Gao FB (2013) Modeling key pathological features of frontotemporal dementia with C9ORF72 repeat expansion in iPSC-derived human neurons. Acta Neuropathol 126:385-399.

Anderson P, Kedersha N (2009) Stress granules. Current Biology 19:R397-R398.

Appel SH, Beers D, Siklos L, Engelhardt JI, Mosier DR (2001) Calcium: the Darth Vader of ALS. Amyotrophic lateral sclerosis and other motor neuron disorders : official publication of the World Federation of Neurology, Research Group on Motor Neuron Diseases 2 Suppl 1:S47-54.

Arai T, Hasegawa M, Akiyama H, Ikeda K, Nonaka T, Mori H, Mann D, Tsuchiya K, Yoshida M, Hashizume Y, Oda T (2006) TDP-43 is a component of ubiquitin-positive tau-negative inclusions in frontotemporal lobar degeneration and amyotrophic lateral sclerosis. Biochemical and biophysical research communications 351:602-611.

Armstrong RA, Gearing M, Bigio EH, Cruz-Sanchez FF, Duyckaerts C, Mackenzie IR, Perry RH, Skullerud K, Yokoo H, Cairns NJ (2011) Spatial patterns of FUS-immunoreactive neuronal cytoplasmic inclusions (NCI) in neuronal intermediate filament inclusion disease (NIFID). Journal of neural transmission (Vienna, Austria : 1996) 118:1651-1657.

Ash PE, Bieniek KF, Gendron TF, Caulfield T, Lin WL, Dejesus-Hernandez M, van Blitterswijk MM, Jansen-West K, Paul JW, 3rd, Rademakers R, Boylan KB, Dickson DW, Petrucelli L (2013) Unconventional translation of C9ORF72 GGGGCC expansion generates insoluble polypeptides specific to c9FTD/ALS. Neuron 77:639-646.

Barbee SA, Estes PS, Cziko AM, Hillebrand J, Luedeman RA, Coller JM, Johnson N, Howlett IC, Geng C, Ueda R, Brand AH, Newbury SF, Wilhelm JE, Levine RB, Nakamura A, Parker R, Ramaswami M (2006) Staufen- and FMRP-containing neuronal RNPs are structurally and functionally related to somatic P bodies. Neuron 52:997-1009.

Baumer D, Hilton D, Paine SM, Turner MR, Lowe J, Talbot K, Ansorge O (2010) Juvenile ALS with basophilic inclusions is a FUS proteinopathy with FUS mutations. Neurology 75:611-618.

Bedford MT, Clarke SG (2009) Protein arginine methylation in mammals: who, what, and why. Molecular cell 33:1-13.

Belzil VV, Bauer PO, Prudencio M, Gendron TF, Stetler CT, Yan IK, Pregent L, Daughrity L, Baker MC, Rademakers R, Boylan K, Patel TC, Dickson DW, Petrucelli L (2013a)

Reduced C9orf72 gene expression in c9FTD/ALS is caused by histone trimethylation, an epigenetic event detectable in blood. Acta Neuropathol 126:895-905.

Belzil VV, Bauer PO, Prudencio M, Gendron TF, Stetler CT, Yan IK, Pregent L, Daughrity L, Baker MC, Rademakers R, Boylan K, Patel TC, Dickson DW, Petrucelli L (2013b) Reduced C9orf72 gene expression in c9FTD/ALS is caused by histone trimethylation, an epigenetic event detectable in blood. Acta Neuropathologica 126:895-905.

Bendotti C, Calvaresi N, Chiveri L, Prelle A, Moggio M, Braga M, Silani V, De Biasi S (2001) Early vacuolization and mitochondrial damage in motor neurons of FALS mice are not associated with apoptosis or with changes in cytochrome oxidase histochemical reactivity. J Neurol Sci 191:25-33.

Bergeron C, Beric-Maskarel K, Muntasser S, Weyer L, Somerville MJ, Percy ME (1994) Neurofilament light and polyadenylated mRNA levels are decreased in amyotrophic lateral sclerosis motor neurons. J Neuropathol Exp Neurol 53:221-230.

Bicker KL, Thompson PR (2013) The protein arginine deiminases: Structure, function, inhibition, and disease. Biopolymers 99:155-163.

Blair IP, Williams KL, Warraich ST, Durnall JC, Thoeng AD, Manavis J, Blumbergs PC, Vucic S, Kiernan MC, Nicholson GA (2010) FUS mutations in amyotrophic lateral sclerosis: clinical, pathological, neurophysiological and genetic analysis. Journal of neurology, neurosurgery, and psychiatry 81:639-645.

Blijham PJ, Schelhaas HJ, Ter Laak HJ, van Engelen BG, Zwarts MJ (2007) Early diagnosis of ALS: the search for signs of denervation in clinically normal muscles. Journal of the neurological sciences 263:154-157.

Boisvert FM, Cote J, Boulanger MC, Richard S (2003) A proteomic analysis of arginine-methylated protein complexes. Molecular & cellular proteomics : MCP 2:1319-1330.

Borchelt DR, Lee MK, Slunt HS, Guarnieri M, Xu ZS, Wong PC, Brown RH, Jr., Price DL, Sisodia SS, Cleveland DW (1994) Superoxide dismutase 1 with mutations linked to familial amyotrophic lateral sclerosis possesses significant activity. Proceedings of the National Academy of Sciences of the United States of America 91:8292-8296.

Borthwick GM, Johnson MA, Ince PG, Shaw PJ, Turnbull DM (1999) Mitochondrial enzyme activity in amyotrophic lateral sclerosis: implications for the role of mitochondria in neuronal cell death. Annals of neurology 46:787-790.

Bosco DA, Lemay N, Ko HK, Zhou H, Burke C, Kwiatkowski TJ, Jr., Sapp P, McKenna-Yasek D, Brown RH, Jr., Hayward LJ (2010) Mutant FUS proteins that cause amyotrophic lateral sclerosis incorporate into stress granules. Hum Mol Genet 19:4160-4175.

Bruijn LI, Becher MW, Lee MK, Anderson KL, Jenkins NA, Copeland NG, Sisodia SS, Rothstein JD, Borchelt DR, Price DL, Cleveland DW (1997) ALS-linked SOD1 mutant G85R mediates damage to astrocytes and promotes rapidly progressive disease with SOD1-containing inclusions. Neuron 18:327-338.

Byrne S, Walsh C, Lynch C, Bede P, Elamin M, Kenna K, McLaughlin R, Hardiman O (2011) Rate of familial amyotrophic lateral sclerosis: a systematic review and meta-analysis. Journal of neurology, neurosurgery, and psychiatry 82:623-627.

Campos-Melo D, Droppelmann CA, He Z, Volkening K, Strong MJ (2013) Altered microRNA expression profile in Amyotrophic Lateral Sclerosis: a role in the regulation of NFL mRNA levels. Mol Brain 6:26.

Celio MR (1990) Calbindin D-28k and parvalbumin in the rat nervous system. Neuroscience 35:375-475.

Cha JR, St Louis KJ, Tradewell ML, Gentil BJ, Minotti S, Jaffer ZM, Chen R, Rubenstein AE, Durham HD (2014) A novel small molecule HSP90 inhibitor, NXD30001, differentially induces heat shock proteins in nervous tissue in culture and in vivo. Cell stress & chaperones 19:421-435.

Chang B, Chen Y, Zhao Y, Bruick RK (2007) JMJD6 Is a Histone Arginine Demethylase. Science 318:444-447.

Cheng D, Cote J, Shaaban S, Bedford MT (2007) The arginine methyltransferase CARM1 regulates the coupling of transcription and mRNA processing. Molecular cell 25:71-83.

Cheng D, Yadav N, King RW, Swanson MS, Weinstein EJ, Bedford MT (2004) Small molecule regulators of protein arginine methyltransferases. J Biol Chem 279:23892-23899.

Cheroni C, Peviani M, Cascio P, Debiasi S, Monti C, Bendotti C (2005) Accumulation of human SOD1 and ubiquitinated deposits in the spinal cord of SOD1G93A mice during motor neuron disease progression correlates with a decrease of proteasome. Neurobiology of disease 18:509-522.

Chesi A, Staahl BT, Jovicic A, Couthouis J, Fasolino M, Raphael AR, Yamazaki T, Elias L, Polak M, Kelly C, Williams KL, Fifita JA, Maragakis NJ, Nicholson GA, King OD, Reed R, Crabtree GR, Blair IP, Glass JD, Gitler AD (2013) Exome sequencing to identify de novo mutations in sporadic ALS trios. Nat Neurosci 16:851-855.

Cheung P, Allis CD, Sassone-Corsi P (2000) Signaling to chromatin through histone modifications. Cell 103:263-271.

Chew J, Gendron TF, Prudencio M, Sasaguri H, Zhang YJ, Castanedes-Casey M, Lee CW, Jansen-West K, Kurti A, Murray ME, Bieniek KF, Bauer PO, Whitelaw EC, Rousseau L, Stankowski JN, Stetler C, Daughrity LM, Perkerson EA, Desaro P, Johnston A, Overstreet K, Edbauer D, Rademakers R, Boylan KB, Dickson DW, Fryer JD, Petrucelli L (2015) Neurodegeneration. C9ORF72 repeat expansions in mice cause TDP-43 pathology, neuronal loss, and behavioral deficits. Science 348:1151-1154.

Chittka A (2010) Dynamic Distribution of Histone H4 Arginine 3 Methylation Marks in the Developing Murine Cortex. PloS one 5:e13807.

Chung YH, Joo KM, Lee YJ, Kim MJ, Cha CI (2003) Immunohistochemical study on the aggregation of ubiquitin in the central nervous system of the transgenic mice expressing a human Cu/Zn SOD mutation. Neurological research 25:395-400.

Coffee B, Zhang F, Ceman S, Warren ST, Reines D (2002) Histone modifications depict an aberrantly heterochromatinized FMR1 gene in fragile x syndrome. American journal of human genetics 71:923-932.

Conte A, Lattante S, Zollino M, Marangi G, Luigetti M, Del Grande A, Servidei S, Trombetta F, Sabatelli M (2012) P525L FUS mutation is consistently associated with a severe form of juvenile amyotrophic lateral sclerosis. Neuromuscul Disord 22:73-75.

Corbo M, Hays AP (1992) Peripherin and neurofilament protein coexist in spinal spheroids of motor neuron disease. Journal of neuropathology and experimental neurology 51:531-537.

Corrado L, Mazzini L, Oggioni GD, Luciano B, Godi M, Brusco A, D'Alfonso S (2011) ATXN-2 CAG repeat expansions are interrupted in ALS patients. Hum Genet 130:575-580.

Cote J, Boisvert FM, Boulanger MC, Bedford MT, Richard S (2003) Sam68 RNA binding protein is an in vivo substrate for protein arginine N-methyltransferase 1. Mol Biol Cell 14:274-287.

Couthouis J, Hart MP, Shorter J, DeJesus-Hernandez M, Erion R, Oristano R, Liu AX, Ramos D, Jethava N, Hosangadi D, Epstein J, Chiang A, Diaz Z, Nakaya T, Ibrahim F, Kim HJ, Solski JA, Williams KL, Mojsilovic-Petrovic J, Ingre C, Boylan K, Graff-Radford NR, Dickson DW, Clay-Falcone D, Elman L, McCluskey L, Greene R, Kalb RG, Lee VM, Trojanowski JQ, Ludolph A, Robberecht W, Andersen PM, Nicholson GA, Blair IP, King OD, Bonini NM, Van Deerlin V, Rademakers R, Mourelatos Z, Gitler AD (2011) A yeast functional screen predicts new candidate ALS disease genes. Proceedings of the National Academy of Sciences of the United States of America 108:20881-20890.

Cruts M, Gijselinck I, Van Langenhove T, van der Zee J, Van Broeckhoven C (2013) Current insights into the C9orf72 repeat expansion diseases of the FTLD/ALS spectrum. Trends Neurosci 36:450-459.

Cudkowicz ME, Andres PL, Macdonald SA, Bedlack RS, Choudry R, Brown RH, Jr., Zhang H, Schoenfeld DA, Shefner J, Matson S, Matson WR, Ferrante RJ (2009) Phase 2 study of sodium phenylbutyrate in ALS. Amyotrophic lateral sclerosis : official publication of the World Federation of Neurology Research Group on Motor Neuron Diseases 10:99-106.

Daoud H, Suhail H, Sabbagh M, Belzil V, Szuto A, Dionne-Laporte A, Khoris J, Camu W, Salachas F, Meininger V, Mathieu J, Strong M, Dion PA, Rouleau GA (2012) C9orf72 hexanucleotide repeat expansions as the causative mutation for chromosome 9p21-linked amyotrophic lateral sclerosis and frontotemporal dementia. Arch Neurol 69:1159-1163.

Das A, Sribnick EA, Wingrave JM, Del Re AM, Woodward JJ, Appel SH, Banik NL, Ray SK (2005) Calpain activation in apoptosis of ventral spinal cord 4.1 (VSC4.1) motoneurons

exposed to glutamate: calpain inhibition provides functional neuroprotection. Journal of neuroscience research 81:551-562.

DeJesus-Hernandez M, Mackenzie IR, Boeve BF, Boxer AL, Baker M, Rutherford NJ, Nicholson AM, Finch NA, Flynn H, Adamson J, Kouri N, Wojtas A, Sengdy P, Hsiung GY, Karydas A, Seeley WW, Josephs KA, Coppola G, Geschwind DH, Wszolek ZK, Feldman H, Knopman DS, Petersen RC, Miller BL, Dickson DW, Boylan KB, Graff-Radford NR, Rademakers R (2011) Expanded GGGGCC hexanucleotide repeat in noncoding region of C9ORF72 causes chromosome 9p-linked FTD and ALS. Neuron 72:245-256.

Deng HX, Zhai H, Bigio EH, Yan J, Fecto F, Ajroud K, Mishra M, Ajroud-Driss S, Heller S, Sufit R, Siddique N, Mugnaini E, Siddique T (2010) FUS-immunoreactive inclusions are a common feature in sporadic and non-SOD1 familial amyotrophic lateral sclerosis. Annals of neurology 67:739-748.

Dormann D, Madl T, Valori CF, Bentmann E, Tahirovic S, Abou-Ajram C, Kremmer E, Ansorge O, Mackenzie IR, Neumann M, Haass C (2012) Arginine methylation next to the PY-NLS modulates Transportin binding and nuclear import of FUS. The EMBO journal 31:4258-4275.

Dormann D, Rodde R, Edbauer D, Bentmann E, Fischer I, Hruscha A, Than ME, Mackenzie IR, Capell A, Schmid B, Neumann M, Haass C (2010) ALS-associated fused in sarcoma (FUS) mutations disrupt Transportin-mediated nuclear import. Embo J 29:2841-2857.

Du K, Arai S, Kawamura T, Matsushita A, Kurokawa R (2011) TLS and PRMT1 synergistically coactivate transcription at the survivin promoter through TLS arginine methylation. Biochemical and biophysical research communications 404:991-996.

Durham HD (1992) An antibody against hyperphosphorylated neurofilament proteins collapses the neurofilament network in motor neurons but not in dorsal root ganglion cells. Journal of neuropathology and experimental neurology 51:287-297.

Durham HD, Roy J, Dong L, Figlewicz DA (1997) Aggregation of mutant Cu/Zn superoxide dismutase proteins in a culture model of ALS. J Neuropathol Exp Neurol 56:523-530.

Eiges R, Urbach A, Malcov M, Frumkin T, Schwartz T, Amit A, Yaron Y, Eden A, Yanuka O, Benvenisty N, Ben-Yosef D (2007) Developmental study of fragile X syndrome using human embryonic stem cells derived from preimplantation genetically diagnosed embryos. Cell stem cell 1:568-577.

Engelhardt JI, Appel SH (1990) IgG reactivity in the spinal cord and motor cortex in amyotrophic lateral sclerosis. Arch Neurol 47:1210-1216.

Eystathioy T, Chan EK, Takeuchi K, Mahler M, Luft LM, Zochodne DW, Fritzler MJ (2003) Clinical and serological associations of autoantibodies to GW bodies and a novel cytoplasmic autoantigen GW182. J Mol Med (Berl) 81:811-818.

Eystathioy T, Chan EK, Tenenbaum SA, Keene JD, Griffith K, Fritzler MJ (2002) A phosphorylated cytoplasmic autoantigen, GW182, associates with a unique population of human mRNAs within novel cytoplasmic speckles. Mol Biol Cell 13:1338-1351.

Farg MA, Sundaramoorthy V, Sultana JM, Yang S, Atkinson RA, Levina V, Halloran MA, Gleeson PA, Blair IP, Soo KY, King AE, Atkin JD (2014) C9ORF72, implicated in amytrophic lateral sclerosis and frontotemporal dementia, regulates endosomal trafficking. Hum Mol Genet 23:3579-3595.

Finelli MJ, Liu KX, Wu Y, Oliver PL, Davies KE (2015) Oxr1 improves pathogenic cellular features of ALS-associated FUS and TDP-43 mutations. Hum Mol Genet 24:3529-3544.

Fischer LR, Culver DG, Tennant P, Davis AA, Wang M, Castellano-Sanchez A, Khan J, Polak MA, Glass JD (2004) Amyotrophic lateral sclerosis is a distal axonopathy: evidence in mice and man. Experimental neurology 185:232-240.

Fridovich I (1995) Superoxide radical and superoxide dismutases. Annual review of biochemistry 64:97-112.

Fridovich I (1997) Superoxide anion radical (O2-.), superoxide dismutases, and related matters. J Biol Chem 272:18515-18517.

Fujii R, Takumi T (2005) TLS facilitates transport of mRNA encoding an actin-stabilizing protein to dendritic spines. J Cell Sci 118:5755-5765.

Gal J, Zhang J, Kwinter DM, Zhai J, Jia H, Jia J, Zhu H (2011) Nuclear localization sequence of FUS and induction of stress granules by ALS mutants. Neurobiol Aging 32:2323 e2327-2340.

Gelpi E, Llado A, Clarimon J, Rey MJ, Rivera RM, Ezquerra M, Antonell A, Navarro-Otano J, Ribalta T, Pinol-Ripoll G, Perez A, Valldeoriola F, Ferrer I (2012) Phenotypic variability within the inclusion body spectrum of basophilic inclusion body disease and neuronal intermediate filament inclusion disease in frontotemporal lobar degenerations with FUS-positive inclusions. Journal of neuropathology and experimental neurology 71:795-805.

Gendron TF, Belzil VV, Zhang Y-J, Petrucelli L (2014) Mechanisms of Toxicity in C9FTLD/ALS. Acta neuropathologica 127:359-376.

Gijselinck I, Van Langenhove T, van der Zee J, Sleegers K, Philtjens S, Kleinberger G, Janssens J, Bettens K, Van Cauwenberghe C, Pereson S, Engelborghs S, Sieben A, De Jonghe P, Vandenberghe R, Santens P, De Bleecker J, Maes G, Baumer V, Dillen L, Joris G, Cuijt I, Corsmit E, Elinck E, Van Dongen J, Vermeulen S, Van den Broeck M, Vaerenberg C, Mattheijssens M, Peeters K, Robberecht W, Cras P, Martin JJ, De Deyn PP, Cruts M, Van Broeckhoven C (2012) A C9orf72 promoter repeat expansion in a Flanders-Belgian cohort with disorders of the frontotemporal lobar degeneration-amyotrophic lateral sclerosis spectrum: a gene identification study. Lancet neurology 11:54-65.

Gitler AD, Shorter J (2011) RNA-binding proteins with prion-like domains in ALS and FTLD-U. Prion 5:179-187.

Giusti SA, Vogl AM, Brockmann MM, Vercelli CA, Rein ML, Trümbach D, Wurst W, Cazalla D, Stein V, Deussing JM, Refojo D (2014) MicroRNA-9 controls dendritic development by targeting REST. eLife 3:e02755.

Goulet I, Gauvin G, Boisvenue S, Cote J (2007) Alternative splicing yields protein arginine methyltransferase 1 isoforms with distinct activity, substrate specificity, and subcellular localization. J Biol Chem 282:33009-33021.

Grad LI, Fernando SM, Cashman NR (2015) From molecule to molecule and cell to cell: prion-like mechanisms in amyotrophic lateral sclerosis. Neurobiology of disease 77:257-265.

Greene E, Mahishi L, Entezam A, Kumari D, Usdin K (2007) Repeat-induced epigenetic changes in intron 1 of the frataxin gene and its consequences in Friedreich ataxia. Nucleic Acids Res 35:3383-3390.

Greenway MJ, Andersen PM, Russ C, Ennis S, Cashman S, Donaghy C, Patterson V, Swingler R, Kieran D, Prehn J, Morrison KE, Green A, Acharya KR, Brown RH, Jr., Hardiman O (2006) ANG mutations segregate with familial and 'sporadic' amyotrophic lateral sclerosis. Nat Genet 38:411-413.

Halgren C, Kjaergaard S, Bak M, Hansen C, El-Schich Z, Anderson CM, Henriksen KF, Hjalgrim H, Kirchhoff M, Bijlsma EK, Nielsen M, den Hollander NS, Ruivenkamp CA, Isidor B, Le Caignec C, Zannolli R, Mucciolo M, Renieri A, Mari F, Anderlid BM, Andrieux J, Dieux A, Tommerup N, Bache I (2012) Corpus callosum abnormalities, intellectual disability, speech impairment, and autism in patients with haploinsufficiency of ARID1B. Clin Genet 82:248-255.

Hardiman O, van den Berg LH, Kiernan MC (2011) Clinical diagnosis and management of amyotrophic lateral sclerosis. Nat Rev Neurol 7:639-649.

Hasegawa M, Arai T, Nonaka T, Kametani F, Yoshida M, Hashizume Y, Beach TG, Buratti E, Baralle F, Morita M, Nakano I, Oda T, Tsuchiya K, Akiyama H (2008) Phosphorylated TDP-43 in frontotemporal lobar degeneration and amyotrophic lateral sclerosis. Annals of neurology 64:60-70.

He CZ, Hays AP (2004) Expression of peripherin in ubiquinated inclusions of amyotrophic lateral sclerosis. Journal of the neurological sciences 217:47-54.

Henkel JS, Beers DR, Siklos L, Appel SH (2006) The chemokine MCP-1 and the dendritic and myeloid cells it attracts are increased in the mSOD1 mouse model of ALS. Molecular and cellular neurosciences 31:427-437.

Henkel JS, Beers DR, Wen S, Rivera AL, Toennis KM, Appel JE, Zhao W, Moore DH, Powell SZ, Appel SH (2013) Regulatory T-lymphocytes mediate amyotrophic lateral sclerosis progression and survival. EMBO molecular medicine 5:64-79.

Herman D, Jenssen K, Burnett R, Soragni E, Perlman SL, Gottesfeld JM (2006) Histone deacetylase inhibitors reverse gene silencing in Friedreich's ataxia. Nature chemical biology 2:551-558.

Hewitt C, Kirby J, Highley JR, Hartley JA, Hibberd R, Hollinger HC, Williams TL, Ince PG, McDermott CJ, Shaw PJ (2010) Novel FUS/TLS mutations and pathology in familial and sporadic amyotrophic lateral sclerosis. Arch Neurol 67:455-461.

Hoell JI, Larsson E, Runge S, Nusbaum JD, Duggimpudi S, Farazi TA, Hafner M, Borkhardt A, Sander C, Tuschl T (2011) RNA targets of wild-type and mutant FET family proteins. Nat Struct Mol Biol 18:1428-1431.

Honda D, Ishigaki S, Iguchi Y, Fujioka Y, Udagawa T, Masuda A, Ohno K, Katsuno M, Sobue G (2013) The ALS/FTLD-related RNA-binding proteins TDP-43 and FUS have common downstream RNA targets in cortical neurons. FEBS open bio 4:1-10.

Howland DS, Liu J, She Y, Goad B, Maragakis NJ, Kim B, Erickson J, Kulik J, DeVito L, Psaltis G, DeGennaro LJ, Cleveland DW, Rothstein JD (2002) Focal loss of the glutamate transporter EAAT2 in a transgenic rat model of SOD1 mutant-mediated amyotrophic lateral sclerosis (ALS). Proceedings of the National Academy of Sciences of the United States of America 99:1604-1609.

Huang S, Litt M, Felsenfeld G (2005) Methylation of histone H4 by arginine methyltransferase PRMT1 is essential in vivo for many subsequent histone modifications. Genes Dev 19:1885-1893.

Ito D, Seki M, Tsunoda Y, Uchiyama H, Suzuki N (2011) Nuclear transport impairment of amyotrophic lateral sclerosis-linked mutations in FUS/TLS. Annals of neurology 69:152-162.

Jaiswal MK, Keller BU (2009) Cu/Zn superoxide dismutase typical for familial amyotrophic lateral sclerosis increases the vulnerability of mitochondria and perturbs Ca2+ homeostasis in SOD1G93A mice. Molecular pharmacology 75:478-489.

Janssens J, Van Broeckhoven C (2013) Pathological mechanisms underlying TDP-43 driven neurodegeneration in FTLD-ALS spectrum disorders. Hum Mol Genet 22:R77-87.

Jiang YM, Yamamoto M, Kobayashi Y, Yoshihara T, Liang Y, Terao S, Takeuchi H, Ishigaki S, Katsuno M, Adachi H, Niwa J, Tanaka F, Doyu M, Yoshida M, Hashizume Y, Sobue G (2005) Gene expression profile of spinal motor neurons in sporadic amyotrophic lateral sclerosis. Ann Neurol 57:236-251.

Kabashi E, Agar JN, Hong Y, Taylor DM, Minotti S, Figlewicz DA, Durham HD (2008a) Proteasomes remain intact, but show early focal alteration in their composition in a mouse model of amyotrophic lateral sclerosis. J Neurochem 105:2353-2366.

Kabashi E, Agar JN, Taylor DM, Minotti S, Durham HD (2004) Focal dysfunction of the proteasome: a pathogenic factor in a mouse model of amyotrophic lateral sclerosis. J Neurochem 89:1325-1335.

Kabashi E, Bercier V, Lissouba A, Liao M, Brustein E, Rouleau GA, Drapeau P (2011) FUS and TARDBP but not SOD1 interact in genetic models of amyotrophic lateral sclerosis. PLoS Genet 7:e1002214.

Kabashi E, Lin L, Tradewell ML, Dion PA, Bercier V, Bourgouin P, Rochefort D, Bel Hadj S, Durham HD, Vande Velde C, Rouleau GA, Drapeau P (2010) Gain and loss of function of ALS-related mutations of TARDBP (TDP-43) cause motor deficits in vivo. Human molecular genetics 19:671-683.

Kabashi E, Valdmanis PN, Dion P, Spiegelman D, McConkey BJ, Vande Velde C, Bouchard JP, Lacomblez L, Pochigaeva K, Salachas F, Pradat PF, Camu W, Meininger V, Dupre N, Rouleau GA (2008b) TARDBP mutations in individuals with sporadic and familial amyotrophic lateral sclerosis. Nat Genet 40:572-574.

Karpati G, Carpenter S, Durham H (1988) A hypothesis for the pathogenesis of amyotrophic lateral sclerosis. Revue neurologique 144:672-675.

Kato M, Han TW, Xie S, Shi K, Du X, Wu LC, Mirzaei H, Goldsmith EJ, Longgood J, Pei J, Grishin NV, Frantz DE, Schneider JW, Chen S, Li L, Sawaya MR, Eisenberg D, Tycko R, McKnight SL (2012a) Cell-free formation of RNA granules: low complexity sequence domains form dynamic fibers within hydrogels. Cell 149:753-767.

Kato M, Han Tina W, Xie S, Shi K, Du X, Wu Leeju C, Mirzaei H, Goldsmith Elizabeth J, Longgood J, Pei J, Grishin Nick V, Frantz Douglas E, Schneider Jay W, Chen S, Li L, Sawaya Michael R, Eisenberg D, Tycko R, McKnight Steven L (2012b) Cell-free Formation of RNA Granules: Low Complexity Sequence Domains Form Dynamic Fibers within Hydrogels. Cell 149:753-767.

Kato S, Sumi-Akamaru H, Fujimura H, Sakoda S, Kato M, Hirano A, Takikawa M, Ohama E (2001) Copper chaperone for superoxide dismutase co-aggregates with superoxide dismutase 1 (SOD1) in neuronal Lewy body-like hyaline inclusions: an immunohistochemical study on familial amyotrophic lateral sclerosis with SOD1 gene mutation. Acta Neuropathol 102:233-238.

Kato S, Takikawa M, Nakashima K, Hirano A, Cleveland DW, Kusaka H, Shibata N, Kato M, Nakano I, Ohama E (2000) New consensus research on neuropathological aspects of familial amyotrophic lateral sclerosis with superoxide dismutase 1 (SOD1) gene mutations: inclusions containing SOD1 in neurons and astrocytes. Amyotrophic lateral sclerosis and other motor neuron disorders : official publication of the World Federation of Neurology, Research Group on Motor Neuron Diseases 1:163-184.

Kawamata T, Akiyama H, Yamada T, McGeer PL (1992) Immunologic reactions in amyotrophic lateral sclerosis brain and spinal cord tissue. The American journal of pathology 140:691-707.

Kedersha N, Stoecklin G, Ayodele M, Yacono P, Lykke-Andersen J, Fritzler MJ, Scheuner D, Kaufman RJ, Golan DE, Anderson P (2005) Stress granules and processing bodies are dynamically linked sites of mRNP remodeling. The Journal of Cell Biology 169:871-884.

Keller BA, Volkening K, Droppelmann CA, Ang LC, Rademakers R, Strong MJ (2012) Co-aggregation of RNA binding proteins in ALS spinal motor neurons: evidence of a common pathogenic mechanism. Acta Neuropathol 124:733-747.

Khan AU, Krishnamurthy S (2005) Histone modifications as key regulators of transcription. Front Biosci 10:866-872.

Kiernan MC, Vucic S, Cheah BC, Turner MR, Eisen A, Hardiman O, Burrell JR, Zoing MC (2011) Amyotrophic lateral sclerosis. Lancet 377:942-955.

Kim SH, Shanware NP, Bowler MJ, Tibbetts RS (2010) Amyotrophic lateral sclerosis-associated proteins TDP-43 and FUS/TLS function in a common biochemical complex to co-regulate HDAC6 mRNA. J Biol Chem 285:34097-34105.

Kino Y, Washizu C, Aquilanti E, Okuno M, Kurosawa M, Yamada M, Doi H, Nukina N (2011) Intracellular localization and splicing regulation of FUS/TLS are variably affected by amyotrophic lateral sclerosis-linked mutations. Nucleic Acids Res 39:2781-2798.

Kovar H (2011) Dr. Jekyll and Mr. Hyde: The Two Faces of the FUS/EWS/TAF15 Protein Family. Sarcoma 2011:837474.

Kroschwald S, Maharana S, Mateju D, Malinovska L, Nuske E, Poser I, Richter D, Alberti S (2015) Promiscuous interactions and protein disaggregases determine the material state of stress-inducible RNP granules. eLife 4:e06807.

Kruman, II, Pedersen WA, Springer JE, Mattson MP (1999) ALS-linked Cu/Zn-SOD mutation increases vulnerability of motor neurons to excitotoxicity by a mechanism involving increased oxidative stress and perturbed calcium homeostasis. Experimental neurology 160:28-39.

Kryndushkin D, Wickner RB, Shewmaker F (2011) FUS/TLS forms cytoplasmic aggregates, inhibits cell growth and interacts with TDP-43 in a yeast model of amyotrophic lateral sclerosis. Protein & cell 2:223-236.

Kumari D, Usdin K (2010) The distribution of repressive histone modifications on silenced FMR1 alleles provides clues to the mechanism of gene silencing in fragile X syndrome. Hum Mol Genet 19:4634-4642.

Kwiatkowski TJ, Jr., Bosco DA, Leclerc AL, Tamrazian E, Vanderburg CR, Russ C, Davis A, Gilchrist J, Kasarskis EJ, Munsat T, Valdmanis P, Rouleau GA, Hosler BA, Cortelli P, de Jong PJ, Yoshinaga Y, Haines JL, Pericak-Vance MA, Yan J, Ticozzi N, Siddique T, McKenna-Yasek D, Sapp PC, Horvitz HR, Landers JE, Brown RH, Jr. (2009) Mutations in the FUS/TLS gene on chromosome 16 cause familial amyotrophic lateral sclerosis. Science 323:1205-1208.

Lagier-Tourenne C, Cleveland DW (2009) Rethinking ALS: the FUS about TDP-43. Cell 136:1001-1004.

Lattante S, Rouleau GA, Kabashi E (2013) TARDBP and FUS mutations associated with amyotrophic lateral sclerosis: summary and update. Hum Mutat 34:812-826.

Lee EB, Russ J, Jung H, Elman LB, Chahine LM, Kremens D, Miller BL, Branch Coslett H, Trojanowski JQ, Van Deerlin VM, McCluskey LF (2013) Topography of FUS pathology

distinguishes late-onset BIBD from aFTLD-U. Acta neuropathologica communications 1:1-11.

Lee JS, Smith E, Shilatifard A (2010) The language of histone crosstalk. Cell 142:682-685.

Lefebvre S, Burglen L, Reboullet S, Clermont O, Burlet P, Viollet L, Benichou B, Cruaud C, Millasseau P, Zeviani M, et al. (1995) Identification and characterization of a spinal muscular atrophy-determining gene. Cell 80:155-165.

Lerga A, Hallier M, Delva L, Orvain C, Gallais I, Marie J, Moreau-Gachelin F (2001) Identification of an RNA Binding Specificity for the Potential Splicing Factor TLS. Journal of Biological Chemistry 276:6807-6816.

Lessard J, Wu JI, Ranish JA, Wan M, Winslow MM, Staahl BT, Wu H, Aebersold R, Graef IA, Crabtree GR (2007) An essential switch in subunit composition of a chromatin remodeling complex during neural development. Neuron 55:201-215.

Levine TP, Daniels RD, Gatta AT, Wong LH, Hayes MJ (2013) The product of C9orf72, a gene strongly implicated in neurodegeneration, is structurally related to DENN Rab-GEFs. Bioinformatics 29:499-503.

Liu-Yesucevitz L, Bassell GJ, Gitler AD, Hart AC, Klann E, Richter JD, Warren ST, Wolozin B (2011) Local RNA translation at the synapse and in disease. J Neurosci 31:16086-16093.

Liu D, Liu C, Li J, Azadzoi K, Yang Y, Fei Z, Dou K, Kowall NW, Choi H-P, Vieira F, Yang J-H (2013) Proteomic Analysis Reveals Differentially Regulated Protein Acetylation in Human Amyotrophic Lateral Sclerosis Spinal Cord. PLoS ONE 8:e80779.

Liu Q, Dreyfuss G (1995) In vivo and in vitro arginine methylation of RNA-binding proteins. Molecular and cellular biology 15:2800-2808.

Loeb C, Mainardi P, Besio G, Lunardi G, Cogliolo I, Pioli F (1994) Plasma and CSF amino acid levels in ALS. Acta neurologica Scandinavica 90:223-224.

Logroscino G, Traynor BJ, Hardiman O, Chio A, Mitchell D, Swingler RJ, Millul A, Benn E, Beghi E, Eurals (2010) Incidence of amyotrophic lateral sclerosis in Europe. Journal of neurology, neurosurgery, and psychiatry 81:385-390.

Lu Y, Ferris J, Gao FB (2009) Frontotemporal dementia and amyotrophic lateral sclerosis-associated disease protein TDP-43 promotes dendritic branching. Molecular brain 2:30.

Mackenzie IR, Bigio EH, Ince PG, Geser F, Neumann M, Cairns NJ, Kwong LK, Forman MS, Ravits J, Stewart H, Eisen A, McClusky L, Kretzschmar HA, Monoranu CM, Highley JR, Kirby J, Siddique T, Shaw PJ, Lee VM, Trojanowski JQ (2007) Pathological TDP-43 distinguishes sporadic amyotrophic lateral sclerosis from amyotrophic lateral sclerosis with SOD1 mutations. Annals of neurology 61:427-434.

Mackenzie IR, Feldman HH (2005) Ubiquitin immunohistochemistry suggests classic motor neuron disease, motor neuron disease with dementia, and frontotemporal dementia of the

motor neuron disease type represent a clinicopathologic spectrum. Journal of neuropathology and experimental neurology 64:730-739.

Mackenzie IR, Rademakers R, Neumann M (2010) TDP-43 and FUS in amyotrophic lateral sclerosis and frontotemporal dementia. Lancet neurology 9:995-1007.

Marks PA, Xu WS (2009) Histone deacetylase inhibitors: Potential in cancer therapy. Journal of Cellular Biochemistry 107:600-608.

McDonald KK, Aulas A, Destroismaisons L, Pickles S, Beleac E, Camu W, Rouleau GA, Vande Velde C (2011) TAR DNA-binding protein 43 (TDP-43) regulates stress granule dynamics via differential regulation of G3BP and TIA-1. Human molecular genetics 20:1400-1410.

Mitchell JD, Borasio GD (2007) Amyotrophic lateral sclerosis. Lancet 369:2031-2041.

Mizielinska S, Lashley T, Norona F, Clayton E, Ridler C, Fratta P, Isaacs A (2013) C9orf72 frontotemporal lobar degeneration is characterised by frequent neuronal sense and antisense RNA foci. Acta Neuropathologica 126:845-857.

Mori K, Lammich S, Mackenzie IR, Forne I, Zilow S, Kretzschmar H, Edbauer D, Janssens J, Kleinberger G, Cruts M, Herms J, Neumann M, Van Broeckhoven C, Arzberger T, Haass C (2013a) hnRNP A3 binds to GGGGCC repeats and is a constituent of p62-positive/TDP43-negative inclusions in the hippocampus of patients with C9orf72 mutations. Acta Neuropathol 125:413-423.

Mori K, Weng SM, Arzberger T, May S, Rentzsch K, Kremmer E, Schmid B, Kretzschmar HA, Cruts M, Van Broeckhoven C, Haass C, Edbauer D (2013b) The C9orf72 GGGGCC repeat is translated into aggregating dipeptide-repeat proteins in FTLD/ALS. Science 339:1335-1338.

Moser JJ, Fritzler MJ (2010) Cytoplasmic ribonucleoprotein (RNP) bodies and their relationship to GW/P bodies. The International Journal of Biochemistry & Cell Biology 42:828-843.

Murphy J, Henry R, Lomen-Hoerth C (2007) Establishing subtypes of the continuum of frontal lobe impairment in amyotrophic lateral sclerosis. Arch Neurol 64:330-334.

Murray ME, DeJesus-Hernandez M, Rutherford NJ, Baker M, Duara R, Graff-Radford NR, Wszolek ZK, Ferman TJ, Josephs KA, Boylan KB, Rademakers R, Dickson DW (2011) Clinical and neuropathologic heterogeneity of c9FTD/ALS associated with hexanucleotide repeat expansion in C9ORF72. Acta Neuropathol 122:673-690.

Nakano I, Hirano A (1987) Atrophic cell processes of large motor neurons in the anterior horn in amyotrophic lateral sclerosis: observation with silver impregnation method. Journal of neuropathology and experimental neurology 46:40-49.

Nakaya T, Alexiou P, Maragkakis M, Chang A, Mourelatos Z (2013) FUS regulates genes coding for RNA-binding proteins in neurons by binding to their highly conserved introns. RNA 19:498-509.

Neale BM, Kou Y, Liu L, Ma'ayan A, Samocha KE, Sabo A, Lin CF, Stevens C, Wang LS, Makarov V, Polak P, Yoon S, Maguire J, Crawford EL, Campbell NG, Geller ET, Valladares O, Schafer C, Liu H, Zhao T, Cai G, Lihm J, Dannenfelser R, Jabado O, Peralta Z, Nagaswamy U, Muzny D, Reid JG, Newsham I, Wu Y, Lewis L, Han Y, Voight BF, Lim E, Rossin E, Kirby A, Flannick J, Fromer M, Shakir K, Fennell T, Garimella K, Banks E, Poplin R, Gabriel S, DePristo M, Wimbish JR, Boone BE, Levy SE, Betancur C, Sunyaev S, Boerwinkle E, Buxbaum JD, Cook EH, Jr., Devlin B, Gibbs RA, Roeder K, Schellenberg GD, Sutcliffe JS, Daly MJ (2012) Patterns and rates of exonic de novo mutations in autism spectrum disorders. Nature 485:242-245.

Nelson JS, Prensky AL (1972) Sporadic Juvenile Amyotrophic Lateral Sclerosis: A Clinicopathological Study of a Case With Neuronal Cytoplasmic Inclusions Containing RNA. Arch Neurol 27:300-306.

Neumann M, Bentmann E, Dormann D, Jawaid A, DeJesus-Hernandez M, Ansorge O, Roeber S, Kretzschmar HA, Munoz DG, Kusaka H, Yokota O, Ang LC, Bilbao J, Rademakers R, Haass C, Mackenzie IR (2011) FET proteins TAF15 and EWS are selective markers that distinguish FTLD with FUS pathology from amyotrophic lateral sclerosis with FUS mutations. Brain : a journal of neurology 134:2595-2609.

Neumann M, Rademakers R, Roeber S, Baker M, Kretzschmar HA, Mackenzie IR (2009) A new subtype of frontotemporal lobar degeneration with FUS pathology. Brain : a journal of neurology 132:2922-2931.

Neumann M, Sampathu DM, Kwong LK, Truax AC, Micsenyi MC, Chou TT, Bruce J, Schuck T, Grossman M, Clark CM, McCluskey LF, Miller BL, Masliah E, Mackenzie IR, Feldman H, Feiden W, Kretzschmar HA, Trojanowski JQ, Lee VM (2006) Ubiquitinated TDP-43 in frontotemporal lobar degeneration and amyotrophic lateral sclerosis. Science 314:130-133.

Nichols RC, Wang XW, Tang J, Hamilton BJ, High FA, Herschman HR, Rigby WF (2000) The RGG domain in hnRNP A2 affects subcellular localization. Experimental cell research 256:522-532.

Nicholson TB, Chen T, Richard S (2009) The physiological and pathophysiological role of PRMT1-mediated protein arginine methylation. Pharmacological Research 60:466-474.

Passos DO, Quaresma AJ, Kobarg J (2006) The methylation of the C-terminal region of hnRNPQ (NSAP1) is important for its nuclear localization. Biochemical and biophysical research communications 346:517-525.

Patel A, Lee Hyun O, Jawerth L, Maharana S, Jahnel M, Hein Marco Y, Stoynov S, Mahamid J, Saha S, Franzmann Titus M, Pozniakovski A, Poser I, Maghelli N, Royer Loic A, Weigert M, Myers Eugene W, Grill S, Drechsel D, Hyman Anthony A, Alberti S (2015) A Liquid-to-Solid Phase Transition of the ALS Protein FUS Accelerated by Disease Mutation. Cell 162:1066-1077.

Perrotti D, Iervolino A, Cesi V, Cirinna M, Lombardini S, Grassilli E, Bonatti S, Claudio PP, Calabretta B (2000) BCR-ABL prevents c-jun-mediated and proteasome-dependent FUS

(TLS) proteolysis through a protein kinase CbetaII-dependent pathway. Molecular and cellular biology 20:6159-6169.

Peters OM, Ghasemi M, Brown RH, Jr. (2015) Emerging mechanisms of molecular pathology in ALS. The Journal of clinical investigation 125:2548.

Piepers S, Veldink JH, de Jong SW, van der Tweel I, van der Pol WL, Uijtendaal EV, Schelhaas HJ, Scheffer H, de Visser M, de Jong JM, Wokke JH, Groeneveld GJ, van den Berg LH (2009) Randomized sequential trial of valproic acid in amyotrophic lateral sclerosis. Annals of neurology 66:227-234.

Qiu H, Lee S, Shang Y, Wang WY, Au KF, Kamiya S, Barmada SJ, Finkbeiner S, Lui H, Carlton CE, Tang AA, Oldham MC, Wang H, Shorter J, Filiano AJ, Roberson ED, Tourtellotte WG, Chen B, Tsai LH, Huang EJ (2014) ALS-associated mutation FUS-R521C causes DNA damage and RNA splicing defects. The Journal of clinical investigation 124:981-999.

Rappsilber J, Friesen WJ, Paushkin S, Dreyfuss G, Mann M (2003) Detection of arginine dimethylated peptides by parallel precursor ion scanning mass spectrometry in positive ion mode. Analytical chemistry 75:3107-3114.

Renton AE, Majounie E, Waite A, Simon-Sanchez J, Rollinson S, Gibbs JR, Schymick JC, Laaksovirta H, van Swieten JC, Myllykangas L, Kalimo H, Paetau A, Abramzon Y, Remes AM, Kaganovich A, Scholz SW, Duckworth J, Ding J, Harmer DW, Hernandez DG, Johnson JO, Mok K, Ryten M, Trabzuni D, Guerreiro RJ, Orrell RW, Neal J, Murray A, Pearson J, Jansen IE, Sondervan D, Seelaar H, Blake D, Young K, Halliwell N, Callister JB, Toulson G, Richardson A, Gerhard A, Snowden J, Mann D, Neary D, Nalls MA, Peuralinna T, Jansson L, Isoviita VM, Kaivorinne AL, Holtta-Vuori M, Ikonen E, Sulkava R, Benatar M, Wuu J, Chio A, Restagno G, Borghero G, Sabatelli M, Heckerman D, Rogaeva E, Zinman L, Rothstein JD, Sendtner M, Drepper C, Eichler EE, Alkan C, Abdullaev Z, Pack SD, Dutra A, Pak E, Hardy J, Singleton A, Williams NM, Heutink P, Pickering-Brown S, Morris HR, Tienari PJ, Traynor BJ (2011) A hexanucleotide repeat expansion in C9ORF72 is the cause of chromosome 9p21-linked ALS-FTD. Neuron 72:257-268.

Ringholz GM, Appel SH, Bradshaw M, Cooke NA, Mosnik DM, Schulz PE (2005) Prevalence and patterns of cognitive impairment in sporadic ALS. Neurology 65:586-590.

Rosen DR (1993) Mutations in Cu/Zn superoxide dismutase gene are associated with familial amyotrophic lateral sclerosis. Nature 364:362.

Rothstein JD, Van Kammen M, Levey AI, Martin LJ, Kuncl RW (1995) Selective loss of glial glutamate transporter GLT-1 in amyotrophic lateral sclerosis. Annals of neurology 38:73-84.

Rouaux C, Jokic N, Mbebi C, Boutillier S, Loeffler J-P, Boutillier A-L (2003) Critical loss of CBP/p300 histone acetylase activity by caspase-6 during neurodegeneration. The EMBO Journal 22:6537-6549.

Roy J, Minotti S, Dong L, Figlewicz DA, Durham HD (1998) Glutamate potentiates the toxicity of mutant Cu/Zn-superoxide dismutase in motor neurons by postsynaptic calcium-dependent mechanisms. J Neurosci 18:9673-9684.

Sama RRK, Ward CL, Kaushansky LJ, Lemay N, Ishigaki S, Urano F, Bosco DA (2013) FUS/TLS assembles into stress granules and is a prosurvival factor during hyperosmolar stress. J Cell Physio 228:2222-2231.

Sareen D, O'Rourke JG, Meera P, Muhammad AK, Grant S, Simpkinson M, Bell S, Carmona S, Ornelas L, Sahabian A, Gendron T, Petrucelli L, Baughn M, Ravits J, Harms MB, Rigo F, Bennett CF, Otis TS, Svendsen CN, Baloh RH (2013) Targeting RNA foci in iPSC-derived motor neurons from ALS patients with a C9ORF72 repeat expansion. Sci Transl Med 5:208ra149.

Sasaki S, Iwata M (1996a) Impairment of fast axonal transport in the proximal axons of anterior horn neurons in amyotrophic lateral sclerosis. Neurology 47:535-540.

Sasaki S, Iwata M (1996b) Ultrastructural study of synapses in the anterior horn neurons of patients with amyotrophic lateral sclerosis. Neurosci Lett 204:53-56.

Scaramuzzino C, Monaghan J, Milioto C, Lanson NA, Jr., Maltare A, Aggarwal T, Casci I, Fackelmayer FO, Pennuto M, Pandey UB (2013) Protein arginine methyltransferase 1 and 8 interact with FUS to modify its sub-cellular distribution and toxicity in vitro and in vivo. PLoS One 8:e61576.

Schwartz JC, Ebmeier CC, Podell ER, Heimiller J, Taatjes DJ, Cech TR (2012) FUS binds the CTD of RNA polymerase II and regulates its phosphorylation at Ser2. Genes & development 26:2690-2695.

Sephton CF, Tang AA, Kulkarni A, West J, Brooks M, Stubblefield JJ, Liu Y, Zhang MQ, Green CB, Huber KM, Huang EJ, Herz J, Yu G (2014) Activity-dependent FUS dysregulation disrupts synaptic homeostasis. Proc Natl Acad Sci U S A 111:E4769-4778.

Shaw PJ, Forrest V, Ince PG, Richardson JP, Wastell HJ (1995) CSF and plasma amino acid levels in motor neuron disease: elevation of CSF glutamate in a subset of patients. Neurodegeneration : a journal for neurodegenerative disorders, neuroprotection, and neuroregeneration 4:209-216.

Shechter D, Dormann HL, Allis CD, Hake SB (2007) Extraction, purification and analysis of histones. Nat Protoc 2:1445-1457.

Shelkovnikova TA, Robinson HK, Connor-Robson N, Buchman VL (2013) Recruitment into stress granules prevents irreversible aggregation of FUS protein mislocalized to the cytoplasm. Cell Cycle 12:3194-3202.

Shen W, Xu C, Huang W, Zhang J, Carlson JE, Tu X, Wu J, Shi Y (2007) Solution structure of human Brg1 bromodomain and its specific binding to acetylated histone tails. Biochemistry 46:2100-2110.

Siklos L, Engelhardt J, Harati Y, Smith RG, Joo F, Appel SH (1996) Ultrastructural evidence for altered calcium in motor nerve terminals in amyotropic lateral sclerosis. Annals of neurology 39:203-216.

Siklos L, Engelhardt JI, Alexianu ME, Gurney ME, Siddique T, Appel SH (1998) Intracellular calcium parallels motoneuron degeneration in SOD-1 mutant mice. Journal of neuropathology and experimental neurology 57:571-587.

Siuda J, Lewicka T, Bujak M, Opala G, Golenia A, Slowik A, van Blitterswijk M, Baker M, Ertekin-Taner N, Wszolek ZK, Rademakers R (2014) ALS-FTD complex disorder due to C9ORF72 gene mutation: description of first Polish family. European neurology 72:64-71.

Sreedharan J, Blair IP, Tripathi VB, Hu X, Vance C, Rogelj B, Ackerley S, Durnall JC, Williams KL, Buratti E, Baralle F, de Belleroche J, Mitchell JD, Leigh PN, Al-Chalabi A, Miller CC, Nicholson G, Shaw CE (2008) TDP-43 Mutations in Familial and Sporadic Amyotrophic Lateral Sclerosis. Science 319:1668-1672.

Staahl BT, Tang J, Wu W, Sun A, Gitler AD, Yoo AS, Crabtree GR (2013) Kinetic analysis of npBAF to nBAF switching reveals exchange of SS18 with CREST and integration with neural developmental pathways. J Neurosci 33:10348-10361.

Stieber A, Gonatas JO, Gonatas NK (2000) Aggregates of mutant protein appear progressively in dendrites, in periaxonal processes of oligodendrocytes, and in neuronal and astrocytic perikarya of mice expressing the SOD1(G93A) mutation of familial amyotrophic lateral sclerosis. Journal of the neurological sciences 177:114-123.

Strahl BD, Briggs SD, Brame CJ, Caldwell JA, Koh SS, Ma H, Cook RG, Shabanowitz J, Hunt DF, Stallcup MR, Allis CD (2001) Methylation of histone H4 at arginine 3 occurs in vivo and is mediated by the nuclear receptor coactivator PRMT1. Current biology : CB 11:996-1000.

Strong MJ, Yang W, Strong WL, Leystra-Lantz C, Jaffe H, Pant HC (2006) Tau protein hyperphosphorylation in sporadic ALS with cognitive impairment. Neurology 66:1770-1771.

Sun L, Wang M, Lv Z, Yang N, Liu Y, Bao S, Gong W, Xu R-M (2011a) Structural insights into protein arginine symmetric dimethylation by PRMT5. Proceedings of the National Academy of Sciences 108:20538-20543.

Sun Z, Diaz Z, Fang X, Hart MP, Chesi A, Shorter J, Gitler AD (2011b) Molecular determinants and genetic modifiers of aggregation and toxicity for the ALS disease protein FUS/TLS. PLoS biology 9:e1000614.

Takeda T, Uchihara T, Nakayama Y, Nakamura A, Sasaki S, Kakei S, Uchiyama S, Duyckaerts C, Yoshida M (2014) Dendritic retraction, but not atrophy, is consistent in amyotrophic lateral sclerosis-comparison between Onuf's neurons and other sacral motor neurons. Acta neuropathologica communications 2:11.

Tateishi T, Hokonohara T, Yamasaki R, Miura S, Kikuchi H, Iwaki A, Tashiro H, Furuya H, Nagara Y, Ohyagi Y, Nukina N, Iwaki T, Fukumaki Y, Kira J (2010) Multiple system degeneration with basophilic inclusions in Japanese ALS patients with FUS mutation. Acta Neuropathol 119:355-364.

Tibshirani M, Tradewell ML, Mattina KR, Minotti S, Yang W, Zhou H, Strong MJ, Hayward LJ, Durham HD (2015) Cytoplasmic sequestration of FUS/TLS associated with ALS alters histone marks through loss of nuclear protein arginine methyltransferase 1. Hum Mol Genet 24:773-786.

Tradewell ML, Cooper LA, Minotti S, Durham HD (2011) Calcium dysregulation, mitochondrial pathology and protein aggregation in a culture model of amyotrophic lateral sclerosis: mechanistic relationship and differential sensitivity to intervention. Neurobiology of disease 42:265-275.

Tradewell ML, Yu Z, Tibshirani M, Boulanger MC, Durham HD, Richard S (2012) Arginine methylation by PRMT1 regulates nuclear-cytoplasmic localization and toxicity of FUS/TLS harbouring ALS-linked mutations. Hum Mol Genet 21:136-149.

Tran LT, Gentil BJ, Sullivan KE, Durham HD (2014) The voltage-gated calcium channel blocker lomerizine is neuroprotective in motor neurons expressing mutant SOD1, but not TDP-43. Journal of neurochemistry 130:455-466.

Tsurusaki Y, Okamoto N, Ohashi H, Kosho T, Imai Y, Hibi-Ko Y, Kaname T, Naritomi K, Kawame H, Wakui K, Fukushima Y, Homma T, Kato M, Hiraki Y, Yamagata T, Yano S, Mizuno S, Sakazume S, Ishii T, Nagai T, Shiina M, Ogata K, Ohta T, Niikawa N, Miyatake S, Okada I, Mizuguchi T, Doi H, Saitsu H, Miyake N, Matsumoto N (2012) Mutations affecting components of the SWI/SNF complex cause Coffin-Siris syndrome. Nat Genet 44:376-378.

Turner MR, Cagnin A, Turkheimer FE, Miller CC, Shaw CE, Brooks DJ, Leigh PN, Banati RB (2004) Evidence of widespread cerebral microglial activation in amyotrophic lateral sclerosis: an [11C](R)-PK11195 positron emission tomography study. Neurobiology of disease 15:601-609.

van Blitterswijk M, Landers JE (2010) RNA processing pathways in amyotrophic lateral sclerosis. Neurogenetics 11:275-290.

Vance C, Rogelj B, Hortobagyi T, De Vos KJ, Nishimura AL, Sreedharan J, Hu X, Smith B, Ruddy D, Wright P, Ganesalingam J, Williams KL, Tripathi V, Al-Saraj S, Al-Chalabi A, Leigh PN, Blair IP, Nicholson G, de Belleroche J, Gallo JM, Miller CC, Shaw CE (2009) Mutations in FUS, an RNA processing protein, cause familial amyotrophic lateral sclerosis type 6. Science 323:1208-1211.

Vehvilainen P, Koistinaho J, Gundars G (2014) Mechanisms of mutant SOD1 induced mitochondrial toxicity in amyotrophic lateral sclerosis. Frontiers in cellular neuroscience 8:126.

Vogel-Ciernia A, Matheos DP, Barrett RM, Kramar EA, Azzawi S, Chen Y, Magnan CN, Zeller M, Sylvain A, Haettig J, Jia Y, Tran A, Dang R, Post RJ, Chabrier M, Babayan AH, Wu JI, Crabtree GR, Baldi P, Baram TZ, Lynch G, Wood MA (2013) The neuron-specific chromatin regulatory subunit BAF53b is necessary for synaptic plasticity and memory. Nat Neurosci 16:552-561.

Waibel S, Neumann M, Rosenbohm A, Birve A, Volk AE, Weishaupt JH, Meyer T, Muller U, Andersen PM, Ludolph AC (2013) Truncating mutations in FUS/TLS give rise to a more aggressive ALS-phenotype than missense mutations: a clinico-genetic study in Germany. European journal of neurology : the official journal of the European Federation of Neurological Societies 20:540-546.

Wang H, Huang ZQ, Xia L, Feng Q, Erdjument-Bromage H, Strahl BD, Briggs SD, Allis CD, Wong J, Tempst P, Zhang Y (2001) Methylation of histone H4 at arginine 3 facilitating transcriptional activation by nuclear hormone receptor. Science 293:853-857.

Wang JW, Brent JR, Tomlinson A, Shneider NA, McCabe BD (2011) The ALS-associated proteins FUS and TDP-43 function together to affect Drosophila locomotion and life span. The Journal of clinical investigation 121:4118-4126.

Wang WY, Pan L, Su SC, Quinn EJ, Sasaki M, Jimenez JC, Mackenzie IR, Huang EJ, Tsai LH (2013) Interaction of FUS and HDAC1 regulates DNA damage response and repair in neurons. Nat Neurosci 16:1383-1391.

Williams TL, Day NC, Ince PG, Kamboj RK, Shaw PJ (1997) Calcium-permeable alpha-amino-3-hydroxy-5-methyl-4-isoxazole propionic acid receptors: a molecular determinant of selective vulnerability in amyotrophic lateral sclerosis. Annals of neurology 42:200-207.

Winkler EA, Sengillo JD, Sullivan JS, Henkel JS, Appel SH, Zlokovic BV (2013) Blood-spinal cord barrier breakdown and pericyte reductions in amyotrophic lateral sclerosis. Acta Neuropathol 125:111-120.

Wu JI, Lessard J, Olave IA, Qiu Z, Ghosh A, Graef IA, Crabtree GR (2007) Regulation of dendritic development by neuron-specific chromatin remodeling complexes. Neuron 56:94-108.

Xiao S, Sanelli T, Chiang H, Sun Y, Chakrabartty A, Keith J, Rogaeva E, Zinman L, Robertson J (2015) Low molecular weight species of TDP-43 generated by abnormal splicing form inclusions in amyotrophic lateral sclerosis and result in motor neuron death. Acta Neuropathol 130:49-61.

Xu Z, Poidevin M, Li X, Li Y, Shu L, Nelson DL, Li H, Hales CM, Gearing M, Wingo TS, Jin P (2013) Expanded GGGGCC repeat RNA associated with amyotrophic lateral sclerosis and frontotemporal dementia causes neurodegeneration. Proc Natl Acad Sci U S A 110:7778-7783.

Yamaguchi A, Kitajo K (2012) The effect of PRMT1-mediated arginine methylation on the subcellular localization, stress granules, and detergent-insoluble aggregates of FUS/TLS. PloS one 7:e49267.

Yamashita S, Mori A, Sakaguchi H, Suga T, Ishihara D, Ueda A, Yamashita T, Maeda Y, Uchino M, Hirano T (2012) Sporadic juvenile amyotrophic lateral sclerosis caused by mutant FUS/TLS: possible association of mental retardation with this mutation. J Neurol 259:1039-1044.

Yoo AS, Staahl BT, Chen L, Crabtree GR (2009) MicroRNA-mediated switching of chromatin-remodelling complexes in neural development. Nature 460:642-646.

Yu MC (2011) The Role of Protein Arginine Methylation in mRNP Dynamics. Mol Biol Int 2011:163827.

Zhang R, Hadlock KG, Do H, Yu S, Honrada R, Champion S, Forshew D, Madison C, Katz J, Miller RG, McGrath MS (2011) Gene expression profiling in peripheral blood mononuclear cells from patients with sporadic amyotrophic lateral sclerosis (sALS). Journal of neuroimmunology 230:114-123.

Zhao Q, Rank G, Tan YT, Li H, Moritz RL, Simpson RJ, Cerruti L, Curtis DJ, Patel DJ, Allis CD, Cunningham JM, Jane SM (2009) PRMT5-mediated methylation of histone H4R3 recruits DNMT3A, coupling histone and DNA methylation in gene silencing. Nature structural & molecular biology 16:304-311.

Zhou Y, Liu S, Liu G, Ozturk A, Hicks GG (2013) ALS-associated FUS mutations result in compromised FUS alternative splicing and autoregulation. PLoS Genet 9:e1003895.

Zu T, Liu Y, Bañez-Coronel M, Reid T, Pletnikova O, Lewis J, Miller TM, Harms MB, Falchook AE, Subramony SH, Ostrow LW, Rothstein JD, Troncoso JC, Ranum LPW (2013) RAN proteins and RNA foci from antisense transcripts in C9ORF72 ALS and frontotemporal dementia. Proceedings of the National Academy of Sciences 110:E4968-E4977.

Supplementary Materials

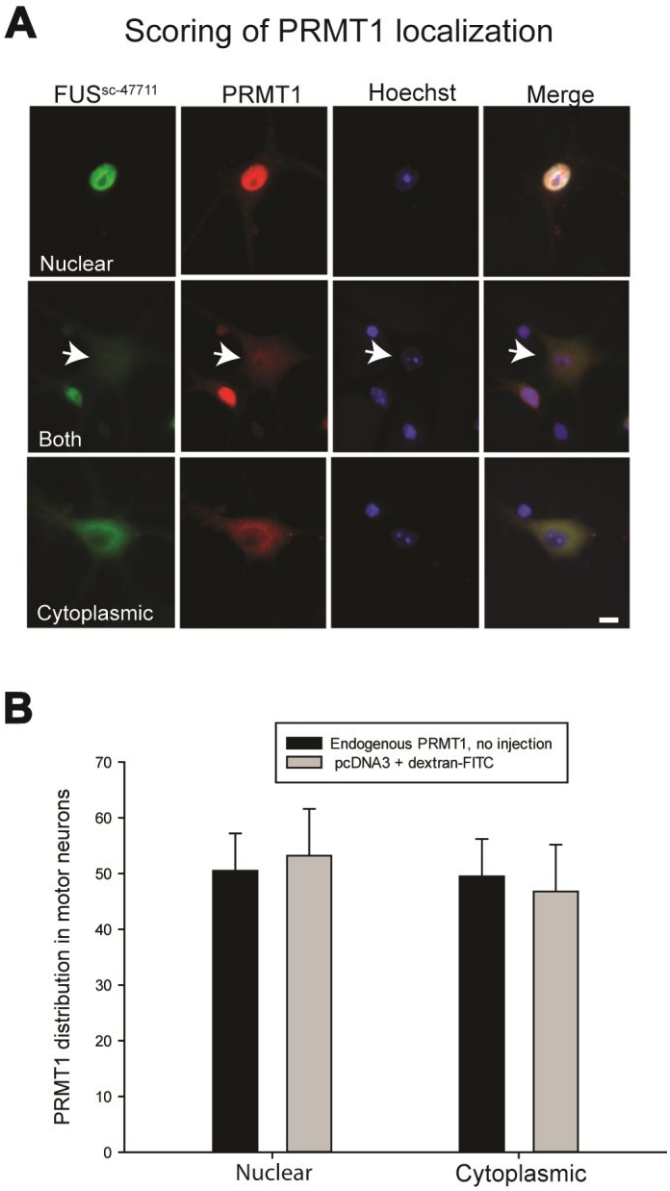

Supplementary Material Fig. S1. Localization of PRMT1 in cultured motor neurons.

(**A)** Double labelling of cultured neurons with anti-FUS/anti-PRMT1 antibodies. PRMT1 localization was scored as nuclear, both nuclear and cytoplasmic, or cytoplasmic and quantified as presented in Fig. 2. Scale bar = 10 µm.

(**B)** Scoring of PRMT1 localization in uninjected neurons and neurons injected with FITC-Dextran, showing that the microinjection procedure has no effect on PRMT1 localization.

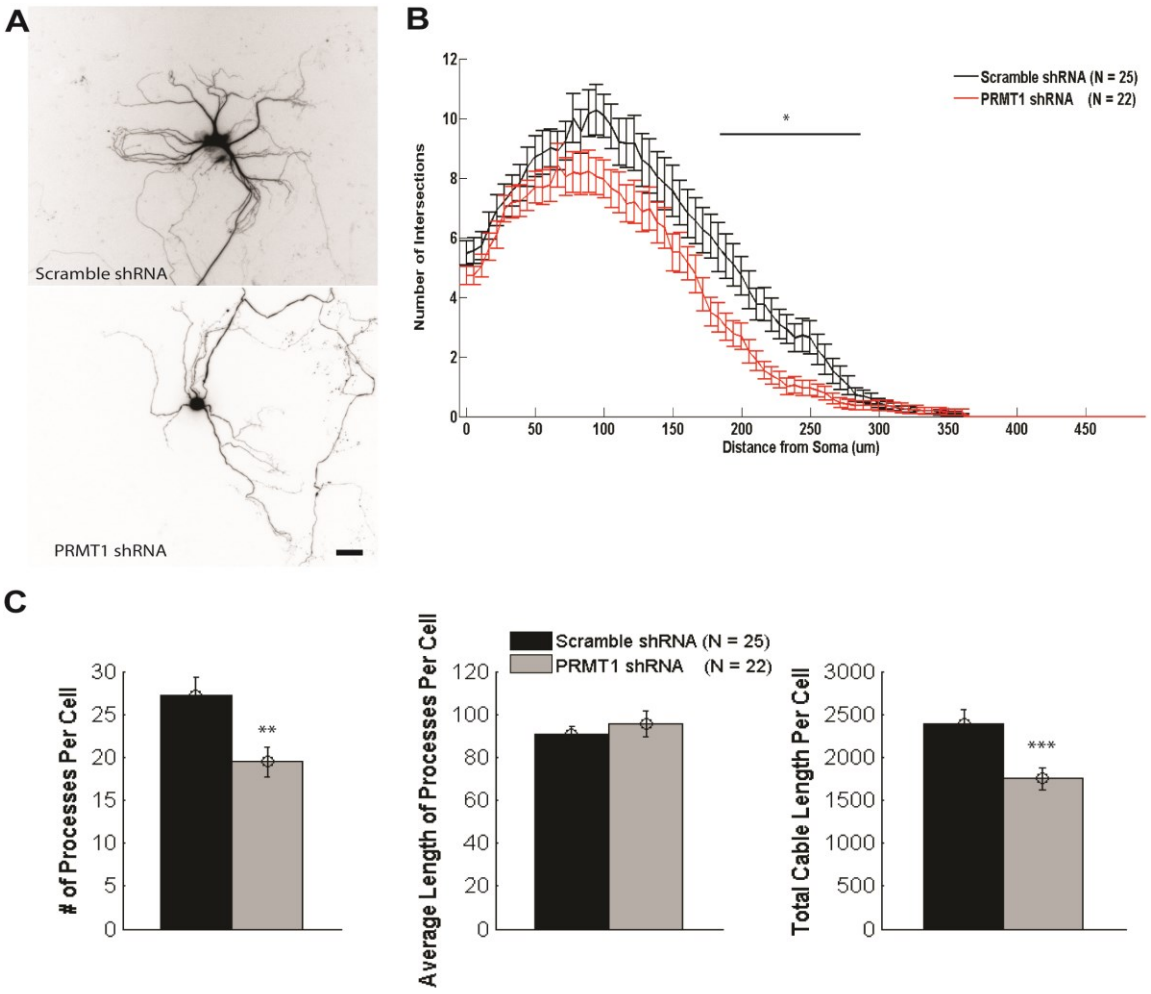

Supplementary Fig. S2. Dendritic attrition is a consequence of PRMT1 knockdown.

Motor neurons were injected with Scramble shRNA or PRMT1 shRNA pool along with mCherry to visualize cell morphology. Measurements of dendritic morphology were performed using Bonfire. Images taken after 3 days using a 10x objective were exported to 8-bit .tif images. Cell body and dendrites were traced using the semi-automated ImageJ tracing plugin, NeuronJ (http://www.imagescience.org/meijering/software/neuronj/). Branching points were designated using NeuroStudio and measurements of dendritic morphology were performed with Bonfire using the resulting .swc file. Significance was determined using a Welch's t-test.

Neurons expressing PRMT1 shRNA showed decreased dendritic branching as indicated by (**A**) mCherry epifluorescence and (**B** and **C**) Sholl analysis compared to scramble shRNA. (B) Sholl curve shows fewer dendritic branches distant from the cell body with PRMT1 knockdown. (**C**) Knockdown of PRMT1 decreased the average number of processes per cell as well as total dendritic output. Asterisks indicate significant difference from scramble shRNA-injected neurons, *p<0.05, **p<0.01, ***p<0.001. Scale bar = 30 μm.

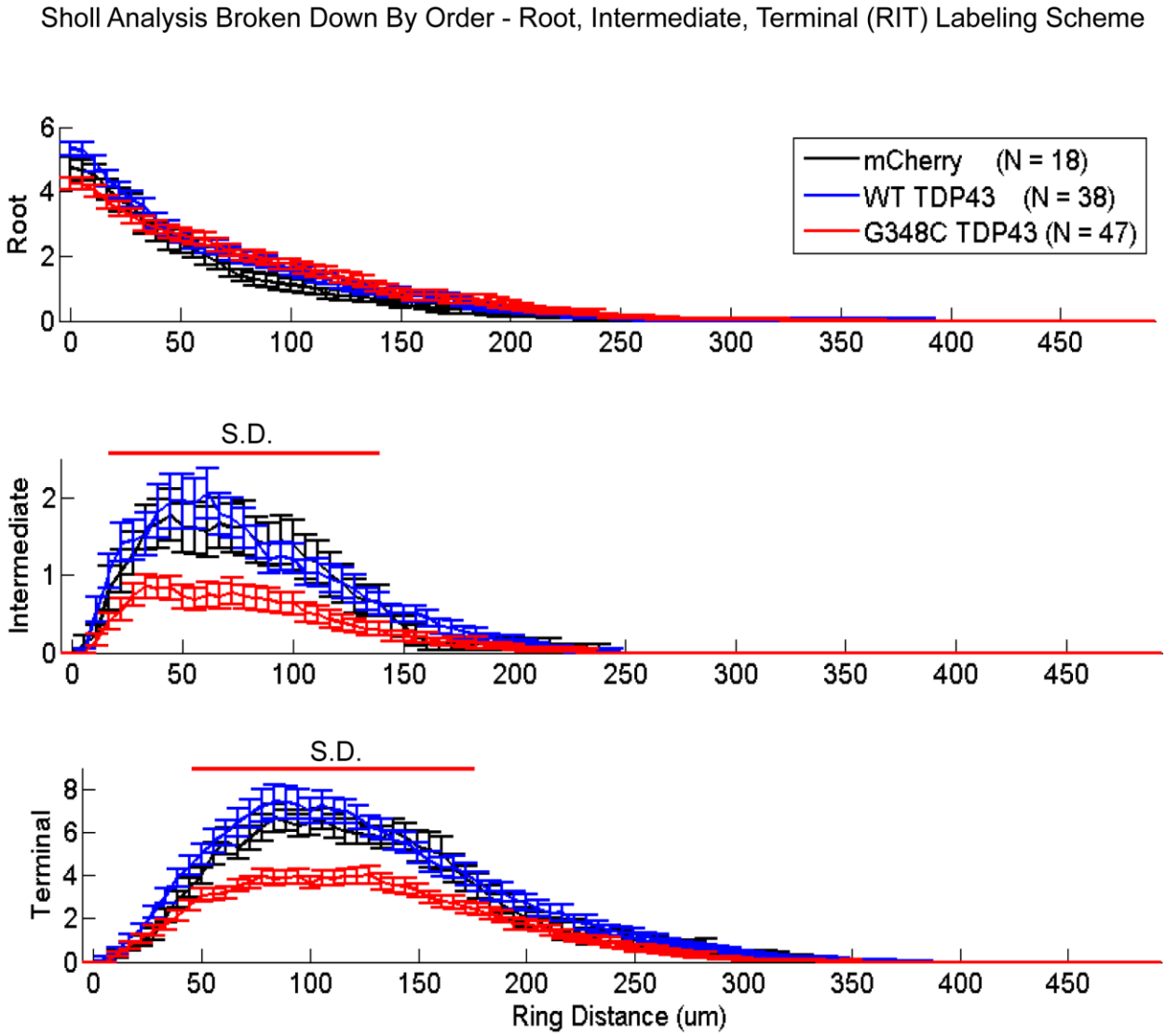

Supplementary Figure S3. Dendritic attrition in mutant TDP43 expressing motor neurons. Motor neurons were injected with pcDNA3, WT TDP43 and mutant TDP43 along with mCherry to visualize cell morphology and imaged on day 3 post-injection. Shown is the root, intermediate and terminal categorization of the sholl analysis. "S.D." indicates significant difference compared to mCherry only control ($p<0.05$; Welch's t-test)

Sequences for G-Blocks ordered for 3'UTR experiments:

*Yellow = 3'UTR sequence

Brg1 3'UTR

GGAGTTCAAGTCCATCTACATGGCCAAGAAGCCCGTGCAGCTGCCCGGCTACTACTA
CGTGGACTCCAAGCTGGACATCACCTCCCACAACGAGGACTACACCATCGTGGAGC
AGTACGAGCGCGCCGAGGGCCGCCACCACCTGTTCCTGTAGTGATCAaccagacattcctgag
tcctgaccccgaggcgctcgtcccagccaagatggagtagcccttagcagtgatgggtagcaccagatgtagtttcgaacttggagaactg
tacacatgcaatcttccacatttttaggcagagaagtataggcctgtctgtcggccctggcctggcctcgagtctctaccagcattaactgtcta
gagaggggacctcctgggagcaccatccacctccccaggccccagtcactgtagctcagtggatgcatgcgcgtgccggccgctccttgt
actgtatcttactggacagggccagctctccaggaggctcacaggcccagcgggtatgtcagtgtcactggagtcagacagtaataaattaa
agcaatgacaagccacGAATTCGCGGCCGCGACTCTAGATCATAATCAGCCATACCACATTT
GTAGAGGTTTTACTTGCTTTAAAAAACCTCCCACACCTCCCCCTGAACCTGAAACAT
AAAATGAATGCA

Scramble sequence for Brg1 UTR#1

GGAGTTCAAGTCCATCTACATGGCCAAGAAGCCCGTGCAGCTGCCCGGCTACTACTA
CGTGGACTCCAAGCTGGACATCACCTCCCACAACGAGGACTACACCATCGTGGAGC
AGTACGAGCGCGCCGAGGGCCGCCACCACCTGTTCCTGTAGTGATCAagtatccattgtggtag
gcgggagagacctctgagtacatctggcgcgcgcaaaccccgagccgtccatgacctcgtagaagacttactttcaggtcgctggagcgc
aacggcctaaggttattagggaatcgacgtgcatcccagccctaccgatgcgacacaactccgcctctaggtagcgttatttaccaagtgcg
gatatttttttgacaaggcgactaggccgcggcgaagcggcagtgtggcgccgccttcagcgcggagaccgataatccccaagccgggga
ccttagactaacaaccctaatacgccgttattgtcgtatctaggtacggacacatgatctacgcgtttcaatgccgacctaatccactcgctctc
cattggcgagagcgctaGAATTCGCGGCCGCGACTCTAGATCATAATCAGCCATACCACATTT
GTAGAGGTTTTACTTGCTTTAAAAAACCTCCCACACCTCCCCCTGAACCTGAAACAT
AAAATGAATGCA

Scramble sequence for Brg1 UTR #2

GGAGTTCAAGTCCATCTACATGGCCAAGAAGCCCGTGCAGCTGCCCGGCTACTACTA
CGTGGACTCCAAGCTGGACATCACCTCCCACAACGAGGACTACACCATCGTGGAGC
AGTACGAGCGCGCCGAGGGCCGCCACCACCTGTTCCTGTAGTGATCAgcccggagacttccg
ggagctaccccggcatcgagaacgcttcttctggtgaaaaactgtcaagcgttgtcgcagcaaatgagctgcctaagcgatatctccgacg
ccgcggacaaagggagattagagggcttgaccgttaatcaagcctcatcactgttgcgaaaggcggtacctggtgggcgacacctcgcgt
cgcctttccaggaagacataccagtgcaaatatcccgttttgctacaatgagttacacactaggaggtggcactagtcgatcgtgggctgaca
tgggtagcagcgccgctggatttggttgacacgcctcaccgcatcttcgcgcctagcaacacaaacgcttcagaggcacaccttactctcac
acgctatgtccctgtttccGAATTCGCGGCCGCGACTCTAGATCATAATCAGCCATACCACATTT
GTAGAGGTTTTACTTGCTTTAAAAAACCTCCCACACCTCCCCCTGAACCTGAAACAT
AAAATGAATGCA

BAF53a 3'UTR

GGACATCACCTCCCACAACGAGGACTACACCATCGTGGAGCAGTACGAGCGCGCCG
AGGGCCGCCACCACCTGTTCCTGTAGTGATCAgggctccaccctgcctgcccgtcacctcaacgtctgtagct
ttagtacactcaggaaaagatgaccatcttttgtagaatgtttatacatgtttgcatatttcaatttccacttaaatttttaaggctttaactggctcta
taaattaaatgagtttgtgctttccttgaaatgcacttattcttattacaggcattttataatttgtatgaatgtctattttctctaaatattttgctttcagt
aagtactctccagctctcctgggggttggttggtggaattactctgtattgacaagtacaagttactgcctatgctttgtaccttaggctacaaaa
ctaaataaaaatcactactgtcctagaagcgtgctggatttgtctgtgtgactggctgctgtcagcgctgcttctaccattacttgatgtggggaa
gcaatcactgactaccagtgtccacatccctttcctgctaacaattatgtatatggataattcacctgcatGAATTCGCGGCCGCG
ACTCTAGATCATAATCAGCCATACCACATTTGTAGAGG